2007-05-15

Cartilage tissue engineering: uses of injection molding and computer aided design for the fabrication of complex geometries with high dimensional tolerances: a dissertation

Morgan E. Hott
University of Massachusetts Medical School

Graduate School of Biomedical Sciences

GSBS Dissertations and Theses

University of Massachusetts Medical School *Year 2007*

Cartilage Tissue Engineering: Uses of injection molding and computer aided design for the fabrication of complex geometries with high dimensional tolerances

Morgan Hott
University of Massachusetts Medical School,

Cartilage Tissue Engineering: Uses of injection molding and computer aided design for the fabrication of complex geometries with high dimensional tolerances

A dissertation presented by
Morgan Hott

Submitted to the Faculty of the
University of Massachusetts Graduate School of Biomedical Sciences, Worcester
in partial fulfillment of the requirements for the degree of
DOCTOR OF PHILOSOPHY

Cartilage Tissue Engineering: Uses of injection molding and computer aided design for the fabrication of complex geometries with high dimensional tolerances

A Dissertation Presented by Morgan Hott

Approved as to style and content by:

_____
Celia Schiffer, Ph.D., Chair of the Committee

_____
Paul Odgren, Ph.D., Member of the Committee

_____
Anthony Carruthers, Ph.D., Member of the Committee

_____
Anthony Carruthers, Ph.D.,
Dean of the Graduate School of Biomedical Sciences

MD/PhD program
University of Massachusetts
May 15, 2007

Acknowledgements

I would like to thank the members of my research advisory committee for sticking with me through this very long process. I will be forever grateful for their continued support and help through the years.

I feel blessed to have many family and friends, all of whom I can rely on. In particular I would like to thank my friends Michael and Shoshanna Gerber for their generous gift of their time and house, where much of my thesis was written

Above all, I would like to thank my father for providing me with a life long example of a hard working, ethical man. Whenever things are tough, his example is the one I seek for guidance. Thanks dad.

Abstract

Cartilage Tissue Engineering. Joint pain and functional impairment due to cartilage damage from osteoarthritis and other means is a major source of disability for adults the world over. Cartilage is an avascular tissue with a very limited capacity for self repair. Current medical and surgical approaches to cartilage repair also have limited efficacy, and in all cases fail to completely restore a normal, healthy cartilage phenotype. Tissue engineering is a relatively new approach to cartilage repair that seeks to fabricate a replacement tissue, indistinguishable from healthy, native tissue.

The basic idea of the tissue engineering approach is to seed tissue synthesizing cells into a shapeable, biocompatible/bioabsorbable scaffold that serves as a temporary extracellular matrix with a localized source of bioactive molecules to direct the development of new tissue. The challenge of tissue engineering is to identify cells, scaffolds, and growth conditions that will be optimal for tissue regeneration. The goal of the current studies was to evaluate one aspect of all three of the major components of cartilage tissue engineering: cell source, scaffolding material and preparation, and controlled growth factor delivery.

We evaluated the chondrogenic potential of human nasal chondrocytes grown in calcium alginate in an in vivo culture system, the potential of computer-aided design and injection molding with calcium alginate to reliably reproduce complex geometries with high dimensional tolerances, and the potential for the controlled

release of TGF-β1 from calcium alginate modified by the covalent addition of a recently discovered TGF-β binding peptide.

We found that adult human nasal chondrocytes show significant chondrogenic potential when grown within an alginate scaffold. We also found that alginate is readily amenable to an injection molding process that utilizes precision made molds from computer-aided design and solid free form fabrication, allowing for the fabrication of tissue engineered constructs with very precise shape fidelity. Additionally, we found that calcium alginate could be reliably modified by the covalent addition of peptides, and that the addition of a newly discovered TGF-β binding peptide delayed the release of pre-loaded TGF-β1. Together these results show some of the encouraging prospects for cartilage tissue engineering.

`**Menière's Syndrome.** Menière's syndrome is an inner ear disorder characterized by idiopathic endolymphatic hydrops with associated periodic tinnitus, vertigo, and progressive sensorineural hearing loss. It affects approximately 0.2% of the population, for whom it can be quite devastating. In addition to progressive hearing loss people with Menière's syndrome are prone to sudden attacks of vertigo and tinnitus that are severe enough that they can lead to falls and potentially serious injury. People subject to frequent attacks are unable to drive, with obvious consequences on standard of living.

In the current studies we evaluated the standard animal model of Menière's syndrome by comparing cochlear turn specific hearing thresholds and the degree of hydrops in that turn. A positive correlation between these had previously been established in the study of human temporal bones from people with Menière's syndrome, but had not been reported in the animal model.

We also evaluated the potential of aminoguanidine, a relatively specific inhibitor of the inducible isoform of nitric oxide synthase, as a neuroprotective therapeutic agent for preservation of hearing in animals with surgically induced endolymphatic hydrops.

We found, for the first time, a partial correlation between cochlear turn specific hydrops and hearing thresholds in the most commonly used animal model of Menière's syndrome, helping to validate the utility of this animal model for future studies. We also found that aminoguanidine did indeed partially preserve hearing in animals with surgically induced Menière's syndrome. This encouraging result appears to be the first report of a medical intervention protective against hearing loss in an animal model of Menière's syndrome, and may help us to understand the etiology pathology seen in Menière's syndrome.

TABLE OF CONTENTS

LIST OF FIGURES

CHAPTER 1:

CHAPTER 2:

CHAPTER 3:

CHAPTER 4:

CHAPTER 5:

Introduction

Cartilage Structure. Articular cartilage, the tissue that lines all diarthrodial joints (freely moving joints), functions as a low friction, wear-resistant tissue that bears and distributes load. It is composed of sparsely scattered chondrocytes in a dense extracellular matrix (ECM) composed primarily of type II collagen, proteoglycans, and water. Other classes of molecules make up a minor, poorly defined, component of cartilage; these include proteins, lipids, phospholipids, and various other minor collagens. The chondrocytes, the only cellular component of cartilage, make up only about 5-10% of the wet weight of cartilage, but their metabolism is entirely responsible for maintaining the appropriate composition of the ECM. Articular cartilage is endowed with its specialized mechanical properties by the highly organized nature of the ECM, which can be structurally and functionally divided into four distinct zones: the superficial zone, the middle zone, the deep zone, and the zone of calcified cartilage. Each of these zones has a distinct organization and function in native cartilage.

The superficial zone is the articulating surface that provides a smooth gliding surface and resists sheer. This zone makes up approximately 10-20% of the thickness of articular cartilage. It has the highest collagen content of the zones, with densely packed fibrils aligned parallel to the articular surface[1]. The superficial zone has the lowest compressive modulus and will deform approximately 25 times more than the

middle zone. The chondrocytes in this layer, characterized by an elongated appearance, preferentially express proteins that have lubricating and protective functions and secrete relatively little proteoglycan[8]. Among the proteins involved in surface lubrication, superficial zone protein (SZP), also known as lubricin, has been identified as a functionally important molecule. SZP has an extremely low coefficient of friction, and together with hyaluronic acid in the synovial fluid creates an almost frictionless articulation. Additionally, the ability to synthesize SZP has been used phenotypically to distinguish superficial zone chondrocytes from those in the deeper layers[9-10].

The middle zone comprises about 40-60% of the articular cartilage volume. This zone has a higher compressive modulus that the superficial zone and a less organized arrangement of collagen fibrils. The fibrils are thicker, more loosely packed, and aligned obliquely to the articular surface. The chondrocytes in this layer are more rounded, and do not secrete SZP.

The deep zone makes up about 30% of the cartilage and consists of large diameter collagen fibrils oriented perpendicular to the articular surface. This layer contains the highest proteoglycan and lowest water concentration, and has the highest compressive modulus. The chondrocytes are typically arranged in columnar fashion parallel to the collagen fibrils and perpendicular to the joint line. The deep zone is partially calcified, and the calcified layer is distinguished histologically by a

boundary with non-calcified cartilage called the tidemark. The calcified zone represents residue from the secondary center of ossification in the epiphysis of the underlying bone. Its chondrocytes frequently exhibit hypertrophy, as is seen in endochondral bone formation. These cells can synthesize type-X collagen, can calcify their extracellular matrix, and are rich in alkaline phosphatase. When cartilage degenerates, as in osteoarthritis, the calcified zone extends further into the deep zone and new tidemarks appear. This is of substantial clinical importance, because with calcification of the extracellular matrix the unique properties of cartilage, especially its ability to recover from deformation, are lost.

Due to the nature of the ECM, cartilage is a highly hydrated tissue, with water making up between 70%-80% of its wet weight. The ECM makes up 90% of the dry weight of cartilage, and more than half of that weight is made up of proteoglycans. Proteoglycans are composed of a large core protein, and covalently bound, sulfated glycosaminoglycan (GAG) chains. In cartilage, a typical large proteoglycan has 100 long chondroitin sulfate chains and 50 much shorter keratin sulfate chains. These GAG chains account for approximately 90% of the molecular weight of the proteoglycan[12]. Proteoglycans are entangled and compacted within the collagen interfibrillar space, which helps to maintain a porous, permeable solid matrix. The charged sulfate groups on proteoglycan GAG chains exhibit electrostatic repulsion, and allow substantial hydration. Proteoglycan swelling in cartilage is limited by the collagen fibril network, which restricts proteoglycan size to as little as 20% of its

potential.[1] The hydrated proteoglycans account for the ability of articular cartilage to resist compressive loads. The collagen mesh, in turn, allows the tissue to resist tension and shear forces.[2]

Cartilage Damage and Osteoarthritis. Articular cartilage is a remarkably durable tissue that provides for almost frictionless motion between the articulating surfaces of diarthrodial joints, while protecting the underlying bones from the mechanical stresses of normal joint use. The architecture of the ECM and the resulting substantial hydration endow cartilage with its ability to cushion the underlying subchondral bone during loading. Chondrocytes continually synthesize, incorporate and degrade ECM proteins, permitting much of the cartilage matrix to undergo turnover and maintenance. Circumstances that impair chondrocyte function can disrupt the balance of synthesis and catabolism in favor of cartilage degradation, which over time can lead to osteoarthritis (OA).

OA afflicts more than 20 million people in the United States, and is the single leading cause of disability in adults.[13] Osteoarthritis is increasingly common with advancing age. About 10% of adults over the age of 50, 50% of adults over the age 65, and nearly all people over the age of 75 have some features of osteoarthritis.[14-17] The total annual societal cost for arthritis, has been estimated at over 2% of the United States gross domestic product, making the understanding of the

pathophysiology and the search for novel treatments of paramount importance in health care science.[18]

There are three main types of cartilage injury: matrix disruption, partial thickness defects, and full thickness defects. Matrix disruption occurs from blunt trauma, such as dashboard injuries in automobile accidents. The ECM is damaged, but if the injury is not extreme, the remaining viable chondrocytes will increase their synthetic activity to repair the tissue. Partial thickness defects demonstrate disruption of the cartilage surface, but this does not extend to the subchondral bone. Immediately following the injury, nearby cells begin to proliferate, but for reasons that remain unclear, cellular attempts to fill the defect cease before it is repaired. It is widely speculated that because of entrapment in the relatively rigid ECM chondrocytes are unable to sufficiently proliferate or migrate to mount an effective wound healing response. Full thickness defects arise from damage that transverses the entire cartilage thickness and penetrates the subchondral bone. In this case, the defect is filled with a fibrin clot and a classic wound healing response ensues. With this type of injury, unlike the others, there is access to a population of progenitor cells from the bone marrow which can migrate to fill the defect[19]. These cells, however, usually cause replacement of the fibrin clot with tissue intermediate between hyaline and fibrocartilage, making a tissue that is usually quite a bit less stiff and more permeable than native cartilage. Consequently this tissue often degrades over a period of months[20-21] .

Whatever the initial etiology, the end-stage of articular cartilage disease, with clinical characteristics including joint pain, stiffness, dysfunction, and deformity, as well as the radiographic manifestations of joint space narrowing, subchondral sclerosis, and osteophyte formation, are easily recognized. However, signs and symptoms in earlier stages, when treatment may alter disease course, are more elusive. Understanding the basic science of cartilage and the changes that occur in OA is imperative to develop novel strategies to diagnose and treat this disorder.

The specialized architecture and limited repair capacity of articular cartilage coupled with the high physical demands on this tissue make it exceedingly difficult to treat medically. There is currently no regimen, either pharmacologic or surgical, that is capable of restoring damaged cartilage to its normal phenotype. The tissue engineering approach to cartilage repair attempts to overcome these difficulties by delivering ECM producing cells entrapped in a space-filling matrix.

Tissue Engineering. Tissue engineering is an interdisciplinary science that combines basic principles of biology, chemistry, physics, and engineering to construct living tissues from their cellular components. A major goal of tissue engineering is the medical application of fabricated tissues for the augmentation or replacement of congenitally defective, impaired, injured, or otherwise damaged human tissue[22]. There has been significant tissue engineering research covering a wide variety of tissues, including: bladder, aorta, skin, breast, muscle, bone, cartilage,

and tendon.[23-29] Regardless of the tissue of interest, the tissue engineering approach always combines three key elements: cells to produce the new tissue, a biocompatible/bioabsorbable scaffold to support and localize the cells, and bioactive molecules to direct tissue development.

Cells for cartilage repair and tissue engineering. Cell-based therapy is a promising approach to cartilage regeneration. Different cell types offer different potential advantages and challenges. There has been research looking at the tissue engineering potential of primary chondrocytes, chondrocytic cell lines, adult mesenchymal stem cells, and embryonic stem cells. The most obvious source for cells that can regenerate cartilage is the cartilage itself. Chondrocytes, the cells which reside within and maintain and remodel cartilage, are readily harvested, but are limited in number, and expansion in standard monolayer culture tends to lead to de-differentiation, with loss of the chondrocyte phenotype. Additionally, donor site morbidity can be a significant issue when harvesting adult chondrocytes.

Clonal chondrocyte-like cell lines derived from chondrosarcomas or immortalization of primary cells with SV40 large T antigen provide an essentially limitless supply of cells with no associated harvesting morbidity, but recent microarray gene expression profiling indicates that while several popular lines (HCS-2/8, SW1353, and C-20/A4) do express cartilage markers, they differ significantly from primary cells.[30-32] Embryonic stem cells have been studied less in this

application, but are widely believed to have significant potential. As with all applications with embryonic stem cells, technical expertise, availability, and ethical issues all provide obstacles.

Scaffolds for cartilage tissue engineering. The function of a tissue engineering scaffold is to provide a temporary structure while cells seeded within this biodegradable matrix synthesize new, natural tissue. New tissue regeneration occurs during scaffold degradation, with the new tissue taking on the shape and size of the original scaffold. Design criteria include controlled biodegradability, suitable mechanical strength and surface chemistry, ability to be processed in different shapes and sizes, and the ability to regulate cellular activities, such as proliferation and differentiation.[33] Both natural and synthetic polymers have been fabricated as scaffolds for cells in a variety of forms, including fibrous structures, porous sponges, woven or non-woven meshes, and hydrogels.

Hydrogels are cross-linked polymer networks that have the ability to absorb large amounts of water, making these materials attractive scaffolds for engineering tissues with high water content, such as cartilage. The unique ability of hydrogel scaffolds to encapsulate cells rather than promote attachment keeps cells in a spherical morphology conducive to maintenance of chondrocyte phenotype. In principle, a cell–polymer suspension could be injected into a cartilage defect just prior to gelation in situ. This would eliminate a separate cell-seeding step post-

scaffold fabrication, and potentially minimize the need for invasive surgical implantation. However, the technical challenge of maintaining precise polymer/cell localization in situ has proven problematic. Alternatively, the cell/polymer suspension can be injected into molds of anatomic shapes and then cross-linked to form an implantable hydrogel.

Signaling molecules in cartilage regeneration. Signaling molecules, including growth factors, cytokines, and non-protein chemical compounds, are commonly used to promote tissue growth in cartilage tissue engineering. It is bioactive signaling molecules that bind to cell surface receptors, activating intracellular pathways that instruct cells to proliferate, differentiate, and synthesize extracellular matrix proteins during tissue regeneration.

Growth factors shown to have regulatory effects on chondrocytes or stem cells for cartilage tissue engineering include members of the TGF-β superfamily, IGFs, fibroblast growth factors (FGFs), platelet-derived growth factors (PDGFs), and the epidermal growth factor (EGF) family. Among these growth factors, TGF-βs are the most potent inducers of both chondrogenesis in MSCs, and enhancement of cartilage ECM synthesis by fully differentiated chondrocytes.[34,35-44]

A successful tissue engineering approach to cartilage repair will require attention to all three of the major elements of tissue engineering: cell source, scaffold design, and delivery of bioactive molecules.

Menière's Syndrome

Menière's syndrome is a disorder of the inner ear which causes episodes of vertigo, tinnitus (ringing in the ear), a feeling of fullness or pressure in the ear, and fluctuating, progressive sensorineural hearing loss. A typical attack of Menière's syndrome is preceded by fullness in one ear. Hearing fluctuation or changes in tinnitus may also precede an attack. A Menière's episode generally involves severe vertigo (spinning), imbalance, nausea and vomiting. The average attack lasts two to four hours. Following a severe attack, most people find that they are exhausted and must sleep for several hours. There is a large amount of variability in the duration of symptoms. Some people experience brief episodes of unsteadiness, and others have constant unsteadiness. Menière's episodes may occur in clusters; that is, several attacks may occur within a short period of time. However, years may pass between episodes. Between the acute attacks, most people are free of symptoms or note mild imbalance and tinnitus.

Menière's syndrome affects roughly 0.2% of the population. It usually starts confined to one ear, but it often extends to involve both ears over time so that after 30 years, more than 50% of patients with Menière's syndrome have bilateral disease.[45]

In almost all cases, a progressive sensorineural hearing loss occurs in the affected ears. This tends to follow a typical course, with low-frequency sensorineural loss

initially, progressing to the classic peaked audiogram seen with low and high frequency loss, and finally a flat audiogram, as hearing is lost across all frequencies.[46]

The exact cause of an acute attack is unknown, but most researchers believe it results from fluctuating pressure of the fluid within the inner ear.[47] Within the inner ear there is a system of membranes, called the membranous labyrinth which contains a fluid called endolymph. The histophathologic hallmark of Menière's syndrome is ballooning of Reisner's membrane within the membranous labyrinth from excess fluid pressure within the endolymph. This process is called endolymphatic hydrops.

It is not currently known why people with Menière's syndrome develop endolymphatic hydrops, but it is presumed to be either from blockage of the endolymph drainage system, the endolymphatic duct and sac, or by excess endolymph production by the stria vascularis. The animal model used for studying Menière's syndrome is endolymph obstruction in the albino guinea pig, created by surgical destruction of the endolymphatic duct and sac, leading to an inability of the inner ear to drain endolymph. These animals do show a progressive sensorineural hearing loss, but it is unknown if they experience tinnitus or vertigo. As with most animal models some controversy exists as to how well the symptoms and pathogenesis of the target disease are replicated.[48]

There is currently no curative medical treatment for Menière's syndrome. The mainstay of treatment involves medications to palliate the symptoms vertigo.

Establishment of treatments to alter the course of the disease will require a better understanding of the pathogenesis.

References

1. Mow VC, Proctor CS, Kelly MA. Biomechanics of articular cartilage. In: Nordin M, Frankel VH, editors. Basic biomechanics of the musculoskeletal system. Philadelphia7 Lea & Febiger;
1989. p. 31– 57.

2. Maroudas A, Bayliss MT, Venn MF. Further studies on the composition of human femoral head cartilage. *Ann Rheum Dis.* 1980;39:514-23.

3. Swann DA, Sotman S, Dixon M, Brooks C. The isolation and partial characterization of the major glycoprotein (LGP-1) from the articular lubricating fraction from bovine synovial fluid. *Biochem J.* 1977;161:473-85.

4. Poole AR. Cartilage in health and disease. In: Koopman WJ, editor. *Arthritis and allied conditions. A textbook of rheumatology.* 14th ed. Volume 1. Philadelphia:
Lippincott Williams and Wilkins; 2001. p 226-84.

5. Kempson GE, Muir H, Pollard C, Tuke M. The tensile properties of the cartilage of human femoral condyles related to the content of collagen and glycosaminoglycans. *Biochem Biophys Acta.* 1973;297:456-72.

6. Mitrovic D, Quintero M, Stankovic A, Ryckewaert A. Cell density of adult human femoral condylar articular cartilage. Joints with normal and fibrillated surfaces. *Lab Invest.* 1983;49:309-16.

7. Mitrovic D, Quintero M, Stankovic A, Ryckewaert A. Cell density of adult human femoral condylar articular cartilage. Joints with normal and fibrillated surfaces. *Lab Invest.* 1983;49:309-16.

8. Wong M, Wuethrich P, Eggli P, Hunziker E. Zone-specific cell biosynthetic activity in mature bovine articular cartilage: a new method using confocal microscopic stereology and quantitative autoradiography. J Orthop Res 1996;14(3):424– 32.

9. Schumacher BL, Hughes CE, Kuettner KE, Caterson B, Aydelotte MB. Immunodetection and partial cDNA sequence of the proteoglycan, superficial zone protein, synthesized by cells lining synovial joints. J Orthop Res 1999;17(1):110–20.

10. Schumacher BL, Block JA, Schmid TM, Aydelotte MB, Kuettner KE. A novel proteoglycan synthesized and secreted by chondrocytes of the superficial zone of articular cartilage. Arch 10. Biochem Biophys 1994;311(1):144–52.

11. Mankin HJ, Mow VC, Buckwalter JA, Iannotti JP, Ratcliffe A. Articular cartilage structure, composition, and function. In: Buckwalter JA, Einhorn TA, Simon SR, editors. Orthopedic basic science: biology and biomechanics of the musculoskeletal system. Rosemont (IL)7 American Academy of Orthopaedic Surgeons; 1999. p. 444– 70.

12. Ateshian GA, Wang H. Rolling resistance of articular cartilage due to interstitial fluid flow. Proc Inst Mech Eng [H] 1997;211(5):419– 24.

13. CDC. Prevalence of disabilities and associated health conditions among adults in the United States, 1999. MMWR 2001;50:120-125

14. Felson DT. Epidemiology of hip and knee osteoarthritis. Epidemiol Rev 988;10:1– 28.

15. Peyron, Jo Epidemiological aspects of osteoarthrits. Scand J Rheumatol Suppl 1988. 77: p. 29-33.

16. Peyron, Jo Clinicalfeatures of osteoarthrits, difuse idiopathic skeletal hyperostosis, and hypermobilty syndromes. Curr Opin Rheumatol, 1991. 3(4): p. 653-61.

17. Bland, J.H. and S.M. Cooper Osteoarthrits: a review of the cell biology involved and evidence for reversibilty. Management rationally related to known genesis and pathophysiology. Semin Arthritis Rheum, 1984. 14(2): p. 106-33.

18. Felson DT, Lawrence RC, Dieppe PA, et al. Osteoarthritis: new insights. Part 1: the disease and its risk factors. Ann Intern Med 2000;133(8):635– 46.

19. Buckwalter JA. Articular cartilage: injuries and potential for healing. J Orthop Sports Phys Ther 1998;28:192-202.

20. Hunziker EB. Growth-factor-induced healing of partial thickness defects in adult articular cartilage. Osteoarthritis Cartilage 2001;9:22-32.

21. Hunziker EB, Rosenberg LC. Repair of partial thickness defects in articular cartilage: cell recruitment from the synovial membrane. J Bone Joint Surg Am 1996;78:721-33.

22. Woolverton CJ, Fulton JA, Lopina ST, Landis WJ. Mimicking the natural tissue environment. In: Lewandrowski K-U, Wise DL, Trantolo DJ, Gresser JD, Yaszemski MJ, Altobelli DE, editors. Tissue engineering and biodegradable equivalents: scientific and clinical applications. New York7 Marcel Dekker; 2002. p. 43– 75.

23. Pariente JL, Kim BS, Atala A. In vitro biocompatibility assessment of naturally derived and synthetic biomaterials using normal human urothelial cells. J Biomed Mater Res 2001;55:33–9.

24. Shum-Tim D, Stock U, Hrkach J, Shinoka T, Lien J, Moses M, et al. Tissue engineering of autologous aorta using a new biodegradable polymer. Ann Thorac Surg 1999;68:2298–305.

25. Vaccariello MA, Javaherian A, Parenteau N, Garlick JA. Use of skin equivalent technology in a wound healing model. In: Morgan JR, Yarmush ML, editors. Methods in molecular medicine: tissue engineering methods and protocols, Vol. Totowa, New Jersey Humana Press; 1999. p. 391– 405.

26. Cao YL, Lach E, Kim TH, Rodriguez A, Arevalo CA, Vacanti CA. Tissue-engineered nipple reconstruction. Plast Reconstr Surg 1998;102:2293– 8.

27. Vandenburgh H, Shansky J, Del Tatto M, Chromiak J. Organogenesis of skeletal muscle in tissue culture. In: Morgan JR, Yarmush ML, editors. Methods in molecular medicine: tissue engineering methods and protocols, Vol. 18. Totowa, New Jersey Humana Press; 1999. p. 217–25.

28. Tubo R, Binette F. Culture and identification of autologous human articular chondrocytes for implantation. In: Morgan JR, Yarmush ML, editors. Methods in molecular medicine: tissue engineering methods and protocols, Vol. 18. Totowa, New Jersey7 Humana Press; 1999. p. 205– 15.

29. Isogai N, Landis WJ, Kim TH, Gerstenfeld LC, Upton J, Vacanti JP. Formation of phalanges and small joints by tissue engineering. J Bone Joint Surg 1999;81A:306–16.

30. Finger F, Schorle C, Soder S, et al. Phenotypic characterization of human chondrocyte cell line C-20/A4: a comparison between monolayer and alginate suspension culture. Cells Tissues Organs 2004; 178:65–77.

31. Gebauer M, Saas J, Sohler F, et al. Comparison of the chondrosarcoma cell line SW1353 with primary human adult articular chondrocytes with regard to their gene expression profile and reactivity to IL-1beta. Osteoarthritis Cartilage 2005; 13:697–708.

32. Saas J, Lindauer K, Bau B, et al. Molecular phenotyping of HCS-2/8 cells as an in vitro model of human chondrocytes. Osteoarthritis Cartilage 2004;12:924–934.

33. Kuo CK, Tuan RS. Tissue engineering with mesenchymal stem cells. *Ieee Engineering In Medicine And Biology Magazine* 2003; 22:51–56.

34. Li WJ, Tuli R, Okafor C, et al. A three-dimensional nanofibrous scaffold for cartilage tissue engineering using human mesenchymal stem cells. Biomaterials 2005; 26:599–609.

35 Stevens MM, Marini RP, Martin I, et al. FGF-2 enhances TGF-beta1-induced periosteal chondrogenesis. J Orthop Res 2004; 22:1114–1119.

36 Lee JE, Kim KE, Kwon IC, et al. Effects of the controlled-released TGF-beta 1 from chitosan microspheres on chondrocytes cultured in a collagen/chitosan/ glycosaminoglycan scaffold. Biomaterials 2004; 25:4163–4173.

37. Barbero A, Grogan S, Schafer D, et al. Age related changes in human articular chondrocyte yield, proliferation and post-expansion chondrogenic capacity. Osteoarthritis Cartilage 2004; 12:476–484.

38 Tay AG, Farhadi J, Suetterlin R, et al. Cell yield, proliferation, and postexpansion differentiation capacity of human ear, nasal, and rib chondrocytes. Tissue Eng 2004; 10:762–770.

39 Hegewald AA, Ringe J, Bartel J, et al. Hyaluronic acid and autologous synovial fluid induce chondrogenic differentiation of equine mesenchymal stem cells: a preliminary study. Tissue Cell 2004; 36:431–438.

40 Glowacki J, Yates K, Maclean R, Mizuno S. In vitro engineering of cartilage: effects of serum substitutes, TGF-beta, and IL-1alpha. Orthod Craniofac Res 2005; 8:200–208.

41. Vunjak-Novakovic G, Meinel L, Altman G, Kaplan D. Bioreactor cultivation of osteochondral grafts. Orthod Craniofac Res 2005; 8:209–218.

42. Chua KH, Aminuddin BS, Fuzina NH, Ruszymah BH. Interaction between insulin-like growth factor-1 with other growth factors in serum depleted culture medium for human cartilage engineering. Med J Malaysia 2004; 59 (Suppl B):7–8.

43. Indrawattana N, Chen G, Tadokoro M, et al. Growth factor combination for chondrogenic induction from human mesenchymal stem cell. Biochem Biophys Res Commun 2004; 320:914–919.

44. Wang Y, Kim UJ, Blasioli DJ, et al. In vitro cartilage tissue engineering with 3D porous aqueous-derived silk scaffolds and mesenchymal stem cells. Biomaterials

2005; 26:7082–7094.

45. Stahle J, Friberg U, Svedberg A. Long-term progression of Meniere's disease. *Acta Otolaryngol (Stockh) 1991*:Suppl 485:75-83

46. Kinney SE, Sandridge SA, Newman CW. Long-term effects of Meniere's disease on hearing and quality of life. *Am J Otol* 1997 Jan;18(1):67-73.HAVIA M,

47. Kentala E. Progression of symptoms of dizziness in Meniere's disease. *Arch Otolaryngol Head Neck Surg* 2004;130:431-5.

48. Kimura RS, Schuknecht JF. Membranous hydrops in the inner ear of guinea pig after obliteration of the endolymphatic sac. *Pract Otorhinolaryngol* 1965;27:343-5.

CHAPTER I

FABRICATION OF TISSUE ENGINEERED CARTILAGE UTILIZING HUMAN NASAL SEPTAL CHONDROCYTES AND INJECTION MOLDING

Abstract

Objectives/Hypothesis. The goal of the current study was to evaluate the chondrogenic potential of first passage human nasal septal chondrocytes grown in injection molded calcium alginate constructs cultured *in vivo* in athymic mice.

Method. Molds of an implantable silicon nasal bridge were cast using a commercial silastic ERTV mold making kit. Human nasal septal chondrocytes were liberated by collagenase digestion, suspended in 2% alginate mixed with $CaSO_4$ (0.2 g/ml) and injected into prepared molds. Un-molded constructs were implanted subcutaneously in the dorsum of athymic mice, and recovered for biochemical, histological, and biomechanical analysis at 2, 4, 6, 12, and 23 weeks.

Results. Recovered constructs demonstrated reasonably good shape fidelity and progressively increasing extracellular matrix deposition, as determined by hydroxyproline and glycosaminoglycan content. Consistent with progressively developing extracellular matrix, equilibrium compressive modulus also continually increased. Safranin-O staining showed progressively increasing proteoglycan production. Consistent with a cartilage phenotype, almost all the collagen produced was type II collagen, as determined by collagen ELISA.

Conclusions. Preliminary data suggest that first passage human nasal septal chondrocytes exhibit good chondrogenic potential in calcium alginate constructs cultured in an *in vivo* system. Because we used first passage cells it was possible to make constructs for implantation that were 80 times more massive than the original septal biopsy from which the cells were harvested: a necessary feature for clinical applications. These results indicate that human nasal septal chondrocytes have potential utility as a cell source for the engineering of cartilage replacements.

Introduction

Annually there are over one million surgeries in the United States that involve the replacement of either bone or cartilage[1]. Craniofacial deformities pose a special set of difficulties for the reconstructive surgeon. Whatever the cause of the defect, be it congenital anomaly or trauma the standard approach to repair is the same. Current clinical practice is to effect a repair using either autologous bone and cartilage or any of a variety of synthetic materials[2-4]. Common donor sites for autologous bone to be used in a reconstruction include calvarial, iliac, and costal areas[5-6]. Cartilage is commonly harvested from auricular, costal, and septal sites[7-9].

Autologous grafting with bone or cartilage is still the standard of care, and is the most common approach[10]. There are, though, a number of inherent difficulties. For any reasonable size defect obtaining sufficient donor site material is associated with an often unacceptable level of morbidity[11-13]. This often makes it necessary to have multiple donor sites used for harvest and can require multiple operations. It also adds the technical difficulty of needing to combine several different tissue harvests into a single unit for reconstruction. Synthetic materials avoid the problems of donor site morbidity and tissue availability, but come with their own set of problems. Synthetic materials can feel unnatural under the skin, and are somewhat more prone to protrusion through the skin and an increased risk for infection[15-16].

Given the current limitations in available clinical options for the treatment of structural craniofacial lesions, the ability to replace damaged or missing tissue with an engineered replacement tissue has the potential to be a valuable new treatment modality. The tissue engineering approach is to combine a space filling matrix with cells and growth factors in a manner that will encourage new tissue growth. Ideally, the initially seeded matrix will be reabsorbed at the same rate that new tissue is formed, so that ultimately the patient will be left with a tissue replacement in the exact shape of the original matrix, but indistinguishable from native tissue. This approach has the potential to combine the best aspects of autologous grafting and synthetic prosthesis. There is no donor site morbidity, material is abundant, and with the reabsorption of the original matrix there should not be the increased risk of protrusion or infection seen with synthetic materials.

Alginate, a linear co-polymer hydrogel of mannuronic acid and guluronic acid, has been known for many years to have value for the three dimensional culture of chondrocytes. Chondrocytes grown in standard monolayer culture tend to dedifferentiate into a fibroblastic phenotype. Chondrocytes grown in three dimensional alginate culture have been shown to maintain their chondrocyte phenotype, and continue to produce proteoglycans[17-20]. There are several properties of alginate that make it appealing as a tissue engineering matrix in addition to its known value for chondrocyte culture. It has already been established to be biocompatible[21], and because of its ability to crosslink and gel in the presence of divalent cations can

be precisely shaped in complex geometries. This has been previously demonstrated with acellular constructs[22] and using freshly harvested bovine articular chondroctyes[23].

An essential component of tissue engineering is the combining of cells with a biocompatible matrix. The ideal cell source for tissue engineering of cartilage is still unknown. Possible cell sources that have been considered include articular chondrocytes, auricular chondrocytes, nasal septal chondrocytes, perichondrial cells, and mesenchymal stem cells. Nasal septal chondrocytes are intriguing as a cell source for several reasons. They are already primary chondrocytes, so there is no need to orchestrate a precise differentiation, and they can be harvested with a minimum of donor site morbidity.

The goal of the current study was to evaluate the chondrogenic potential of human nasal septal chondrocytes when used in injection molded calcium alginate constructs grown *in vivo* on the dorsum of athymic mice.

Methods And Materials

Chondrocyte Isolation. Chondrocytes were isolated from human nasal septa obtained from septoplasty patients at Englewood hospital, Englewood, NJ. A total of 30 septa were used. Donor age ranged between 16-62 years and had a mean age of 32 ± 6 years. Twenty-one septa were from women and nine from men. Upon surgical excision all septa were stored immediately in sterile 50 ml conical tubes (BD Biosciences, Bedford, MA) containing 30 mls of sterile Hamm's F-12 culture media (Gibco, Grand Isand, NY) with 100 μg/ml antibiotic/antimycotic (10,000 U/ml penicillin G sodium, 10,000 μg/ml streptomycin sulfate, and 25 μg/ml amphotericin B, Gibco, Grand Island NY). Excised nasal septa were then shipped by overnight mail to the University of Massachusetts Medical School, where all future work was done. Immediately upon arrival at the University of Massachusetts individual septa were washed thoroughly two times in phosphate buffered saline (PBS, Sigma-Aldrich, Irvine, CA) supplemented with antibiotic/antimycotic. Washed septa were then cut into approximately 0.5 cm^2 slices and again washed thoroughly two times in PBS with antibiotic/antimycotic. Cartilage slices were then digested enzymatically in 0.3 % collagenase (Worthington Biochemical Corp, Freehold, N.J.) for approximately 10 hours. The resultant digest was filtered through a sterile 100 μm cell strainer (BD Biosciences, Bedford, MA,) in order to separate the liberated chondrocytes from any remaining undigested cartilage. Recovered cells were washed thoroughly 2 times in sterile PBS supplemented with antibiotic/antimycotic, pelleted by centrifugation at

7000 rpm and resuspended in sterile Hamm's F-12 culture media. Resuspended cells were counted on a hemocytometer, and cell viability was determined by the trypan blue dye exclusion assay (Sigma-Aldrich, Irvine, CA). Individual septa yielded between three hundred thousand and 2 million cells. Only tissue digests that demonstrated better then 90% cell viability were used in the study.

Chondrocyte Culture. Isolated chondrocytes were cultured in standard monolayer culture in T-225 culture flasks (BD Biosciences, Bedford, MA), at an initial plating density of approximately 1,500 cells per cm^2. Culture medium was comprised of Hamm's F-12 culture media with 10% heat inactivated fetal bovine serum (FBS, Gibco, Grand Island, NY), 50 µg/ml ascorbate (Sigma-Aldrich, Irvine, CA, USA), and 1% antibiotic/antimycotic (10,000 U/ml penicillin G sodium, 10,000 µg/ml streptomycin sulfate, and 25 µg/ml amphotericin B) (Gibco, Grand Island NY, USA). Culture medium was changed every second day and the cells were grown until near confluence. Nearly confluent cultures were trypsinized (0.05% trypsin-EDTA, Gibco, Grand Island, NY), the cells collected and washed twice in PBS with antibiotic/antimycotic, resuspended in Hamm's F-12 for counting, and replated, again in T-225 culture flasks at 1,500 cells per cm^2.

Mold Fabrication. Negative molds for injection were made using a commercially available Silastic ERTV mold-making kit (Dow Corning, Midland, MI). The silastic and catalyst were mixed 10:1 as per the manufacturer's instructions

and poured into the bottom of a beaker to a height of approximately 1 cm. A non-implantable model of an implantable silicon nasal bridge (Implantech, Ventura, CA) was used as a positive structure for the casting of a negative mold. The silicon nasal bridge was coated with petroleum jelly to facilitate its release and embedded in the catalyzed silastic until halfway submerged. After 24 hours at room temperature the solidified silastic and embedded nasal bridge were coated with a thin layer of petroleum jelly all across their top surface except for a small area near one edge. A second layer of catalyzed silastic was poured on top and allowed to set at room temperature. After 24 hours the silicon nasal bridge was removed and the fully cast mold was cleaned and autoclave sterilized.

Alginate Construct Fabrication. Methods for generating chondrocyte-seeded alginate constructs were based on previous studies documenting generation of cartilage by injection molding (Figure 1). Passage 1 human nasal chondrocytes were suspended in filter sterilized 2% low viscosity alginate (FMC Biopolymer, Drammen, Norway) in PBS at a seeding density of 50 x 10^6 cells/ml. Immediately prior to injection into the mold the alginate/chondrocyte suspension was combined with a solution of autoclave sterilized $CaSO_4$ in PBS (0.25g/ml) by thorough mixing through a sterile stopcock (David Scott, MA). The $CaSO_4$ solution was combined with the alginate/chondrocyte mixture at a ratio of 0.04 mls of $CaSO_4$ per milliliter of alginate. The alginate/chondrocyte/$CaSO_4$ mixture was then injected into the mold using a 3 ml syringe with an 18.5 gauge needle. After 45 minutes a fully gelled construct was

un-molded. Molded constructs were implanted subcutaneously in the dorsum of athymic mice and harvested at 2, 4, 6, 12, and 23 weeks. Harvested constructs were frozen at -20º C in preparation for histological, biochemical, and biomechanical testing.

All animals were treated in accordance with the NIH Guide for the Care and Use of Laboratory Animals, and the protocol was approved by the Animal Care Committee at the University of Massachusetts Medical School and with the approval of the institutional review boards of UMass Medical School and Englewood Hospital.

Histological Analysis. Specimens for histology were fixed in 10% phosphate buffered formalin for at least 24 hours and then embedded in paraffin. Paraffin embedded engineered tissues were sectioned by microtome and placed on glass microscope slides. Sections on slides were de-paraffinized and GAG content visualized by staining with Safranin-O.

Biochemical and Molecular Analysis. Chondrogenic potential of the human nasal chondrocytes was assessed by several biochemical measures. Cell number was determined by DNA quantification. Extracellular matrix accumulation was assessed by quantification of glycosaminoglycans as a marker for proteoglycans, hydroxyproline as a marker for total collagen, and a collagen ELISA to determine

collagen type and quantity. All biochemical assays were well established techniques that have been described elsewhere in detail.

DNA Qunatification. Samples for biochemical analysis were digested overnight at 60º C in 1 ml of papain digest buffer (0.5 mls papain (Sigma-Aldrich, Irvine, CA, USA), 176 mg L-Cysteine (Sigma-Aldrich, Irvine, CA, USA), and 100 mls PBS with EDTA). DNA was quantified by the PicoGreen DNA assay (Molecular Probes, CA) according to the manufacturers instructions. Briefly, 5 µl of the papain digest was added to 195 µl of the PicoGreen dye solution in a 96-well plate and the contents excited at 485 nm and fluorescence read at 535 nm on an HTS 7000+ spectrophotometer (Perkin-Elmer, Wellesley, MA). DNA content was then determined by linear interpolation with calf thymus DNA standards. All samples and standards were measured in duplicate.

GAG Quantification. Sulfated GAG content was measured using 1,9-dimethylmethylene blue dye (DMB) at pH 1.5. This pH assures a sufficiently acidic environment that the dye binds to the sulfate groups on glycosaminoglycans, but not to the carboxyl groups on alginate[24]. Aliquots of 50 µls of papain digest were combined with 950 µls of DMB and optical density was measured at an absorbance of 525 nm. GAG content was quantified by quadratic interpolation using chondroitin-6-sulfate from shark cartilage (Sigma-Aldrich, USA) as a standard. All samples and standards were measured in duplicate.

Hydroxyproline Quantification. Hydroxyproline content was measured by acid hydrolysis of samples of papain digests, as described in detail elswhere[25-26]. Briefly, equal volume aliquots of 6N HCL and papain digest were combined and incubated overnight at 115°C. Chloramine T hydrate (Sigma-Aldrich, USA) and *p*-dimethylamino-benzaldehyde (Ehrlich's reagent) (Sigma-Aldrich, USA) were added to the hydroxylated samples and absorbance was measured at 560 nm on an HTS 7000+ spectrophotometer (PE Wellesley, MA). Hydroxyproline content was determined by linear interpolation using chondroitin 6-sulfate from shark cartilage (Sigma-Aldrich) as a standard. All samples and standards were analyzed in duplicate.

Collagen Type II ELISA. Collagen type was assessed by ELISA using the Native Type II Collagen Detection Kit #6009 (Chondrex Inc, Redmond, WA), according to the manufacturer's instructions. First, the collagen molecules were extracted from the engineered samples using methods supplied with the ELISA Kit. Briefly, samples were lyophilized, and then incubated overnight at 4°C in 3M guanidine/0.05M Tris-HCl buffer at pH 7.5 to extract the proteoglycans. The tissue was then homogenized and the collagen digested into soluble monomers by successive treatment with pepsin and pancreatic elastase. The supplied 96 well ELISA plate was incubated overnight with the capture antibody, washed, and loaded with the solubulized collagen from the tissue samples and a supplied collagen

standard. After a two hour incubation the plate was washed and incubated with the supplied biotinylated detection antibody for another two hours, washed again, then incubated with streptavidin peroxidase, washed and incubated with the OPD chromagen in a H_2O_2 buffer. The reaction was stopped with 2.5 N sulfuric acid and the plate was read on an HTS 7000+ spectrophotometer at 490 nm. Type II collagen was quantified by linear interpolation with the supplied collagen standard.

Total collagen from biochemical assessment of hydroxyproline content was compared to the ELISA values to estimate the percent of total collagen that was the desired type II. This estimate is based on prior reports that show hydroxyproline to make up a consistent percentage of collagen from a wide variety of tissues. In many studies this percentage has consistently ranged from 12.3%-14.4%[26-29]

Biomechanical Analysis. Samples of engineered cartilage for mechanical testing were cut into regular right cylindrical discs 1 mm in height and 6 mm in diameter using a razor blade and a 6 mm diameter dermal biopsy punch. Discs of engineered cartilage were placed in a 6 mm diameter well in an electrically insulated confining chamber mounted to a servo-controlled Dynastat mechanical spectrometer (IMASS, Hingham, MA) interfaced with a computer. Samples in the confining chamber were equilibrated in PBS at pH 7.4 (Gibco, Grand Island, NY) and compressed between a porous polyethylene platen and the base of the confining chamber. Each sample was compressed in ten sequential steps of 3% static strain to a

maximum 30% strain. After each strain step the signal detected by the load cell was recorded every 0.5 seconds for 100 seconds. Recorded stress relaxation data was fit to a poroelastic model of material behavior to determine the engineered tissue's equilibrium modulus.[30-31].

.

Statistical Analysis. The statistical changes over time in GAG content, hydroxyproline content, DNA content, equilibrium modulus, and hydraulic permeability were assessed by computing the Pearson product moment correlation coefficient. This value was compared to a critical value for the number of samples used in order to determine the statistical significance of any observed changes (*p* value).

Results

Shape Duplication. The injection molding process allowed for the reasonably easy and fast duplication of a desired geometry with reasonably good fidelity immediately upon un-molding. Chondrocyte/alginate implants continued to show reasonably good shape fidelity through 23 weeks of in-vivo culture (Figure 2). There was some early loss in overall volume, presumably due to an initial re-absorption of the thin peripheral portions of the alginate construct.

Histology. On staining with Safranin O after two weeks of in vivo culture engineered tissue showed significant alginate matrix containing a large number of cells with the characteristic, rounded chondrocyte morphology. Staining of GAGs at two weeks was extremely faint, indicating very little extracellular matrix production. After four weeks of in vivo culture staining with Safranin-O still shows abundant alginate and rounded cells, but also shows small, densely staining islands rich in proteoglycans. After 6 weeks of *in vivo* culture staining with Safranin-O showed large densely staining proteoglycan rich areas surrounded by now much smaller areas of alginate. By 12 weeks of in vivo culture all of the alginate appears to have been reabsorbed and the islands of developing matrix have coalesced into solid, normal appearing cartilage, with uniform and significant extracellular matrix (Figure 3). Tissue samples for 23 week histology were inadvertently damaged by improper processing, so are not presented here.

Biochemistry. Biochemical evaluation of the engineered tissue demonstrated that GAG, hydroxyproline, and equilibrium modulus all increased significantly with time ($p < 0.01$). At 23 weeks GAG, hydroxyproline, and equilibrium modulus were respectively 68%, 54%, and 44% of average native septal values. DNA did not change appreciably over time from what was initially seeded ($p > 0.05$), consistent with the observation that proliferation is inhibited at high cell seeding densities (Figures 4-7).

Quantification of collagen type II by ELISA showed that the developing tissue was synthesizing almost exclusively type II collagen, consistent with the cartilage phenotype. The lack of type I collagen demonstrates consistency with the cartilage phenotype and the lack of scar tissue formation. The amount of collagen identified by ELISA was consistent with the indirect quantification by hydroxyproline assessment, and ranged from 82%-96% of the total collagen depending on the correction factor used (Figure 8).

Discussion

The goal of the current study was to assess the chondrogenic potential of first passage human nasal chondrocytes grown in geometrically complex calcium alginate constructs cultured *in vivo* in athymic mice. After subcutaneous implantation the implants developed a gross morphology over time that began to resemble native cartilage. The chondrocytes remained metabolically active, producing new extracellular matrix. Collagen and proteoglycan content, the two major components of the extracellular matrix, increased continuously over time. Consistent with this, the equilibrium compressive modulus increased continuously, as the developing tissue became stiffer.

The nasal bridges that were duplicated are very thin along the edges, and in these areas shape duplication was not as precise as in thicker areas, or as has been demonstrated with larger constructs. For clinical applications, where dimensional tolerances of constructs would have to be quite precise, this is potentially a serious problem. This difficulty with the duplication of small shapes will be addressed in a separate publication by introducing computer aided design and solid free form fabrication into the molding process.

Our preliminary data show that adult human nasal chondrocytes represent a possible cell source for clinical applications of tissue engineered neo-cartilage with several very attractive features. Using injection molding technology and calcium-

alginate, adult human nasal septal chondrocytes expanded through 1 passage enable the production of engineered constructs as large as 8 grams from an initial septal biopsy as small as 100 milligrams. The biochemical data on matrix deposition presented here show similar initial results to an earlier study by Rotter et al[32] using human nasal septal chondrocytes seeded onto PGA/PLA discs, cultured briefly in vitro, and then in-vivo in athymic mice to twelve weeks. In that study, in contrast to the present one, the matrix deposition peaked quickly and then tended to level off or decline by 4 weeks. The continual deposition of matrix seen in the current study may indicate a stronger chondrogenic potential for nasal septal chondrocytes when grown in alginate compared to PGA/PLA. The high variability in DNA content may represent technical imprecision, but also may represent a differing tendency for proliferation or matrix deposition depending on the age of the donor cartilage. This possibility will be examined in future studies.

There are several outstanding questions from the current study that could prove important. With this system matrix deposition was seen to continue for the entire length of the study, close to six months. At this time it remains unclear how long tissue development would continue with this system, or if the current technologies would produce similar results in an *in vitro* culture system. Future work will look to improve the quality of shape duplication by the application of computer aided design and solid free form fabrication in the mold making process, and possible

modifications of alginate to allow it to serve as a growth factor deliver system. These ideas will be explained in detail in the following chapters.

References

1. Langer R, Vacanti JP. Tissue engineering. *Science* 1993;920:260–266.

2. Nishiyama, T., Nakajima, T., Yoshimura, Y., et al. Utilizing solid models for preoperative shaping of HAP-TCP ceramic bone substitute: Application for craniomaxillofacial surgery. *Eur. J. Plast. Surg.* 1994; 17(4):173-177.

3. Magee Jr., W.P., Ajkay, N., Freda, N., and Rosenblum, R. S. Use of fast-setting hydroxyapatite cement for secondary craniofacial contouring. 2004 *Plast. Reconstr. Surg* .114(2): 289-297

4. Zeng, Y., Wu, W., Yu, H., et al. Silicone implants in augmentation rhinoplasty. *Aesthetic Plast. Surg.*2002; 26(2):85-88.

5. Cutting, BC, McCarthy, JG, and Knize, DM. Repair and grafting of bone. In JG McCarthy (Ed), *Plastic Surgery* Philadelphia: Saunders, 1998. p. 605-13.

6. Tatum, SA, and Kellman, RM. Cranial bone grafting in maxillofacial trauma and reconstruction. *Facial Plast. Surg.*1998; 14(1):117-29

7. Brent, B. Repair and grafting of cartilage and perichondrium. In JG McCarthy

(Ed), *Plastic Surgery*. 1990; p 559-68.

8. Gurley, JM, Pilgram, T, Perlyn, CA, and Marsh, JL. Long-term outcome of autogenous rib graft nasal reconstruction. *Plast. Reconstr. Surg* 2001; 108(7):1895-1905.

9. Mottura, A. A. Chin augmentation with nasal osteocartilaginous graft. *Plast. Reconstr. Surg.* 2002; 109(2):783-787.

10. Lovice DB, Mingrone MD, Toriumi DM. Grafts and implants in rhinoplasty and nasal reconstruction. *Otolaryngol Clin North Am* 1999;32:113–139.

11. Laurie, SW, Kaba, LB, Mulliken, JB, and Murray, JE. Donor site morbidity after harvesting rib and iliac bone. *Plast.Reconstr. Surg.* 1984; 73(6): 933-938.

12. Skouteris, CA, and Sotereanos, GC. Donor site morbidity following harvest of autogenous rib grafts. *J. Oral Maxillofac. Surg.* 1989; 47:808-812.

13. Kline, RM, and Wolfe, SA. Complications associated with the harvesting of cranial bone grafts. *Plast. Reconstr. Surg.* 1995; 95(1):5-13.

14. Matarasso, A, Elias, AC, and Elias, RL. Labial incompetence: A marker for progressive bone resorption in silastic chin augmentation. *Plast. Reconstr. Surg.*

1996; 98(6):1007-1014.

15. Peled, IJ, Wexler, MR, Ticher, S, et al. Mandibular resorption from silicone chin implants in children. *J. Oral Maxillofac. Surg.* 1986; 44(4):346-348.

16. Cohen MS, Constantino PD, Friedman CD. Biology of implants used in head and neck surgery. *Facial Plast Surg Clin North Am* 1999;7:17–41.

17. Beekman B, Verzijl N, Bank RA, von der Mark K, TeKoppe JM. Synthesis of collagen by bovine chondrocytes cultured in alginate: Posttranslational modifications and cell-matrix interaction. *Exp Cell Res* 1997;237(1):135–141.

18. Guo JF, Jourdian GW, MacCallum DK. Culture and growthcharacteristics of chondrocytes encapsulated in alginate beads. *Connect Tissue Res* 1989;19(2–4):277–297.

19. Hauselmann HJ, Fernandes RJ, Mok SS, Schmid TM, Block JA, Aydelotte MB, Kuettner KE, Thonar EJ. Phenotypic stability of bovine articular chondrocytes after long-term culture in alginate beads. *J Cell Sci* 1994;107(1):17–27.

20. Hauselmann HJ, Aydelotte MB, Schumacher BL, Kuettner KE, Gitelis SH, Thonar EJ. Synthesis and turnover of proteoglycans by human and bovine adult

articular chondrocytes culture in alginate beads. *Matrix* 1992;12(2):116–129.

21. Klock G, Pfeffermann A, Ryser C, Grohn P, Kuttler B, Hahn HJ, Zimmerman U. Biocompatibility of mannuronic acid-rich alginates. *Biomaterials* 1997;18:707–713.

22. Huband ML. Intranasal conformers: A case report. *J Dent Technol* 1997;14:12–15.

23. Chang SCN, Rowley JA, Tobias G, Genes NG, Roy AK, Mooney DJ, Vacanti CA, Bonassar LJ. Injection molding of chondrocyte/alginate constructs in the shape of facial implants. *J Biomed Mater Res* 2001; 55(4):503-511

24. Enobakhare, B.O., D.L. Bader, and D.A. Lee, Quantification of sulfated glycosaminoglycans in chondrocyte/alginate cultures, by use of 1,9-dimethylmethylene blue. *Anal Biochem*, 1996. 243(1): p. 189-91.

25. Beekman B, Verzijl N, Bank RA, von der Mark K, TeKoppeJM. Synthesis of collagen by bovine chondrocytes cultured in alginate: Posttranslational modifications and cell-matrix interaction. *Exp Cell Res* 1997;237(1):135–141.

26. Stegemann H, Stadler K. Determination of hydroxyproline. *Clin Chim Acta* 1967;18:267–273.

27. Gallop PM, Paz MA. Posttranslational protein modifications, with special attention to collagen and elastin. *Physiol Rev* 1975;55:418–487

28. Woessner JFJ. Determination of hydroxyproline in connective tissues. In: *The Methodology of Connective Tissue Research,* edited by Hall D. Oxford, UK: Johnson-Bruvvers, 1976, p. 235–245.

29. Wong MY, Harmanli OH, Agar M, Dandolu V, and Grody TM, Collagen content of nonsupport tissue in pelvic organ prolapse and stress urinary incontinence *Am J Obstet Gynecol* 2003;189:1597-600

30. Mow VC, Kuei SC, Lai WM, Armstrong CG. Biphasic creep and stress relaxation of articular cartilage in compression: Theory and experiment. *J Biomech Eng* 1980;102(1):73–84.

31. Quinn TM, Grodzinsky AJ. Longitudinal modulus and hydraulic permeability of poly(methacrylic acid) gels: Effects of charge density and solvent content. *Macromolecules* 1993;26: 4332–4338.

32. Rotter N, Aigner J, Naumann A, Planck H, Hammer C, Burmester G, Sittinger M. Cartilage reconstruction in head and neck surgery: Comparison of resorbable

polymer scaffolds for tissue engineering of human septal cartilage. *J Biomed Mater Res* 1998;42(3)347-356

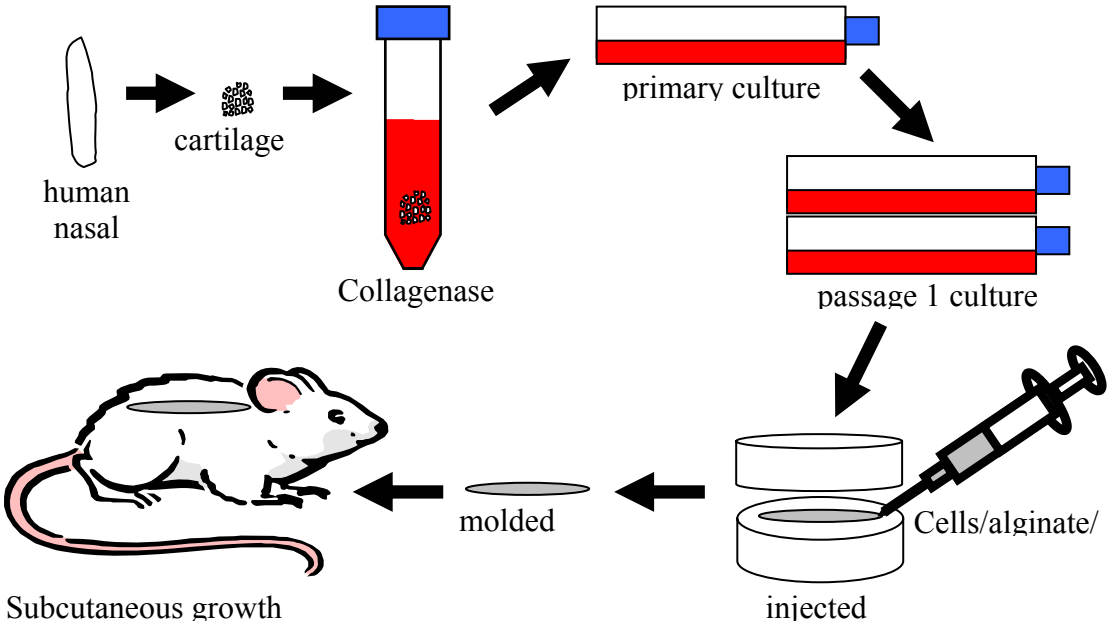
human
nasal
cartilage
Collagenase
primary culture
passage 1 culture
Cells/alginate/
injected
molded
Subcutaneous growth

Figure 1

Schematic of injection molding process. Human nasal septal cartilage was digested in type II collagenase, grown in monolayer culture, passaged, mixed with calcium alginate, injected into a negative mold, unmolded, and implanted subcutaneously into the dorsum of an athymic mouse.

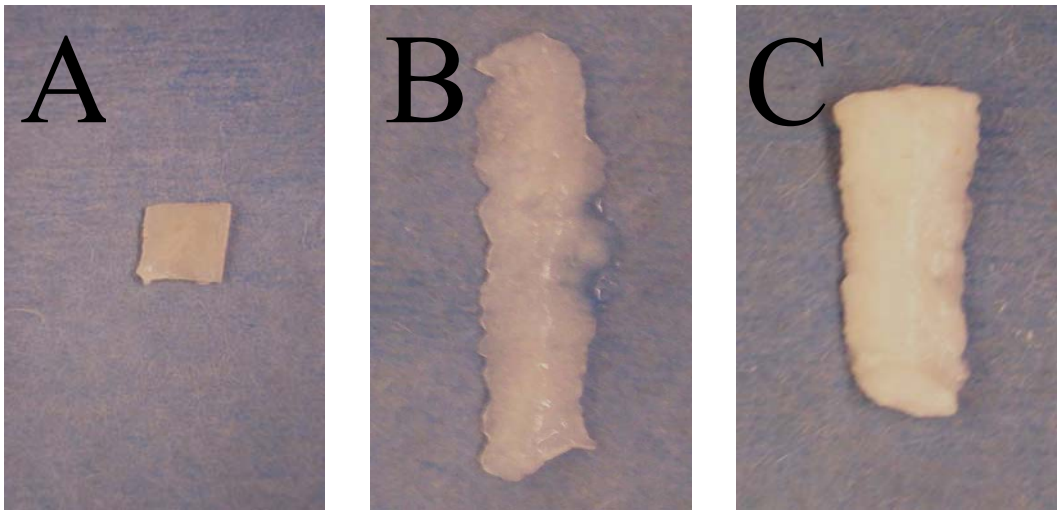
A
B
C

Figure 2

Nasal septal biopsy before digestion (A), formed construct immediately after un-molding (B), and engineered tissue after 12 weeks of in vivo growth (C).

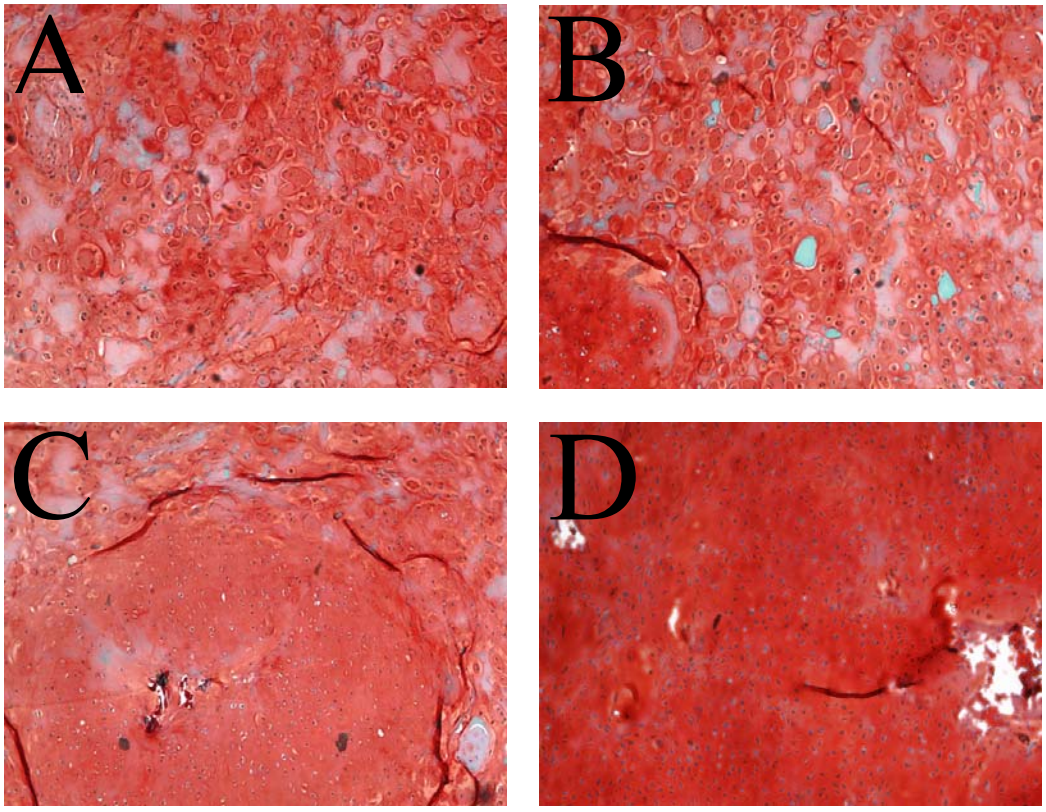
A
B
C
D

Figure 3

Safranin-O staining of engineered constructs at (A) 2 weeks, (B) 4 weeks, (C) 6 weeks, and (D) 12 weeks after subcutaneous implantation.

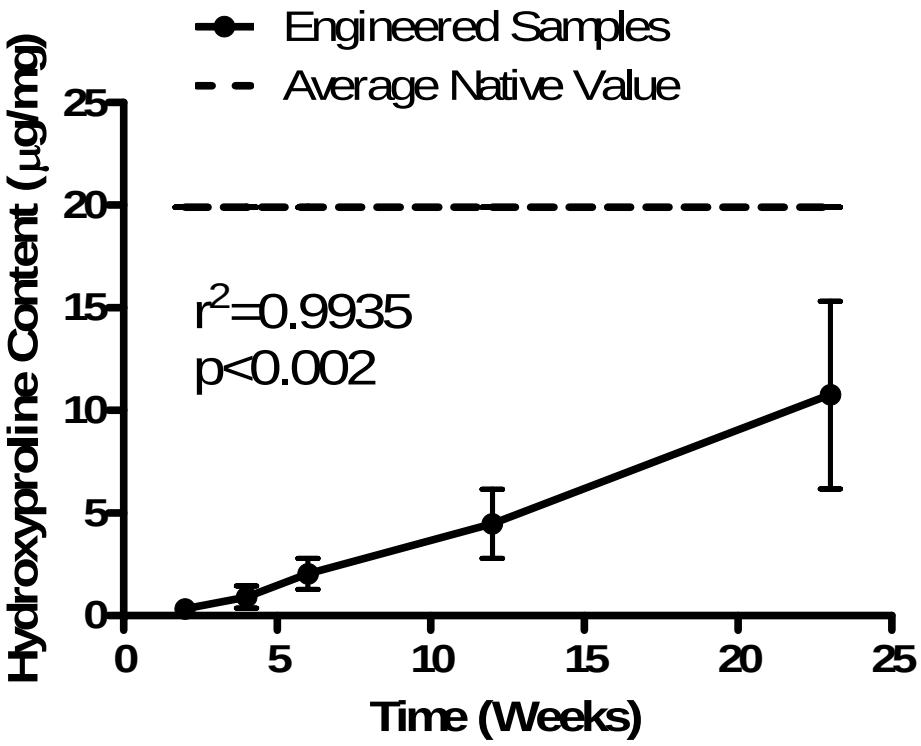
Engineered Samples
Average Native Value
Hydroxyproline Content (µg/mg)
25
20
15
10
5
0
r2=0.9935
p<0.002
0
5
10
15
20
25
Time (Weeks)

Figure 4

Hydroxyproline content measured after removal from subcutaneous implantation. Each data point represents n = 6 ± standard deviation. The correlation coefficient and p values indicate levels of significance of change in hydroxyproline with time.

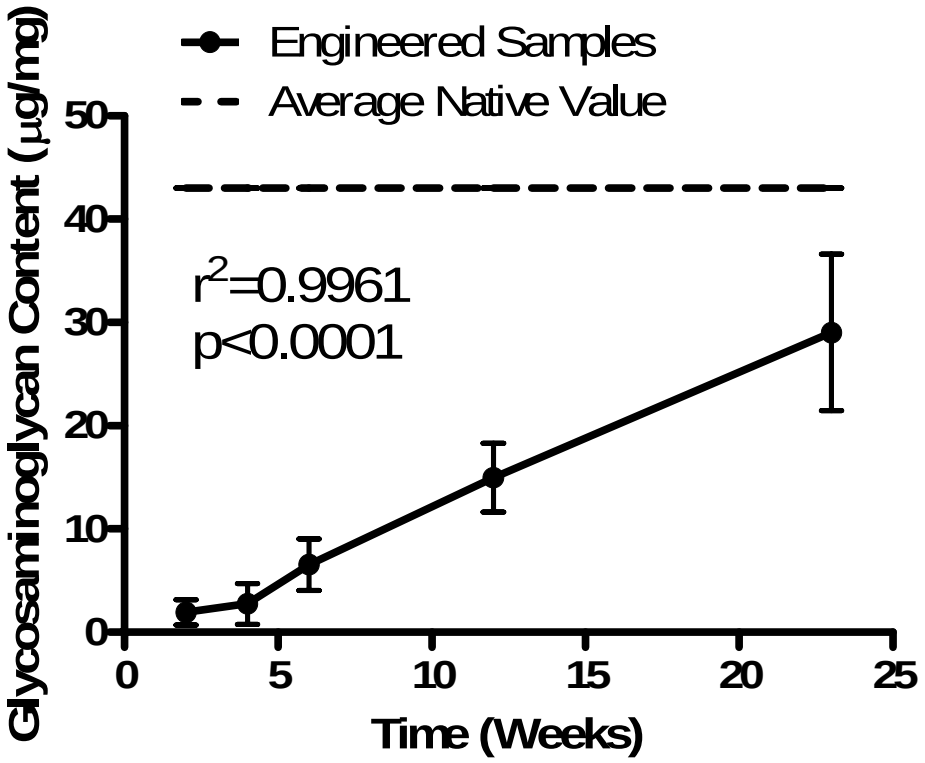
Engineered Samples
Average Native Value
r^2=0.9961
p<0.0001
Glycosaminoglycan Content (μg/mg)
Time (Weeks)
0
10
20
30
40
50
0
5
10
15
20
25

Figure 5

Glycosaminoglycan content measured after removal from subcutaneous implantation. Each data point represents n = 6 ± standard deviation. The correlation coefficient and p values indicate levels of significance of change in Glycosaminoglycan with time.

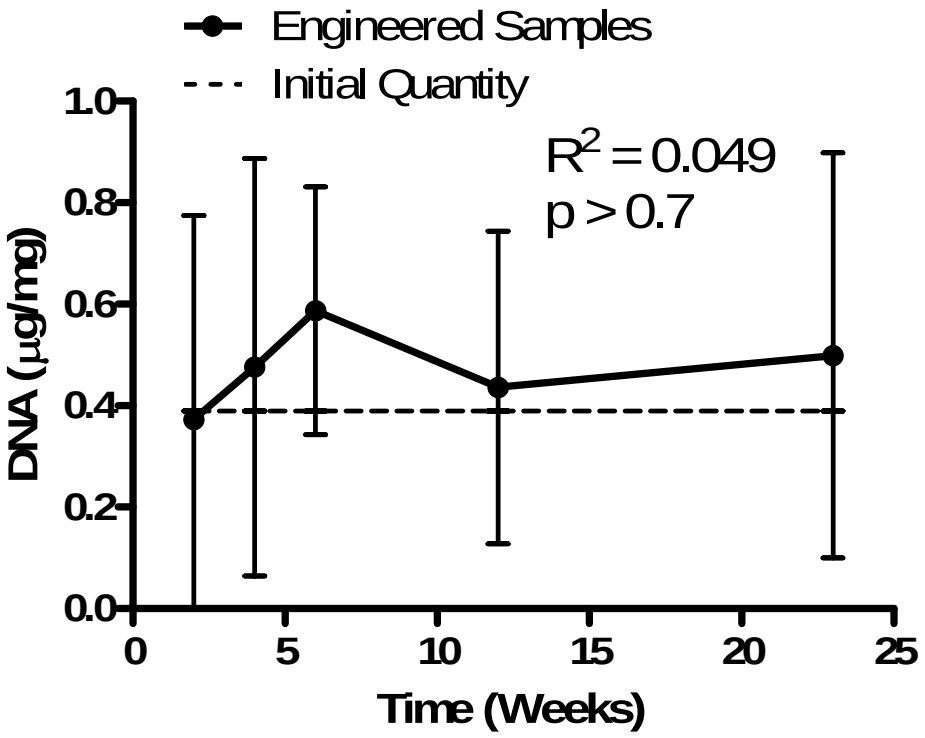
Engineered Samples
Initial Quantity
$R^2 = 0.049$
$p > 0.7$
DNA (μg/mg)
1.0
0.8
0.6
0.4
0.2
0.0
0
5
10
15
20
25
Time (Weeks)

Figure 6

DNA content measured after removal from subcutaneous implantation. Each data point represents n = 6 ± standard deviation. The correlation coefficient and p values indicate levels of significance of change in DNA with time.

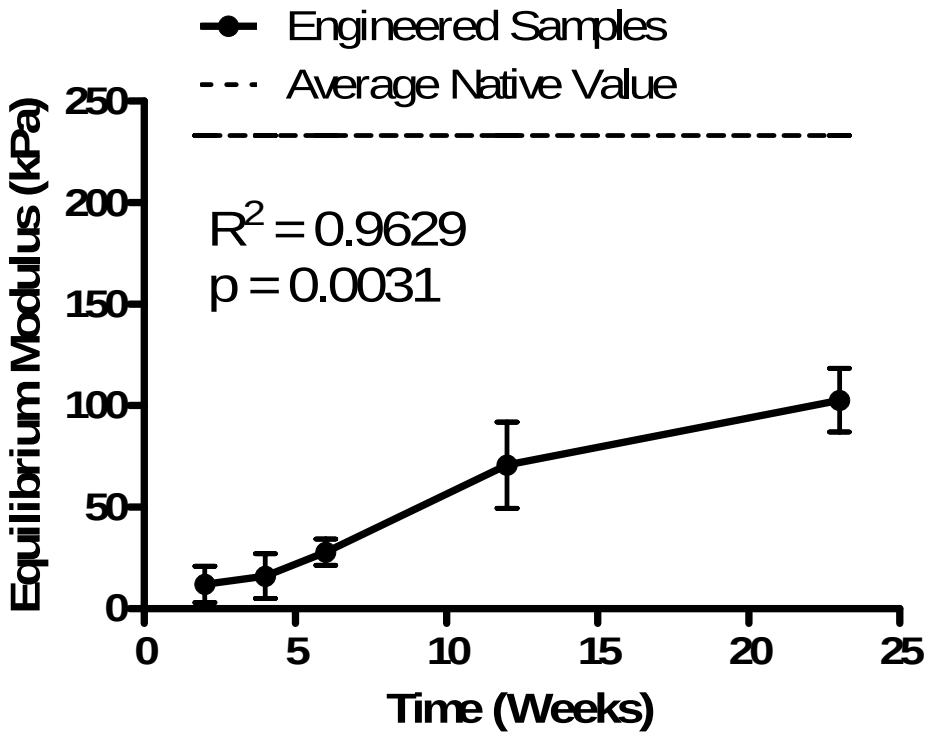
Engineered Samples
Average Native Value
$R^2 = 0.9629$
$p = 0.0031$
Equilibrium Modulus (kPa)
250
200
150
100
50
0
0
5
10
15
20
25
Time (Weeks)

Figure 7

Compressive equilibrium modulus of molded constructs after removal from subcutaneous implantation. Each data point represents n = 6 ± standard deviation. The correlation coefficient and p values indicate levels of significance of change in compressive equilibrium modulus with time.

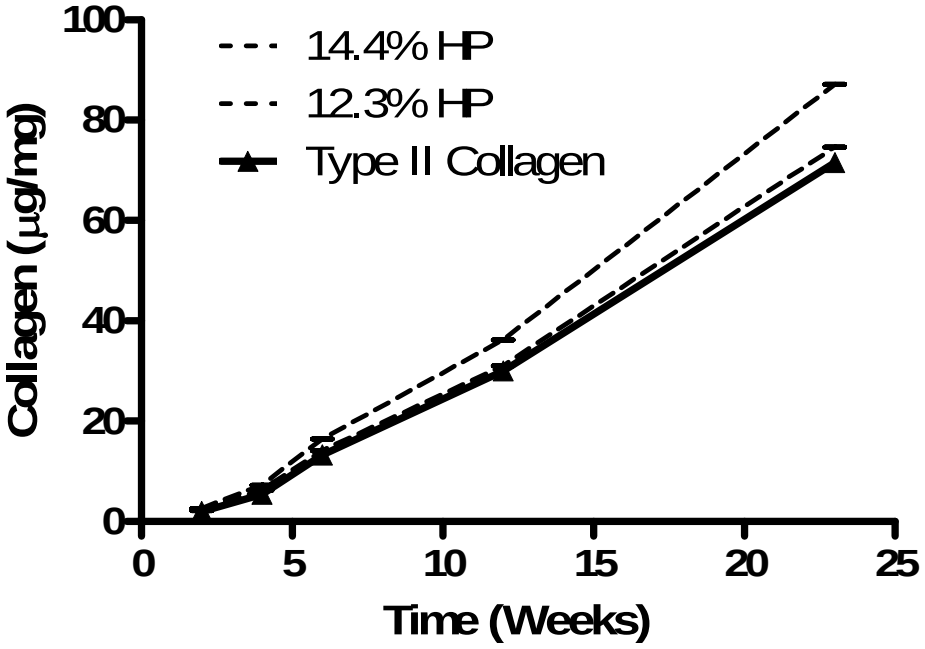
14.4% HP
12.3% HP
Type II Collagen
Collagen (µg/mg)
100
80
60
40
20
0
0
5
10
15
20
25
Time (Weeks)

Figure 8

Collagen content measured after removal from subcutaneous implantation. Dashed lines represent the predicted total collagen range calculated with hydroxyproline content taken to range from 12.3%-14.4% of the total collagen content. The solid line is type II collagen as measure by ELISA. Each data point represents n = 6 ± standard deviation.

CHAPTER 2

FABRICATION OF TISSUE ENGINEERED TYMPANIC MEMBRANE PATCHES USING COMPUTER-AIDED DESIGN AND INJECTION MOLDING

Abstract

Objectives/Hypothesis. The goal of the current study was to utilize computer aided design and injection molding technologies to tissue engineer precisely shaped cartilage in the shape of butterfly tympanic membrane patches out of chondrocyte seeded calcium alginate gels.

Methods. Molds were designed on Solid works 2000 and built out of acrylonitrile butadiene styrene (ABS) utilizing fused deposition modeling (FDM). Tympanic membrane patches were fabricated using bovine articular chondrocytes seeded at 50 x 10^6 cells/ml in 2% calcium alginate gels. Molded patches were cultured in vitro for up to ten weeks, and assessed biochemically, morphologically, and histologically.

Results. Un-molded patches demonstrated outstanding dimensional fidelity with a volumetric precision of at least 3µls, and maintained their shape well for up to ten weeks of in vitro culture. Glycosaminoglycan and collagen content increased steadily over ten weeks in culture, demonstrating continual deposition of new extracellular matrix, consistent with new tissue development.

Conclusions. The use of computer aided design and injection molding technologies allows for the fabrication of very small, precisely shaped chondrocyte-seeded calcium alginate structures that faithfully maintain their shape during in vitro

culture. In vitro fabrication of tympanic membrane patches with a precisely controlled geometry may have the potential to provide a minimally invasive alternative to traditional methods for the repair of chronic tympanic membrane perforations.

Introduction

Over two million tympanostomy tubes are inserted annually in the United States, making this the most commonly performed of all surgical procedures[1]. In up to ten percent of cases the patient treated with tympanostomy tubes is left with a permanent perforation of the tympanic membrane that requires surgical repair[2]. Because of the enormous number of chronic tympanic membrane perforations that need to be treated surgically every year, any new treatment that can simplify the repair process without sacrificing outcome quality has significant potential benefits. Current surgical reparative techniques require harvesting autologous tissue such as temporalis fascia or tragal cartilage to close the defect[3]. The tragal cartilage, or so called cartilage butterfly technique, is a relatively new and very promising transcanal inlay procedure that, in many cases, has several distinct advantages over more traditional tympanoplasty. It demonstrates excellent results in closing the tympanic membrane, and effectively restores and maintains normal audiometric function without requiring removal of contiguous myringosclerosis plaques or the creation a tympanomeatal flap. For these reasons the cartilage butterfly approach can sometimes be performed with mask anesthesia in an outpatient surgery setting[4].

Any highly effective treatment for chronic tympanic membrane perforations that could be performed reliably in an outpatient setting without the need for general anesthesia would provide an easier experience for patients and their families as well as potentially greatly reduce the cost of treatment. The cartilage butterfly approach to

tympanic membrane repair is a positive step in this direction, but is often limited by the invasiveness of harvesting the tragal cartilage as well as by the time and discomfort associated with shaping the harvested cartilage to make the appropriate geometry needed for repair.

Tissue engineering is an area of science in which investigators strive to repair or regenerate damaged or lost tissue. There is currently active investigation into the tissue engineering of a wide variety of specific tissues[5]. The common theme unifying the tissue engineering approach is the principle that a wide variety of cell types can be coaxed into synthesizing new tissue if they are seeded onto an appropriate three dimensional scaffold in an appropriate growth environment[6]. Seeding chondrocytes into a biocompatible and bioabsorpable three dimensional scaffold, such as alginate localizes the cells to a desired area and geometry allowing for new extracellular matrix (ECM) production in a desired location and shape[7,8]. Cartilage regeneration occurs as the chondrocytes are cultured in-vitro, seeded in a three dimensional polymer scaffold of the desired shape. As new tissue develops the polymer scaffold is reabsorbed so that ultimately new tissue is formed in the shape of the polymer in which the cells were seeded.

For many tissue engineering purposes it is desirable to precisely control the geometry of the newly generated tissue. The most common approach researchers have taken to controlling shape is to press fibrous scaffolds such as polyglycolic acid

(PGA) or polylglycolic-co-lactic acid (PLGA) into a rigid mold and then seed this scaffold with a cell solution [9]. This process works to some degree, but has inherent difficulties. It is technically challenging in this process to control the homogeneity of both polymer and cell distribution, complicating the ability to reliably produce consistent results. Additionally, cell-seeding efficiency tends to be low[10] and shape generation somewhat operator dependent. To our knowledge there are no reports to date of this approach being used to successfully fabricate very small precisely shaped constructs. Previously published work demonstrated calcium alginate production of complex geometries utilizing injection molding[11]. In this work silicon maxillofacial implants were used as positives to generate negative molds from a commercially available silastic mold making kit. Calcium alginate was then injected into the molds to duplicate the silicon shapes. The results demonstrated the utility of the process, but also some inherent limitations. Complete filling of the molds was difficult, and the process was not capable of reliably generating very small constructs. Additionally, in order to create an injection mold one needed a structure serving as a positive that already possessed the desired geometry. This study addresses these limitations by incorporating computer aided design (CAD), which eliminates the need for the existing positive, and solid free form fabrication which allows for the fabrication of sophisticated mold elements.

We propose that the cartilage butterfly approach to tympanic membrane repair would benefit from using a tissue engineered autologous cartilage patch in lieu of

intra-operatively harvesting and shaping tragal cartilage. Our tissue engineering approach strives to generate new cartilage in the shape of a butterfly tympanic membrane patch from a very small number of autologous chondrocytes harvested from an unobtrusive retro-auricular or tragal site using local anesthesia.

In the current study we have sought to demonstrate the feasibility of a tissue engineering approach for tympanic membrane perforation repair by fabricating cartilage butterfly patches of three different sizes using bovine articular chondrocytes seeded in shaped calcium-alginate constructs. Toward this end we evaluated the ability of CAD and injection molding technologies for their ability to reliably reproduce very small and precisely shaped cell-seeded calcium alginate gels that maintain a complex geometry during in vitro culture, as well as the chondrogenic potential of these gels in a standard in vitro culture system.

To insure precise geometry and dimensional tolerances for the patches we utilized an injection molding technology specially adapted for an alginate/cell mixture with a mold designed by computer-aided design (CAD), and fabricated by fused deposition modeling (FDM), a kind of solid freeform fabrication.

Methods and Materials

Chondrocyte Isolation. Bovine articular chondrocytes were isolated from the glenohumoral joint of freshly slaughtered calfs. Cartilage slices were excised from the

joint and washed thoroughly two times in phosphate buffered saline (PBS) (Sigma-Aldrich, Irvine, CA, USA) supplemented with antibiotic/antimycotic (10,000 U/ml penicllin G sodium, 10,000 µg/ml streptomycin sulfate, and 25 µg/ml amphotericin B) (Gibco, Grand Island NY). Cartilage slices were then enzymatically digested in 0.3% collagenase type II (Worthington Biochemical Corp, Freehold, N.J. USA.) in Hamms F-12 media (Sigma-Aldrich, Irvine CA) at 37° for 12-16 hours[12]. The resultant digest was filtered through a sterile 180 um polypropylene filter (Millipore, Bedford, MA) to separate the chondrocytes from any undigested cartilage. The filtered collagenase solution was centrifuged at 7000 rpm, and the pelleted cells were washed thoroughly twice in antibiotic/antimycotic supplemented PBS. Isolated chondrocytes were re-suspended in Hamm's F-12 media supplemented with antibiotic/antimycotic, and counted on a hemocytometer. Cell viability was assessed by trypan blue dye exclusion assay (Sigma-Aldrich, Irvine, CA). All cells used in construct fabrication were taken from digests that demonstrated better than 90% cell viability.

Mold Design and fabrication. An injection mold for fabricating tissue engineered tympanic membrane patches was designed using SolidWorks 2000 (Computer-Aided Products, Peabody, MA) and fabricated out of acrylonitrile butadiene styrene (ABS) using fused deposition modeling (FDM), on a Stratysys Inc.'s Prodigy (Stratysys Inc, Eden Prairie, MN). The mold was designed with a part-line along an axis of symmetry to avoid undercuts, and had two alignment pins at one

end to ensure proper marriage of the two halves (Fig 1). The mold was designed with an injection port at one end and off-gassing slits at the far end of each individual patch to insure proper filling of the mold cavity (Fig 1). The injected mold makes two copies each of three different sizes of "butterfly" tympanic membrane patches. Same size patches are molded in parallel and the different sizes in series (Fig 1). The butterfly shape patch was modeled after the target shape of surgically carved tragal cartilage, (two circular flanges flanking a central connector). In the injected mold the patches sit on top of two inserts that can be pushed out from the back to facilitate removal from the mold (Fig 1). All three patches are 2 mm long across their major axis and have flanges with outer diameters ranging from 2 mm-3 mm. The thickness of the flanges is roughly 0.40 mm.

Construct Fabrication and Handling. Methods for generating chondrocyte-seeded alginate patches were based on previous studies documenting generation of cartilage by injection molding[11]. Chondrocytes isolated from enzymatic digestion of bovine articular cartilage were suspended in filter sterilized 2% low viscosity alginate (Pronvoa, Norway) in PBS at a seeding density of 50×10^6 cells/ml. Immediately prior to injection into the mold the alginate/cell suspension was mixed thoroughly, using a sterile stopcock, with autoclave sterilized $CaSO_4$ in PBS (0.25g/ml). The alginate/chondrocyte/ $CaSO_4$ mixture was injected into the mold using a 3 ml syringe with an 18.5 gauge needle. Over time the Ca^{++} in the alginate/chondrocyte/$CaSO_4$ solution continually cross-links individual alginate strands, leading to a progressively

stiffer and stiffer gel. The injected molds were allowed to stand for one hour, after which fully formed solid gelled patches were removed. (Fig. 2) The individual patches were cultured in vitro for up to 10 weeks in Hamm's F-12 media supplemented with antibiotic/antimycotic), 10% heat inactivated fetal bovine serum (FBS), and ascorbate (50 μg/ml). (Fig 4) All patches were cultured in 6 well culture dishes, with different size patches isolated from each other. A maximum of six patches were cultured in any individual well. Cultured patches were covered with 8 mls of culture medium which was changed every second day.

Histological Evaluation of Constructs. At 0 and 10 weeks samples were removed from culture and frozen for histological and biochemical evaluation. Specimens for histology were fixed in 10% unbuffered formalin supplemented to be 0.1M in $CaCl_2$ for at least 24 hours and then embedded in paraffin, sectioned by microtome, and stained with Safranin-O.

Biochemical Evaluation of Constructs. In parallel with histological studies, samples were removed from culture at 2, 4, 6, and 10 weeks for biochemical evaluation. Cell number in the constructs was evaluated by quantifying the amount of DNA. Extracellular matrix accumulation in the constructs was evaluated by quantifying the amount of sulfated glycosaminoglycans (GAGs) as a marker of proteoglycans, and hydroxyproline as a marker of collagen content. All biochemical analysis used standard methods that have been described elsewhere in detail. Briefly,

all samples were digested in 1 ml of a papain digest buffer (0.1M sodium phosphate, 10 mmol sodium EDTA (BDH), 10 mmol cysteine hydrochloride (Sigma), and 3.8 U/ml papain (Sigma) at 60° for 24 hours. DNA content of samples was measured by quantitating the amount of fluorescence (358/458 nm) due to bound Hoechst 33258 dye. Measured fluorescence from the samples was compared to a standard curve created with calf thymus DNA[13]. Sulfated GAG content was measured using 1,9-dimethylmethylene blue dye at pH 1.5, and quantitating the absorbances at 595 nm, using C-6-S from shark cartilage (Sigma) as a standard[14]. Hydroxyproline content was measured by acid hydrolysis of samples of papain digests, addition of Chloramine T and *p*dimethylamino-benzaldehyde, and quantitating the absorbance at 560 nm[15].

Mass Evaluation of Constructs. In order to determine if the mold was faithfully reproducing the shape of the patches, we compared the masses of the three different size patches immediately after un-molding to the expected mass for each size patch. Each measured mass used for comparison was the average mass of thirty individually weighed patches. Expected masses were determined based upon the designed patch volumes and a measured density of the cross-linked alginate gel. Each sample was weighed to 0.0001g using a microbalance (Ohaus, Pine Brook, NJ) and the weights were recorded.

Statistical Analysis. Mean differences in GAG, hydroxyproline, and DNA content at 2, 4, 6, and 10 weeks were analyzed by a one factor ANOVA with tukey post-hoc multiple comparisons.

Results

The ABS mold faithfully reproduces the computer generated design, yielding tympanic membrane patches which can be separated and removed from the mold. The average masses of the three different size patches immediately after un-molding were 30.2 ± 3.1 mg, 21.6 ± 2.2 mg, and 10.6 ± 2.2 mg (90%, 89%, and 88% of expected values) (Fig 3). For each size patch this represents a volume discrepancy of 3 µl or less, demonstrating an excellent ability to accurately duplicate small shapes. The gross morphology of the patches was maintained through 10 weeks of in-vitro culture, and over time the patches gradually became more opaque, grossly consistent with developing extracellular matrix. This is most apparent between 6 and 10 weeks (Fig 4).

Immediately after un-molding the samples show good shape fidelity, and air bubbles generated from mixing alginate with $CaSO_4$ can be seen (Fig 5). At 10 weeks samples still show excellent shape retention, with Safranin-O staining throughout, indicating relatively uniform deposition of proteoglycans, an important component of the cartilage extracellular matrix. The periphery of the samples contained a thin (10-20 µm) layer that did not stain with Safranin-O.

GAG and hydroxyproline content increased significantly between each measured time point ($p<0.002$). DNA content showed no statistically measurable difference over time. At 2, 4, 6, and 10 weeks GAG content was 1.1 ± 0.56 µg/mg ,

2.02 ± 0.91 μg/mg, 3.83 ± 1.60 μg/mg, and 9.33 ± 2.3μg/mg. (Fig. 6) These values are roughly 2%, 3%, 6% and 13% respectively of native values. At 2, 4, 6, and 10 weeks hydroxyproline content was 0.07 ± 0.03 μg/mg, 0.14 ± 0.05 μg/mg, 0.67 ± 0.27μg/mg. and 0.94 ± 0.27 μg/mg. (Fig. 8) These values are approximately 1%, 2%, 10%, and 15% respectively of native values measured as an internal control. Increasing GAG and hydroxyproline content indicate that the chondrocytes were alive and metabolically active. DNA content over time remained consistent with the DNA content initially loaded, indicating that the chondrocytes did not proliferate in the course of this culture. (Fig. 6)

Discussion

The goal of the present study was to assess the potential of CAD and injection molding technologies to generate chondrocyte seeded calcium alginate gels in the shape of cartilage butterfly tympanic membrane patches, and to then assess the chondrogenic potential of those constructs to determine their potential suitability for therapeutic application in the treatment of chronic tympanic membrane perforations.

Alginate, an anionic copolymer of manuronic and guluronic acids, has been used for many years for in vitro culture systems, and in more recent years has gained interest as a scaffold for tissue engineering[16]. Because of the relatively low aqueous solubility of the alginate cross-linking solution used in this study, $CaSO_4$ (0.209 g/ml), the amount of the cross-linking agent, free Ca^{++}, available at equilibrium is scant enough that cross-linking of alginate occurs slowly enough that the alginate/cell/ $CaSO_4$ mixture can be injected into a mold as a liquid, but in a reasonably short time forms a stiff enough gel to be un-molded as a solid.

The most commonly used scaffold in tissue engineering has been polyglycolic acid (PGA), which has demonstrated the ability to facilitate new tissue development, but has provoked a severe inflammatory reaction when implanted in immunocompetent animals[17]. An appealing element of alginate as a tissue engineering scaffold is that it allows for new tissue development in a three

dimensional matrix while, unlike PGA, seems to provoke little or no immune response in immunocompetent hosts[17].

The tympanic membrane patches fabricated in this study demonstrated good dimensional fidelity, with volumetric precision to within 3 µl of design specifications for all size patches, indicating excellent potential for making very small precisely shaped cell-seeded constructs. Increasing GAG and hydroxyproline content indicate that the chondrocytes were alive and metabolically active, continually producing new extracellular matrix. The DNA data indicate that the chondrocytes did not proliferate, which is consistent with metabolic energy being conserved for extracellular matrix development, as was desired. These biochemical data are reasonably consistent with reports on similar in vitro cartilage development, and are consistent with the development of new cartilage[18]. Chondrogenic potential of the cultured constructs was further demonstrated by progressive staining with Safranin-O during in vitro culture. Good cross-sectional morphology was difficult to see on histology due to the technical challenge in preparing the constructs. Upon removal from the mold the alginate gel is still quite soft and subject to deformation during the imbedding process, particularly at the very thin outer flanges.

The increasing trend in matrix components shows that tissue development was continuing with time in culture. Also, while ECM development, which strongly correlates with the developing tissue's mechanical properties, is for some cartilage

tissue engineering applications perhaps the most crucial indication of tissue utility, that is not necessarily the case here. Using a cartilage tympanic membrane patch is fundamentally different from trying to create load bearing, structural cartilage. For this application, it is unclear, as of now, how crucial the mechanical properties of the new tissue will be, but by ten weeks of in vitro culture the patches had solidified sufficiently that they could be picked up and handled with forceps.

Conclusion

We have demonstrated the ability to tissue engineer cartilage implants with the precise shape necessary for repair of non-healing perforated tympanic membranes caused by long term use of tympanostomy tubes. Determination of how well these constructs work for the clinical repair of non-healing tympanic membrane perforations will require an in vivo study using an animal model of non-healing tympanic membrane perforations. In future studies we will also compare tissue engineered cartilage patches with patches made from other tissue engineered tissues. The clinical use of a tissue engineered patch for repair of tympanic membranes has the potential to allow repair of small tympanic membrane perforations to be accomplished at an office visit, with no need for general anesthesia in select cases. Moving the routine repair of non-healing tympanic membrane perforations due to long term tympanostomy tube use from the operating room to the office has the potential to greatly reduce the time and stress of treatment for patients and additionally to greatly reduce the cost of providing treatment. To accomplish the long-term goal of this work, though, much work needs to be done in the animal model in order to optimize the formulation and design of the implants. In addition, future work utilizing alternative cell types may facilitate an “off-the-shelf”, one-step tympanic membrane patch.

References

1. Isaacson G, Rosenfeld R. Care Of The Child With Tympanostomy Tubes. *Pediatric Otolaryngolgoy* 1996;43(6):1183-1193.

2. Siddiqui N, Toynton S, Mangat KS. Results of middle ear ventilation with 'Mangat' T-tubes. *Int J Pediatr Otorhinolaryngol* 1997;40(2-3): 91-6.

3. Patterson M, Papatella M. Ottitis Media: Surgical Principles Based on Pathogenesis. *Otolaryngology Clinics of North America* 1999;32 (3):391-399.

4. Eavey RD. Inlay Tympanoplasty: Cartialge Butterfly Technique. *Laryngoscope* 1998;108(5):657-661.

5. Langer R. Tissue Engineering. *Mol Ther*. 2000;1(1):12-15.

6. Vacanti JP; Langer R. Tissue engineering: the design and fabrication of living replacement devices for surgical reconstruction and transplantation. *Lancet* 1999;354 Suppl 1:SI32-4

7. Atala A, Cima LG, Kim W, Paige KT, Vacanti JP, Retik AB, Vacanti CA. Injectable alginate seeded with chondrocytes as a potential treatment for vesicoureteral reflux. *J Urol* 1993;150(2 Pt 2):745–747.

8. Paige KT, Cima LG, Yaremchuk MJ, Schloo BL, Vacanti JP, Vacanti CA. *De novo* cartilage generation using calcium alginate-chondrocyte constructs. *Plast Reconstr Surg* 1996;97(1): 168–178; discussion 179–180.

9. Cao Y, Vacanti JP, Paige KT, Upton J, Vacanti CA. Transplantation of chondrocytes utilizing a polymer-cell construct to produce tissue-engineered cartilage in the shape of a human ear. *Plast Reconstr Surg* 1997;100:297–302.

10. Morran JM, Pazzano D, Bonassar LJ. Characterization of Polylactic Acid-Polyglycolic Acid Composites for Cartilage Tissue Engineering. *Tissue Engineering* 2003;9(1):63-70.

11. Chang SCN, Rowley JA, Tobias G, Genes NG, Roy AK, Mooney DJ, Vacanti CA, Bonassar LJ. Injection Molding Of Chondrocyte/Alginate Constructs In The Shape Of Facial Implants. *J Biomed Mat Res* 2001;55(4):503-511

12. Klagsburn M. Large-scale preparation of chondrocytes. *Methods Enzymol* 1979;58:560–564.

13. Kim YJ, Sah RLY, Doong JYH, Grodzinsky AJ. Fluorometric assay of DNA in cartilage explants using Hoechst 33258. *Analyt Biochem* 1988;174: 168-176

14. Enobakhare BO, Bader DL, Lee DA. Quantification of sulfated glycoaminoglycans in chondrocyte/alginate culture, by use of 1,9-dimethylmethylene blue. *Anal Biochem* 1996;243:189-191.

15. Stegemann H, Stadler K. Determination of hydroxyproline. *Clin Chim Acta* 1967;18:267-273.

16. Draget KI, Skjak-Braek G, Smidsrod O. Alginate based new materials. *Int J Biol Macromol* 1997;21(1–2):47–55.

17. Cao Y; Rodriguez A; Vacanti M; Ibarra C; Arevalo C; Vacanti CA. Comparative study of the use of poly(glycolic acid), calcium alginate and pluronics in the engineering of autologous porcine cartilage. *J Biomater Sci Polym Ed* 1998;9(5):475-87.

18. Pazzano D, Mercier KA, Moran JM, Fong SS; DiBiasio DD, Rulfs JX; Kohles SS, Bonassar LJ. Comparison of chondrogensis in static and perfused bioreactor culture. *Biotechnol Prog*. 2000;16(5):893-6

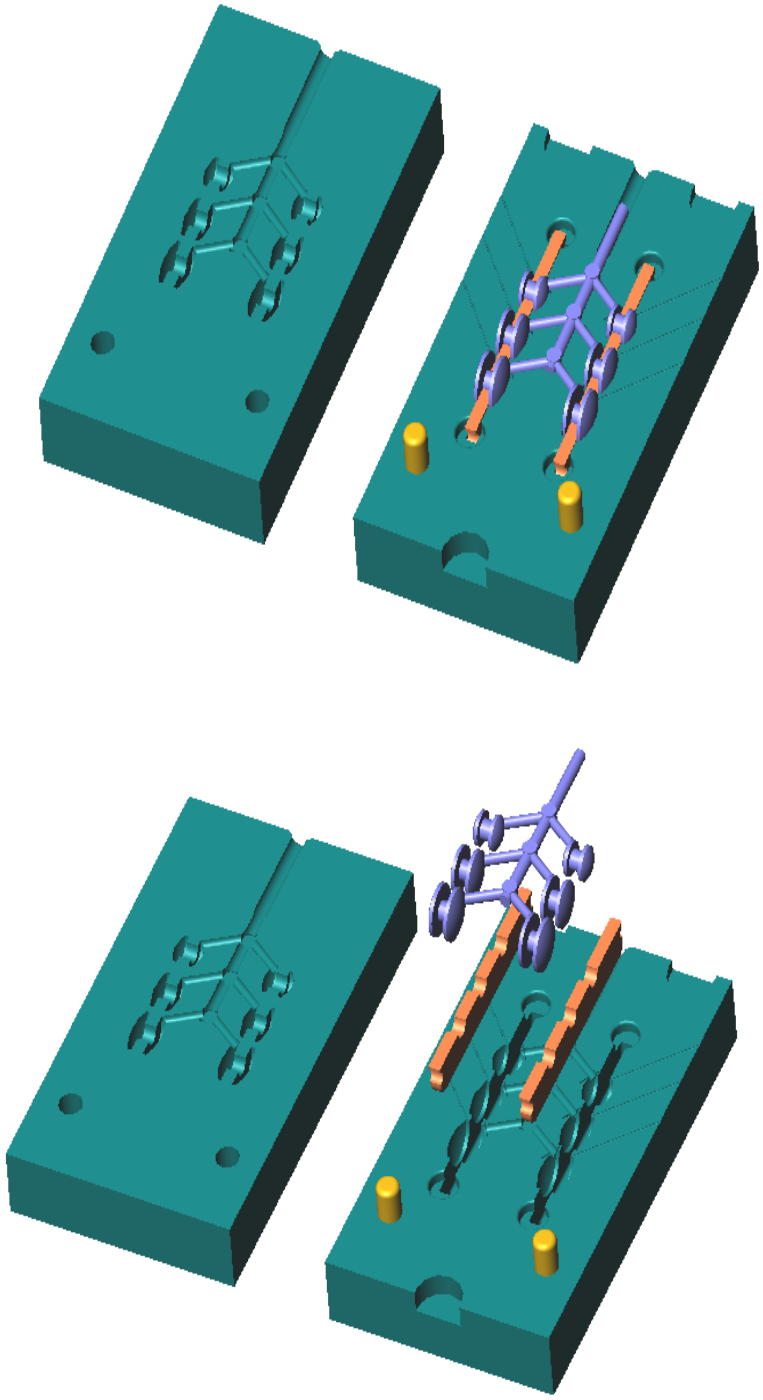

Figure 1.

CAD rendering of the mold generated in SolidWorks 2000 Unexploded (A), and Exploded (B).

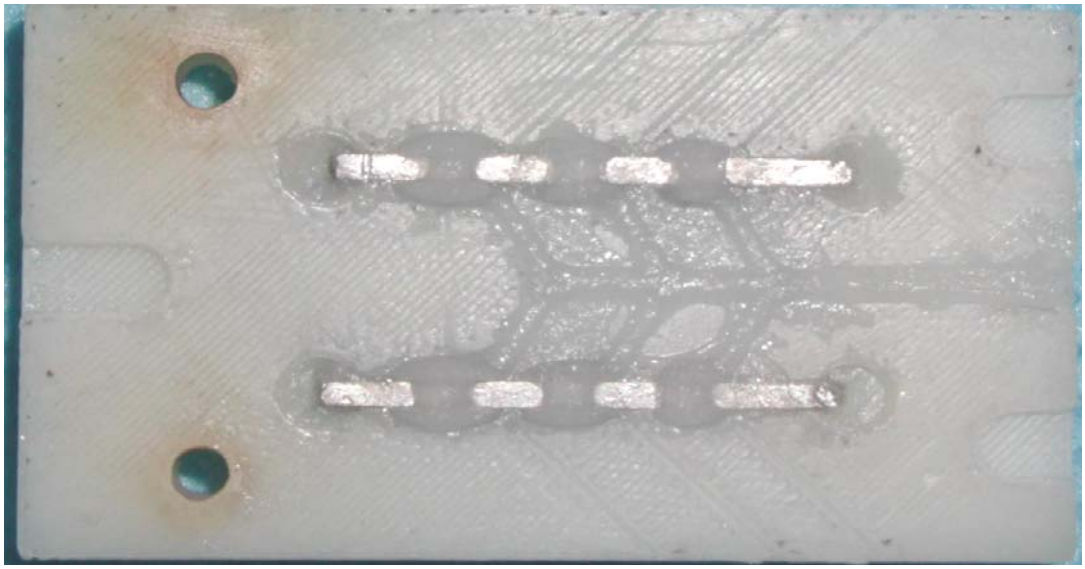

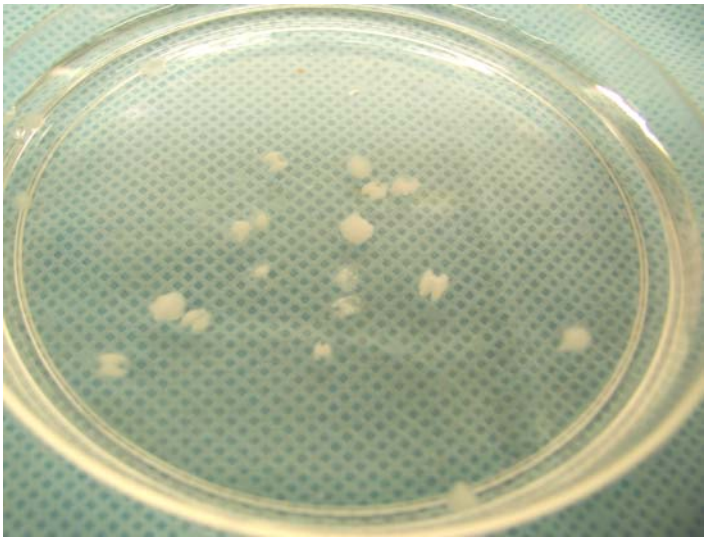

Figure 2.

ABS mold filled with alginate seeded with 50 x 10^6 chondrocytes/ml immediately before un-molding (A), and molded patches immediately prior to culture (B).

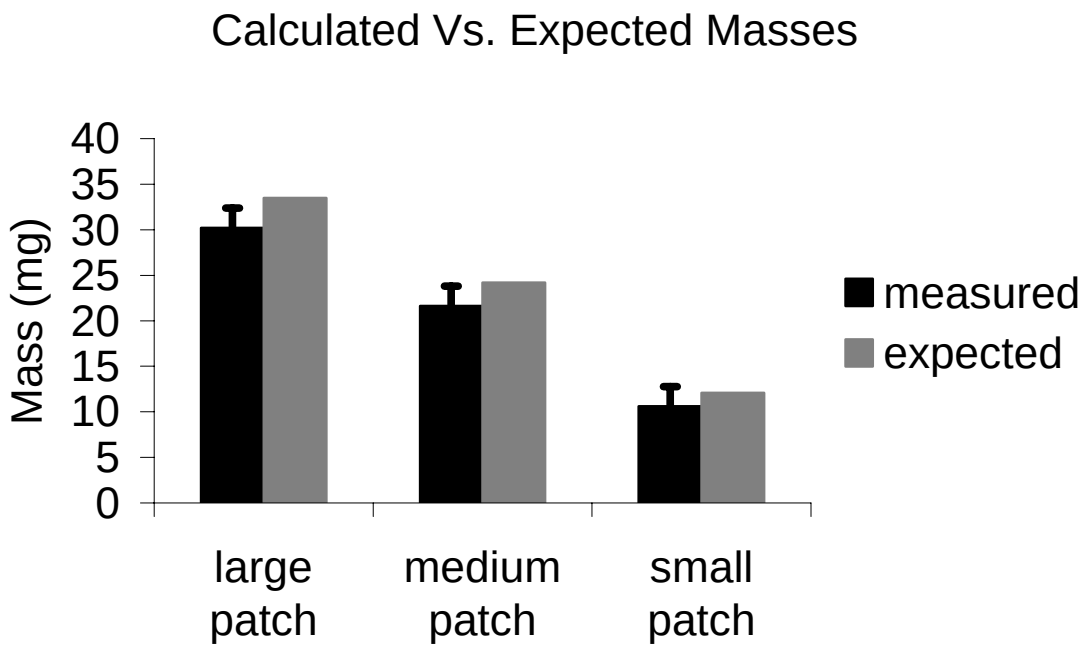
Calculated Vs. Expected Masses
Mass (mg)
40
35
30
25
20
15
10
5
0
large patch
medium patch
small patch
measured
expected

Figure 3.

Calculated and expected masses of small medium, and large tympanic membrane patches immediately after un-molding.

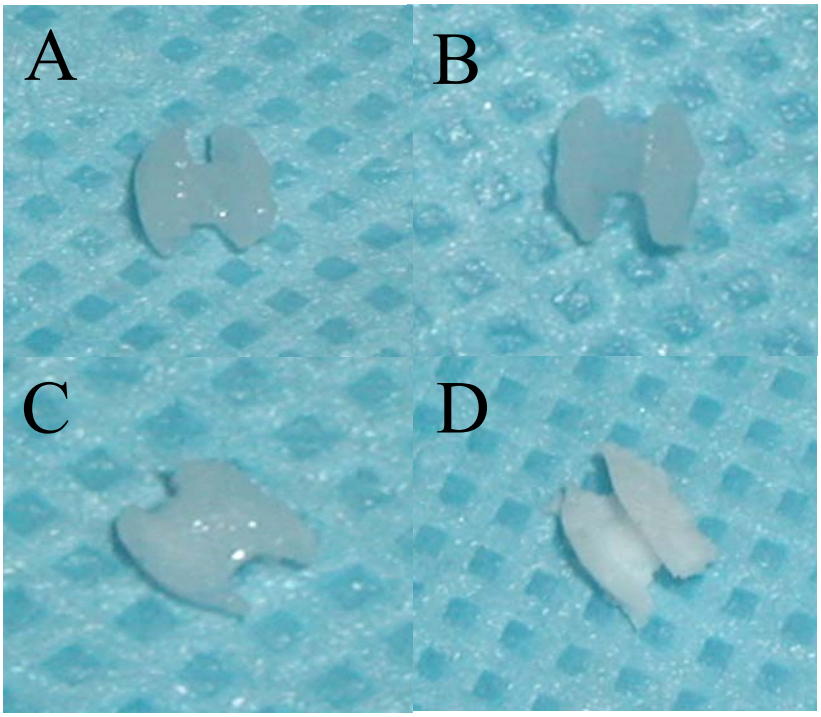
A
B
C
D

Figure 4.

Gross morphology at 2 weeks (A), 4 weeks (B), 6 weeks (C), and 10 weeks (D) in culture.

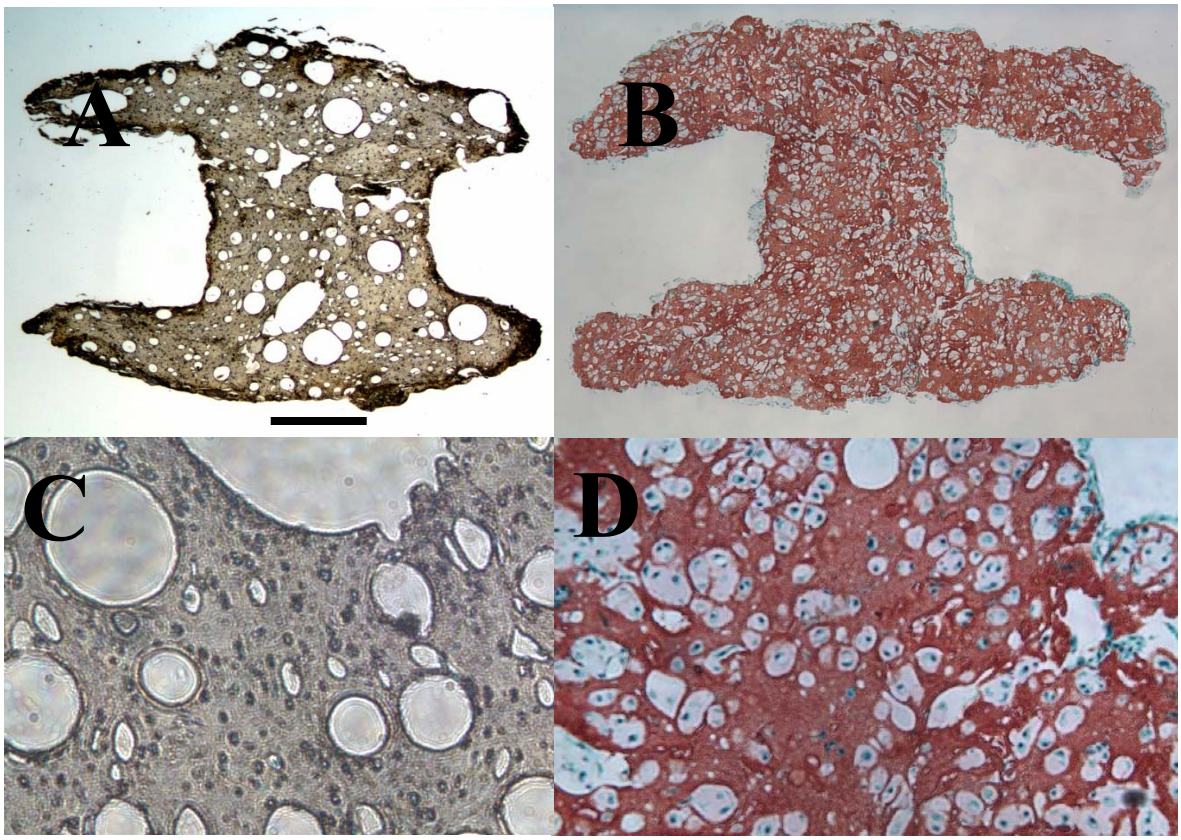
A
B
C
D

Figure 5.

Safranin O staining of a small tympanic membrane patch to detect cartilage proteoglycans immediately after un-molding (A at 40x magnification and C at 200x magnification), and a large tympanic membrane patch after 10 weeks in culture (B at 40x magnification and D at 200x magnification). Bar = 500 μm.

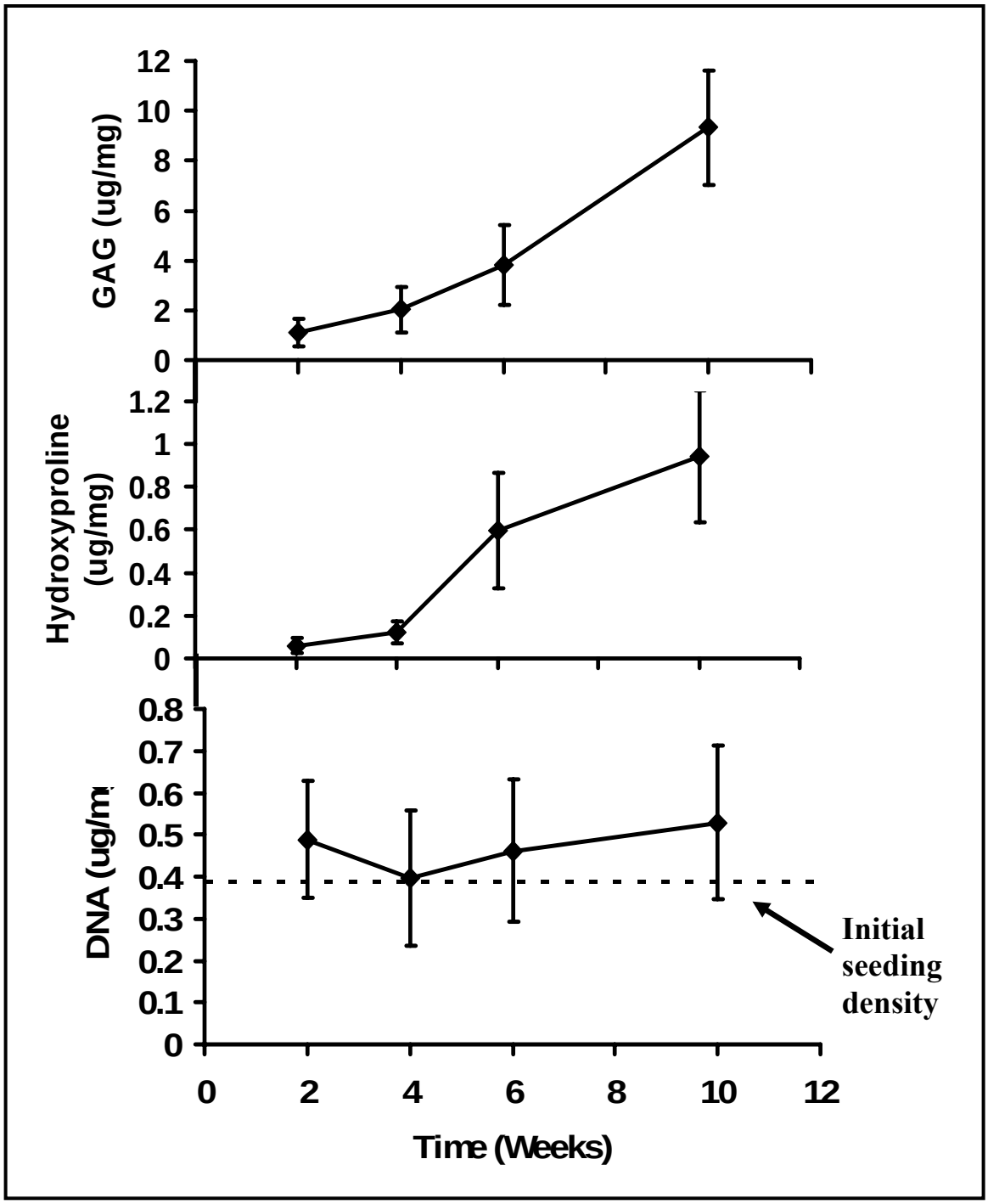
GAG (ug/mg)
12
10
8
6
4
2
0
Hydroxyproline (ug/mg)
1.2
1
0.8
0.6
0.4
0.2
0
DNA (ug/m
0.8
0.7
0.6
0.5
0.4
0.3
0.2
0.1
0
Initial seeding density
0
2
4
6
8
10
12
Time (Weeks)

Figure 6.

Glycosaminoglycan (GAG) content (A), hydroxyproline content (B), and DNA content (C) of tympanic membrane patches at times in culture up to 10 weeks. All data are represented as mean ± SD for n = 24 samples.

CHAPTER 3

PEPTIDE MODIFIED ALGINATE HYDROGELS: A POTENTIAL VEHICLE FOR THE CONTROLLED RELEASE OF TGF-β1 IN A TISSUE ENGINEERING SCAFFOLD

Abstract

Objectives/Hypothesis. The goal of the current study was twofold: first, to evaluate the efficiency of carbodiimide chemistry for adding a novel growth factor binding peptide to sodium alginate; second, to compare the TGF-β1 release characteristics from peptide-modified alginate and control alginate.

Methods. A novel growth factor binding peptide was covalently bonded to sodium alginate using standard carbodiimide chemistry to form amide linkages between the N-terminal region of the peptide and the free carboxylate moieties on the alginate backbone. The efficiency of the reaction was determined using the BCA Protein Assay. Control and peptide-modified alginate were loaded with 30 ng/ml TGF-β1 and stored in PBS at 37ºC. TGF –β1 release from experimental and control constructs was quantified by ELISA over 16 days

Results. Carbodiimide addition of the novel growth factor binding peptide proceeded at 60% efficiency, consistent with previously published reports on carbodiimide addition of peptides to sodium alginate. The peptide-modified alginate displayed different release characteristics than control alginate, delaying a burst release of growth factor by approximately three days.

Conclusions. Carbodiimide chemistry can reliably add a variety of growth factors to calcium alginate in a predictable manner. Peptide modification of alginate

resulted in altered release characteristics for TGF-β1. This may have been due to specific binding to the peptide or alterations in the properties of the alginate construct.

Introduction

Osteoarthritis effects as many as twenty-one million people in the United States, and is responsible for over 50% of all hip replacements. This alone results in annual medical costs exceeding fifteen billion dollars[1]. There are over one million surgical procedures annually in the United States that involve the replacement of bone or cartilage[2]. Given this enormous societal cost and the debilitating nature of severe joint pain, medical science has striven for decades to find ways to encourage cartilage regeneration and repair. This work is difficult because of the inherently poor ability of cartilage for self repair. Because cartilage is an avascular tissue, partial thickness injuries that do not extend down to the level of the subchondral bone are incapable of spontaneous healing. Without a vascular supply, cells, growth factors and cytokines cannot be recruited to the site of injury to aid in repair as happens in most other tissues.

For severely damaged articular cartilage with debilitating joint pain the only currently available treatment is prosthetic joint replacement. While this does provide symptomatic relief, prosthetic joints have a limited life span and cannot fully replicate cartilage's resistance to compression and ability to evenly distribute load[3]. Thus, the ability to repair native cartilage, or replace damaged or diseased cartilage with an engineered replacement would be of tremendous benefit in the treatment of joint disease. The tissue engineering approach to repairing cartilage acknowledges that tissue repair will require a space filling matrix, cells, and appropriate biologics.

Alginate, a copolymer of mannuronic and guluronic acids, is a hydrogel that has been used extensively for three dimensional chondrocyte culture, and more recently as a tissue engineering scaffold, effectively serving as synthetic extracellular matrix (ECM)[4-7]. A primary goal of tissue engineering is to be able to take a very small amount of tissue, and transform it into a much greater amount of tissue that can be used for therapeutic purposes. This is accomplished by liberation and expansion of the cells from donor tissue, followed by seeding into a polymer scaffold. The idea in using a scaffold is to provide an environment that essentially replaces the function of the ECM. Namely, it allows cells to organize in a three dimensional structure, provides mechanical stability, provides for localization of cells, and provides a hydrated space for the diffusion of nutrients and cellular metabolites[8-9].

Alginate has been used for decades for the three dimensional culture of chondrocytes, where it has been shown to maintain the chondrocyte phenotype, which is lost in standard monolayer culture[10-13]. Alginate has been previously shown to have utility as a tissue engineering scaffold for fabricating chondrocyte seeded structures with complex geometries that have outstanding structural fidelity in *in vitro* culture[14]. Alginate is also intriguing as a tissue engineering scaffold for its chemical properties. As a hydrogel, it is subject to solution chemistry, making it easier to modify than rigid polymers. As a copolymer of two acids it has abundant free carboxylic acid moieties that are highly reactive and naturally subject to condensation reactions. This

makes it possible to conceive numerous peptide modifications of alginate to regulate such important functions as cell adhesion and growth factor delivery.

The necessity of growth factors and other biologically active molecules for orchestrating tissue development in tissue engineering applications has long been accepted. Numerous growth factors have been investigated for the engineering of articular cartilage, including the TGF-β superfamily, IGFs, FGFs, PDGF, EGFs, VEGF, and numerous others[15-24]. From this increasingly dizzying array, TGF-β1 stands out for a number of reasons. TGF-β is the most studied growth factor for chondrogenesis, and TGF-β1 is the most abundant naturally occurring isoform in articular cartilage[25]. TGF-β1 has consistently been shown to be a potent stimulatory of chondrogenic differentiation, and extracellular matrix production[26-31]. How best to deliver TGF-β to chondrocytes in tissue engineered constructs is not known. While in principal this can be done in a number of ways, the key element, if it is to be effective, is that the growth factor must be supplied in a controlled manner.

One of the major carriers of TGF-β endogenously is the homotetrameric glycoprotein, α_2-Macroglobulin (α_2M). α_2M functions as broad spectrum proteinase inhibitor in plasma and other extracellular spaces. It functions in this manner by presenting multiple peptide bonds in its so called “bait” region to proteinases. When these peptide bonds are cleaved by an attacking proteinase it causes a conformational change in the entire α_2M protein, trapping the attacking proteinase[32-33]. Recently a

linear 16 amino acid sequence has been isolated from the bait region of α_2M that appears able to bind a wide variety of growth factors, including TGF-β1[34]. Modification of alginate by biochemical addition of this peptide could potentially allow for the controlled release of TGF-β1 from calcium alginate constructs. In the current study we will attempt to modify alginate by covalent addition of this TFG-β binding peptide, and characterize the subsequent release of TGF-β1 from this modified alginate compared to control alginate.

Methods and Materials

Custom Peptide Synthesis. Medium viscosity alginate was purchased from FMC Biopolymer (Drammen Norway), and the modified TGF-β binding peptide, glycine, glycine, glycine, glycine, tryptophan, aspartic acid, leucine, valine, valine, valine, asparagine, serine, alanine, glycine, valine, alanine, glutamic acid, valine, glycine, valine, tyrosine, tyrosine, abbreviated as, GGGGWDLVVVNSAGVAEVGVYY, was purchased as a custom synthesis order from New England Peptide Inc. (Gardner, MA). The N-terminal GGGG sequence was added to the known TGF-β binding peptide as a known linking sequence used with alginate, and the C-Terminal YY sequence was added to aid in peptide detection by the BCA Protein Assay Kit. All other reagents were purchased through Sigma Aldrich in Irvine, CA.

Fabrication of Peptide Modified Alginate. The TGF-β binding peptide sequence, GGGGWDLVVVNSAGVAEVGVYY, was covalently bonded to alginate utilizing aqueous carbodiimide chemistry as has been previously described for fabricating alginate gels modified with other peptide sequences[33].

Briefly, in what is essentially a protected nucleophilic acyl substitution reaction, the carbodiimide approach to peptide bonding was used to form amide linkages between the N-terminus of the binding peptide and the carboxylate moieties on the mannuronic acid and guluronic acid residues of the alginate backbone. Medium viscosity alginate (FMC Biopolymer, Drammen, Norway) was suspended in 100 mM

MES (2-N-Morpholino ethane sulfonic acid) buffer with 300 mM NaCl at pH 6.5 to make a 1% alginate solution. EDAC (l-ethyl-dimethylaminopropyl carbodiimide) and Sulfo-NHS ((N-hydroxy-sulfosuccinimide) were added to the alginate solution at molar ratios of 5% and 2.5% of the guluronate content of the alginate respectively. Finally, the TGF-β binding peptide was added as 49.2 mg in 1 mg/ml MES buffer. The reaction was allowed to proceed at room temperature for approximately 20 hours and then the solution was transferred to 3500 MWCO dialysis tubing in a 4 liter solution of ddH_2O and NaCl. The dialysis bath was changed every 8 hours for three days, with the NaCl concentration being progressively lowered with each change. The peptide was dialyzed against pure water for the last 24 hours. The final contents of the dialysis tube was transferred to 50 ml conical tubes, frozen at -86ºC and lyophilized for approximately 48 hours, until dry. Unmodified alginate to be used as a control was processed exactly in parallel with the one exception that no peptide was added. The lyophilized alginates were resuspended as a 2% solution in PBS.

Reaction Efficiency. The efficiency of covalent addition of peptide addition to alginate was assessed using the BCA Protein Assay kit, (Pierce, Rockford, Il), according to the manufacturers instructions. Briefly, 25 µl of the of the peptide modified alginate in a 2% solution of PBS was combined with 200 µl of the BCA working reagent in a 96 well microplate. The plate was covered and mixed on a plate shaker for 30 seconds, and then incubated at 37ºC for 30 minutes. After incubation the plate was cooled to room temperature and absorbance was measured at 562 nm on an HTS 7000+ spectrophotometer (PE Wellesley, MA). Peptide content of the

modified alginate was determined by linear interpolation using 2% control alginate with varying concentrations of peptide directly added as a standard. All samples and standards were analyzed in triplicate, and the results averaged.

TGF-β1 Loaded Alginate Preparation. TGF-β1 (PeproTech) stock solution (50 μg/ml) was diluted 10:1, and 12 μl of the diluted stock solutions was combined with a separate 2 ml aliquot of a 2% solution of low viscosity alginate (FMC Biopolymer, Drammen, Norway) in PBS, making the concentration of TGF-β1 loaded alginate, 30 ng/ml. The alginate was then combined with a sterile solution of $CaSO_4$ (0.25g/ml) by thorough mixing through a sterile stopcock (David Scott, MA). The $CaSO_4$ solution was used at 0.04 milliliters per milliliter of alginate. The alginate/TGF-β1/$CaSO_4$ solution was then injected between two sterile glass electrophoresis plates with a 1 mm spacer, and allowed to gel for 30 minutes. Uniform alginate discs were cut from the gelled alginate with a 6mm dermal biopsy punch. Discs were collected and placed in an 8 well culture dish at 1.0 mg per well, covered with 9 mls of sterile PBS per well, sealed, and stored at 37ºC. Control alginate was prepared in parallel, without the addition of the TGF-β1 binding peptide.

In Vitro Release Studies. The *in vitro* release of TGF-β1 was analyzed for two conditions: peptide modified and control alginate at an initial loading concentration of 30 ng/ml. At each time point (days 0, 0.5, 1, 1.5, 2, 3, 4, 8, 12 and 16), the total fluid was collected for analysis, and replaced with fresh PBS.

Cumulative release of TGF-β1 over 16 days was determined by ELISA. Each condition was run in duplicate and the results averaged.

TGF-β1 Elisa. TGF-β1 content was determined using the TGF-β1 E_{max} ImmunoAssay System (Promega, Maddison, WI), according to the manufacturer's instructions. Briefly, 10 µl of the provided TGF-β1 capture antibody was combined with 10 mls of carbonate coating buffer (025M $NaHCO_3$, 0.025 $NaCO_3$), mixed thoroughly, and added at 100 µl per well to a 96 well polystyrene ELISA plate (Corning Life Sciences, Lowell, MA). This plate was sealed and incubated statically at 4ºC overnight. The plate was allowed to return to room temperature, emptied, and 270 µl of the supplied TGF-β1 blocking buffer was added to each well, statically incubated at 37ºC for 35 minutes, then washed once in prepared TBST wash buffer (20mM Tris-HCl (pH 7.6), 150mM NaCl, 0.05% Tween 20). Serial dilutions of the provided TGF-β1 standard was added at 100 µl per well to make a standard curve with a range from 0-1000 pg/ml. Samples were added at 100 µl per well, and the plates were incubated for 90 minutes on a plate shaker at room temperature. The provided anti-TGF-β1 antibody, diluted 1000:1 in the sample buffer, was added at 100µl per well, the plate was incubated on plate shaker at room temperature for two hours, then washed 5 times with TBST wash buffer. TGF-β1 HRP Conjugate diluted 1:100 was added at 100µl/well, incubated on a plate shaker for 2 hours at room temperature, and washed 5 times with TBST wash buffer. The provided TMB One Solution was added at 100 µl per well, and statically incubated at room temperature

for 15 minutes. The reaction was stopped by adding 1N hydrochloric acid at 100 µl per well. The plate was read on an HTS 7000+ spectrophotometer (Perkin-Elmer, Wellesley, MA) plate reader at 450 nm, and TGF-β1 was calculated by linear interpolation with the provided TGF-β1 standard. All samples and standards were analyzed in duplicate and the results averaged.

Statistical Analysis. The results are displayed as the mean ± a standard deviation. Statistical difference between means at each time point was evaluated by an unpaired two-tailed t-test. The threshold for statistical significance was taken to be $p < 0.05$.

Results

Carbodiimide Efficiency. The efficiency of covalent peptide addition to alginate was determined by the BCA Protein Assay Kit and linear interpolation of prepared standards of alginate with known amounts of added peptide. The calculated efficiency of the reaction was 60%, which is consistent with prior report of the efficiency of the carbodiimide process using alginate and different peptides[34]. (Figure 1) This consistency substantiates that hydrogel polymers, such as alginate, that are subject to solution chemistry and have abundant free carboxylate moieties that are readily and predictably modified by carbodiimide chemistry.

TGF-β1in vitro release. The *in vitro* release of TGF-β1 from peptide-modified and control alginate was determined using a commercially available TGF-β1 ELISA kit. The releasate was analyzed at 0, 0.5, 1, 1.5, 2, 3, 4, 8, 12, and 16 days. The release of TGF-β1 was affected by incorporation into the peptide-modified alginate compared to control alginate. The release profile from the control alginate was notable for an early burst, with 42% of the originally loaded TGF-β1 being released within the first 12 hours. After this there was a fairly slow, but steady release of TGF-β1 of about 2 ng per day. The peptide-modified alginate also demonstrated a burst release pattern, but the burst was delayed until day 3. Then again, as with the unmodified control alginate, there was a fairly slow and steady release of TGF-β1 through 16 days. At the end of 16 days more than 90% of the originally loaded TGF-β1 from both peptide-modified and control alginate had been released. The difference

between the mean release of TGF-β1 from peptide-modified and control alginate was only statistically significant ($p < 0.001$) through 3 days.

Discussion

The goal of the current study was to evaluate the efficiency of carbodiimide chemistry to covalently add a newly discovered growth factor binding peptide to sodium alginate, and to then characterize the effect that peptide had on the release of TGF-β1 from gelled 2% calcium alginate constructs *in vitro*.

The carbodiimide chemistry achieved an efficiency of 60%, which is remarkably consistent with published results for the covalent addition of other peptides to alginate. For a polymer scaffold to effectively serve as a temporary synthetic ECM in tissue engineering applications it will have to do more than simply provide a rigid framework. The ability to easily and reproducibly add a wide variety of peptides to alginate in principal should allow it to more precisely fulfill its intended role. Alginate gels with attached peptides can begin to take on the regulation of cell adhesion and the sequestration and controlled release of growth factors and other biologically active molecules.

The peptide-modified alginate showed different release kinetics compared to control alginate, principally in delaying a burst release of TGF-β1 from within the first 12 hours, to between 48 and 72 hours. These results are encouraging, as any ability to control the timing and dose of growth factor delivery has enormous potential utility for tissue engineering applications. Further work will need to be done to fully characterize the system in this study. Control alginate in the next phase will use a

"dummy" peptide with no growth factor binding properties to establish that the peptide itself does not alter the alginate gel in some way as to alter release kinetics. The concentration of TGF-β1 and growth factor binding peptide in future studies will be varied in order to evaluate whether or not the reported specific binding of TGF-β1 is retained after covalent addition to alginate, and if so, what the affinity is. With a known affinity, fabricating constructs with appropriate peptide density and TGF-β1 concentration, it might be possible to control the rate of TGF-β1 release.

REFERENCES

1. www.arthritis.org; accessed May 2003

2. Langer R, Vacanti JP. Tissue engineering. *Science* 1993; 920:260–266.

3. Cohen NP, Foster RJ, Mow VC. Composition and dynamics of articular cartilage: structure, function, and maintaining healthy state. *J Orthop Sports* Phys Ther 1998; 28:203-15.

4. Crooks CA, Dougles JA, Broughton RL, Sefton MV. A submerged jet process for the microencapsulation of mammalian cells in a HEMA-MMA copolymer. *J Biomed Mater Res* 1990; 24:1241-62.

5. Lim F, Sun AM. Microencapsulated islets as bioartificial endocrine pancreas. *Science* 1980; 210:908-10.

6. Atala A, Kim W, Paige KT, Vacanti CA, Retik AB. Endoscopic treatment of vesicoureteral reßux with a chondrocyte-alginate suspension. *J Urol* 1994;152:641-3.

7. Jen AC, Wake MC, Mikos AG. Review: hydrogels for cell immobilization. *Biotechnol Bioeng* 1996;50:357-64.

8. Putnam AJ, Mooney DJ. Tissue engineering using synthetic extracellular matrices. *Nature Med* 1996;2:82-6.

9. Shoichet MS, Li RH, White ML, Winn SR. Stability of hydrogels used in cell encapsulation: an in vitro comparison of alginate and agarose. *Biotechnol Bioeng* 1996;50:37-81.

10. Beekman B, Verzijl N, Bank RA, von der Mark K, TeKoppe JM. Synthesis of collagen by bovine chondrocytes cultured in alginate: Posttranslational modifications and cell-matrix interaction. *Exp Cell Res* 1997;237(1):135–141.

11. Guo JF, Jourdian GW, MacCallum DK. Culture and growth characteristics of chondrocytes encapsulated in alginate beads. *Connect Tissue Res* 1989;19(2–4):277–297.

12. Hauselmann HJ, Fernandes RJ, Mok SS, Schmid TM, Block JA, Aydelotte MB, Kuettner KE, Thonar EJ. Phenotypic stability of bovine articular chondrocytes after long-term culture in alginate beads. *J Cell Sci* 1994;107(1):17–27.

13. Hauselmann HJ, Aydelotte MB, Schumacher BL, Kuettner KE, Gitelis SH, Thonar EJ. Synthesis and turnover of proteoglycans by human and bovine adult articular chondrocytes culture in alginate beads. *Matrix* 1992;12(2):116–129.

14. ME Hott, CA Megerian, R Beane, LJ Bonassar. Fabrication of Tissue Engineered Tympanic Membrane Patches Using Computer-Aided Design and Injection Molding *Laryngoscope* 2004;114(7):1290-1295

15. Stevens MM, Marini RP, Martin I, et al. FGF-2 enhances TGF-beta1-induced periosteal chondrogenesis. *J Orthop Res* 2004; 22:1114–1119.

16. Lee JE, Kim KE, Kwon IC, et al. Effects of the controlled-released TGF-beta 1 from chitosan microspheres on chondrocytes cultured in a collagen/chitosan/glycosaminoglycan scaffold. *Biomaterials* 2004; 25:4163–4173.

17. Barbero A, Grogan S, Schafer D, et al. Age related changes in human articular chondrocyte yield, proliferation and post-expansion chondrogenic capacity. *Osteoarthritis Cartilage* 2004; 12:476–484.

18. Tay AG, Farhadi J, Suetterlin R, et al. Cell yield, proliferation, and

postexpansion differentiation capacity of human ear, nasal, and rib chondrocytes. *Tissue Eng* 2004; 10:762–770.

19. Hegewald AA, Ringe J, Bartel J, et al. Hyaluronic acid and autologous synovial fluid induce chondrogenic differentiation of equine mesenchymal stem cells: a preliminary study. *Tissue Cell* 2004; 36:431–438.

20. Glowacki J, Yates K, Maclean R, Mizuno S. In vitro engineering of cartilage: effects of serum substitutes, TGF-beta, and IL-1alpha. *Orthod Craniofac Res* 2005; 8:200–208.

21. Vunjak-Novakovic G, Meinel L, Altman G, Kaplan D. Bioreactor cultivation of osteochondral grafts. *Orthod Craniofac Res* 2005; 8:209–218.

22. Chua KH, Aminuddin BS, Fuzina NH, Ruszymah BH. Interaction between insulin-like growth factor-1 with other growth factors in serum depleted culture medium for human cartilage engineering. *Med J Malaysia* 2004; 59 (Suppl B):7–8.

23. Indrawattana N, Chen G, Tadokoro M, et al. Growth factor combination for chondrogenic induction from human mesenchymal stem cell. *Biochem Biophys* Res Commun 2004; 320:914–919.

24. Wang Y, Kim UJ, Blasioli DJ, et al. In vitro cartilage tissue engineering with 3D porous aqueous-derived silk scaffolds and mesenchymal stem cells. Biomaterials 2005; 26:7082–7094.

25. Morales TI, Joyce ME, Sobel ME, Danielpour D, Roberts AB. Transforming growth factor-beta in calf articular cartilage organ cultures: synthesis and distribution. Arch Biochem Biophys 1991;288(2):397–405.

26. Ferguson CM, Schwarz EM, Puzas JE, *et al*: Transforming growth factor-1 induced alteration of skeletal morphogenesis in vivo. *J Ortho Res* 2004;22: 687–696.

27. Caterson EJ, Li WJ, Nesti LJ, *et al*: Polymer/alginate amalgam for cartilage tissue engineering. *Ann N Y Acad Sci* 2002;961: 134–138.

28. Miura Y, Parvizi J, Fitzsimmons JS, *et al*: Brief exposure to high dose transforming growth factor-1 enhances periosteal chondrogenesis in vitro. *J Bone and Joint Surg Am* 2002; 84: 793–799.

29. Lee KH, Song SU, Hwang TS, *et al*: Regeneration of hyaline cartilage by cell-mediated gene therapy using transforming growth factor-1 producing

fibroblasts. *Hum Gene Ther* 2001;12:1805–1813.

30. Rosier RN, O'Keefe, RJ, Crabb ID, *et al*: Transforming growth factor beta: an autocrine regulator of chondrocytes. *Connect Tissue Res* 1989; 20: 295–301, 1989.

31. Redini F, Min W, Demoor-Fossard M, *et al*: Differential expression of membrane-anchored proteoglycans in rabbit articular chondrocytes cultured in monolayers and in alginate beads: Effect of transforming growth factor-beta1. *Biochem Biophys Acta* 1997; 1355:20–32.

32. Barrett AJ, Starkey PM. The interaction of α2-macroglobulin with proteinases. Characteristics and specificity of the reaction and a hypothesis concerning its molecular mechanism. *Biochem J* 1973; 133:709–724.

33. Sottrup-Jensen L, Stepanik,TM, Kristensen T, Wierzbicki DM, Jones CM, Lonblad LB, Magnusson S, Petersen TE. Primary structure of human α2-macroglobulin. V. The complete structure. *J Biol Chem* 1984; 259:8318–8327.

34. Rowley JG, Madlambayan, and DJ. Mooney. Alginate hydrogels as synthetic extracellular matrix materials. *Biomaterials* 1999. 20(1):45-5334.

35. Webb DJ, Roadcap DW, Dhakephalkar A, and Gonias SL. A 16-amino acid peptide from human α2-macroglobulin binds transforming growth factor-b and platelet-derived growth factor-BB *Protein Science* 2000; 9:1986–1992

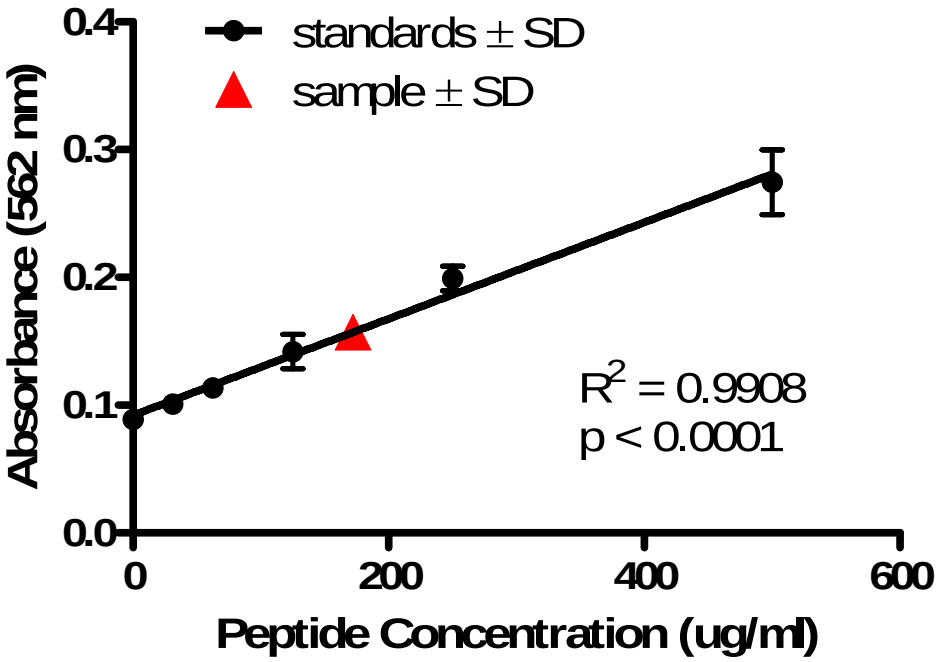
standards ± SD
sample ± SD
Absorbance (562 nm)
0.4
0.3
0.2
0.1
0.0
0
200
400
600
Peptide Concentration (ug/ml)
R2 = 0.9908
p < 0.0001

Figure 1

Characterization of efficiency of carbodiimide peptide linkage to sodium alginate. Using standard carbodiimide chemistry 60% of the added peptide was successfully incorporated, via peptide linkages, to the alginate backbone.

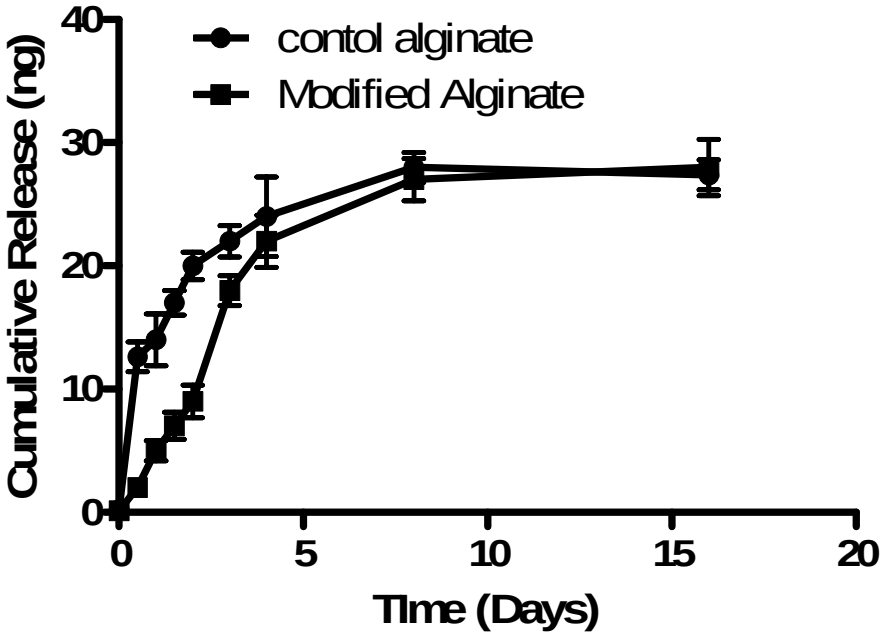
contol alginate
Modified Alginate
Cumulative Release (ng)
40
30
20
10
0
0
5
10
15
20
TIme (Days)

Figure 2

Cumulative release of TGF-β1 from peptide-modified and control alginate. All points represent mean ± a standard deviation. Means at all time points were compared by an unpaired two-tailed t-test. There was significantly more TGF-β1 released in the control alginate ($p < 0.001$) until day three.

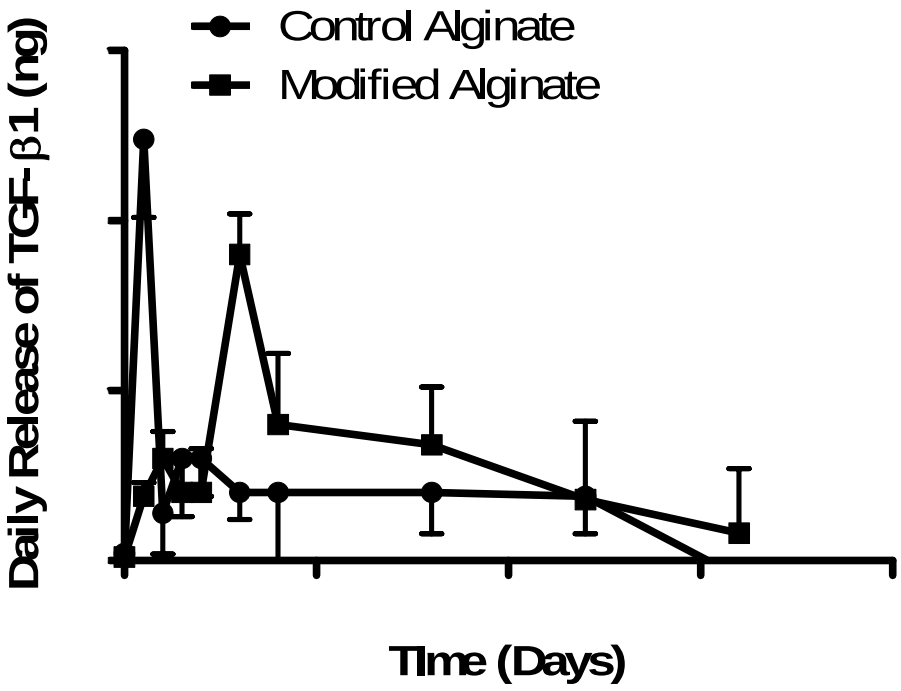
Control Alginate
Modified Alginate
Daily Release of TGF-β1 (ng)
Time (Days)

Figure 3

Daily release of TGF-β1 from peptide-modified and control alginate. A burst release of TGF-β1 can be seen at day 0.5 in the control and at day 3 in the peptide-modified alginate.

CHAPTER 4

EXPERIMENTAL ENDOLYMPHATIC HYDROPS QUANTIFICATION VERSUS HEARING THRESHOLDS IN THE ALBINO GUINEA PIG

Abstract

Hypothesis. Histological analysis of hydropic and normal guinea pig cochleae was undertaken to assess potential correlation between the magnitude of endolymphatic hydrops and hearing loss. We hypothesize that a greater correlation than previously reported may be found by looking at well developed hydrops and high frequency range hearing.

Background. Surgically induced endolymphatic hydrops in guinea pigs is the most widely used animal model for the study of human Menière's syndrome (endolymphatic hydrops, tinnitus, and progressive sensorineural hearing loss). A strong correlation between magnitude of hydrops and severity of hearing loss has been reported in the human condition, but not in animal models.

Methods. Nine guinea pigs were operated on to destroy the endolymphatic sac of the right ear, with left ears remaining as internal controls. Hearing was assessed from 2 kHz to 32 kHz by auditory brain stem response for 6 to 25 weeks post surgery. Histological morphometry post sacrifice was used to quantify both turn-specific, and weighted, overall hydrops These measures were correlated with hearing loss in each animal at all tested frequencies.

Results. A statistically significant relationship between the magnitude of hydrops and the severity of hearing loss was found for 2 kHz and 16 kHz. These frequencies correlated with both turn-specific hydrops and overall hydrops.

Conclusions. There may be a greater correlation between hydrops and hearing loss in guinea pigs with surgically induced hydrops than previously reported. This helps to validate the model and highlights the necessity of treatment modalities aimed at reducing hydrops.

Introduction

Since its introduction by Kimura and Schuknecht in 1965, surgical induction of endolymphatic hydrops in the guinea pig has become the standard model for the study of Menière's syndrome.[1] This procedure works by blocking the resorption of endolymph, and has been readily adopted because it reliably produces both histological hydrops and hearing loss. There remain, though, issues regarding the model's utility. At this time it is not clear that the characteristic vestibular symptoms of Menière's syndrome are reproduced in the animal model, or even whether the basic physiology of hydrops production is the same as in the human condition. Endolymphatic hydrops is a state of excess endolymph in the scala media, so it can occur due to insufficient resorption of endolymph, excess production of endolymph, or some combination of the two. At this time it is unknown what causes hydrops in Menière's syndrome, so it remains a challenge to understand how best to model the human condition. In contrast to the surgical model there are "over production" models that have been developed that like the surgical model produce both histological hydrops and hearing loss. These include the introduction of cholera toxin into the inner ear and various techniques for the induction of inner ear autoimmune disease.[2-4] Because the mechanism of hydrops production is different in overproduction models than in the surgical model it is possible that the pathophysiology of hearing loss is also different. At this time it is still unclear whether one of these models better replicates the auditory and cochlear pathology seen in Menière's syndrome, so it is important to continue the work of characterizing

all animal models as thoroughly as possible. Since surgical induction is still by far the most common method for producing experimental endolymphatic hydrops it is particularly important to characterize the pathology in this model so that its relevance to Menière's syndrome can be fully appreciated.

While many of the morphological changes in the hydropic cochlea have been described, the mechanism for hearing loss in surgically induced hydrops remains controversial. It has been noted that distortion of the scala media secondary to hydrops is associated with loss of hair cells in the upper two turns of the cochlea in both human Menière's syndrome and surgically induced hydrops.[5-6] Since high frequency hearing is ultimately affected, though, these same studies imply a poor relationship between hair cell loss and degree of hearing loss. In this regard the model fits the disease well, but does not explain the phenomenon.

The chief morphological feature of Menière's syndrome is the distention of Reisner's membrane. While it is widely known that this distention does not occur uniformly throughout the cochlea, there remains no good explanation as to why one part of Reisner's membrane might distort differently than another. It has also been noted that in both the human condition and the animal model hearing loss follows a distinctive pattern: the so called "peak audiogram", followed finally by a uniform hearing loss. That is to say, hearing is lost initially in the low frequencies, then the high frequencies, followed lastly by the mid frequencies.[7-8] Because of the tonotopic

tuning of the cochlea and the fact that neither hearing loss nor Reisner's membrane distension occur uniformly, it is natural to question whether or not there is a correlation between the two phenomena. Several studies have looked for a quantitative relationship between the degree of hydrops that develops and the severity of hearing loss in the animal model, but on the whole have found little or no direct correlation.[4, 9-10] This is important because in a very thorough study by Fraysse et al. a strong correlation between the magnitude of hydrops and hearing loss was established in a study of audiograms and archived temporal bones from patients with diagnosed Menière's syndrome.[11]

Comparisons between previous studies correlating a mathematically quantified measure of hydrops and hearing loss in animal models with Fraysse et al.'s human findings are difficult for several reasons. Researchers comparing hydrops and hearing loss in animals have used the guinea pig, but no studies attempting to quantitatively correlate hydrops and hearing loss to date have looked at any hearing frequencies beyond 8 kHz. Because guinea pigs can hear up to around 50 kHz, none of these studies has looked into the higher ranges for evidence of hearing loss (12). Interestingly, in Frassye et al.'s study the only area where there was not a strong correlation was in the low (0.25 kHz) frequency range. Hence, the possibility exists that animal studies that exclude the high frequency will miss a correlation between hearing loss and hydrops. Also, almost without exception previous studies have only looked at hydrops very early in its course of development. Fraysse et al. examined

temporal bones from patients with long-standing hydrops. For these reasons a thorough histological analysis of well developed surgically induced hydrops in the guinea pig was undertaken with an effort to fully characterize the pattern and magnitude of hydrops via detailed measurements and determine the correlation to hearing loss severity across a more representative length of the guinea pig dynamic range (2 kHz-32 kKz). In addition, this study is designed to better describe the distribution and severity of hydrops across the four turns of the guinea pig cochlea in order to document the relative turn specific severity of hydrops and any correlation to magnitude and frequency of hearing loss.

Methods and Materials

Materials. The experiment was carried out using 9 female albino guinea pigs (Duncan-Hartley strain) each initially weighing 250-300 grams obtained from the Charles River Breeding Labs (Wilmington, MA). Guinea pigs were anesthetized by administration of pentobarbital (16.67mg/kg, IP), xylazine (3.46mg/kg. IM), and ketamine (17.28mg/kg, IM). Body temperature was maintained with an electric heating pad (Harvard Apparatus, Holliston, MA). All animals were treated in accordance with the NIH Guide for the Care and Use of Laboratory Animals, and the protocol was approved by the Animal Care Committee at the University of Massachusetts Medical School.

Measurement of Hearing Thresholds. All hearing thresholds were obtained using Intelligent Hearing Systems' Auditory Brainstem Response (ABR) system, version 3.6x (Intelligent Hearing Systems, Miami, Fl) A custom made sound source was used that is described in detail elsewhere (14). Briefly, the sound source was fit securely into the external auditory canal of the guinea pig. The sound source consisted of a Radio Shack 40-1377 'Super Tweeter' high-frequency dynamic speaker, a brass ear bar to direct sound into the ear canal, and a coupler to attach the ear bar to the speaker. Subdermal needle electrodes were placed at the midline scalp and retroauricularly. Electrical activity was amplified 100,000 times and was filtered (0.1-3 kHz) with a bioamplifier. The signal was digitized by an MII signal averaging system and an IBM PC clone. Each response was the average of 1024 sweeps

presented at a rate of 19.3 Hz and was stored on the PC clone. Threshold of hearing was determined to plus or minus 5 dB SPL for frequencies of 2 kHz, 4kHz, 8kHz, 16kHz, and 32kHz. Examples of audiograms are shown in FIGURES 1 and 2.

Induction of hydrops. Guinea pigs were anesthetized as described earlier and right-side unilateral endolymphatic hydrops was induced as described by Kimura and Schuknecht (1). Briefly, the endolymphatic sac and duct were entered through a posterior cranial fossa approach, and a small surgical drill was used to enter and obliterate the endolymphatic sac and duct, the remains of which were packed with bone wax. All right ears were operated on and all left ears were kept as internal controls. Post-operatively sulfonamide antibiotics and one dose of liquid Tylenol were included in the drinking water of all animals.

Histology Processing. All animals were sacrificed between 16 and 25 weeks post surgery. Animals were deeply anesthetized by administration of pentobarbital (33.33mg/kg, IP), xylazine (6.9mg/kg. IM), and ketamine (34.57mg/kg, IM). Following induction of deep anesthesia, animals were transcardially perfused with normal saline supplemented with heparin (10 units/liter) and sodium nitrite (69mg/liter), followed by transcardial perfusion with 10% buffered formalin. Fully fixed animals were decapitated and their temporal bones dissected out en-bloc. The bullae were opened and the temporal bones were stored fully submerged in 10% buffered formalin. After all animals had been sacrificed the temporal bones were sent

to the University of Minnesota temporal bone lab where they were decalcified and embedded in celloidin. After hardening the specimens were cut into 14 μm sections along the mid-modiolar plane. Every 5th slide was mounted and stained with Hematoxylin and Eosin for histologic analysis.

Histological Analysis. Quantification of hydrops requires some measure of the relative volume of scala media in a hydropic ear compared to a normal ear. The most widely used methods for making this determination involve using histological morphometry. Two approaches researchers have taken are to either use a ratio of the measured length of Reisner's membrane in a hydropic cochlea to the straight distance between its normal lateral and medial attachment points,[4] or to directly measure the scala media area.[11] We chose to take scala media measurements because this more directly relates to scala media volume, the true measure of hydrops.

Sections were photographed with a Spot Jr. digital camera (Micro Video Instruments, Avon MA) connected to a Nikon TE300 microscope. All image analysis was done with MetaView 4.0 (Universal Imaging Corporation, Downington, PA). Representative images are shown in FIGURES 3 and 4. Hydrops was determined by a modified version of a technique described by Klis et al.[10] Every slide where it was possible to measure the area of both the scala media (SM) and the scala vestibuli (SV) on both sides of the modiolus was studied. In order to determine a relative measure of the degree of hydrops in the operated versus the control ear we first calculated a value

we refer to as the proportion scala media (PSM). This is simply the proportion of the combined SM and SV space that is made up by SM. In formula:

$$PSM = \frac{\text{SM area}}{\text{SM area + SV area}}$$

We used this proportional measurement, as suggested by Klis et al. in order to compensate for any slight deviations in the plane of section between animals. The measurements taken on each slide were summed to give a measure of the total PSM for each cochlear turn. We then calculated a relative measure of hydrops in the operated versus the control ear that we refer to as the hydropic ratio (HR). This was calculated for each turn by dividing each turn's total PSM in the right ear by the total PSM for the same turn from the left ear. In formula:

$$HR = \frac{\text{Total right ear PSM}}{\text{Total left ear PSM}}$$

A hydropic ratio of 1 for a given turn would indicate that no hydrops had developed in that turn. Likewise, a hydropic ratio of 3 would indicate a 3-fold increase in volume in the scala media of a turn in the operated ear compared to the control ear. This differs from the technique of Klis et al. in that they took as a measure of hydrops the average of 2 representative measurements from each ear. Each measurement they used was from the most hydropic turn from a slide that clearly showed all four turns. With this technique one develops an overall measure of hydrops, but not one that is turn specific. For guinea pig 31 in our study histology for the left ear was inadequate to make measurements, so in lieu of measurements from that ear we used an average of the area measurements from the left ears of the other eight animals. By taking

measurements at all turns our technique allows for generation of both a turn specific hydropic ratio and an overall measure of hydrops. The overall measure of hydrops was made by averaging all the measurements for each turn in a single animal and then normalizing that value to the percentage of the total length of the cochlea made up by that turn and then adding the weighted values for each turn. As an alternative method we also divided the sum of the measurements taken in the right ear by the sum of the measurements taken in the left ear. Because of the different number of sections in different turns this inherently weights the measurements. The results were indistinguishable.

Determination of cochlear frequency position. To determine if the degree of hearing loss at a particular frequency was correlated with the degree of hydrops in the turn where that frequency is localized we needed to determine the location on the basilar membrane characteristic for the frequencies we tested. This information can be obtained from the cochlear frequency-position mapping done by Greenwood.[14-15] Greenwood developed a function that relates characteristic frequencies to a specific location along the basilar membrane. This function is $CF=A(10^{ax/L}-K)$, where A, a, and K are species specific constants, L is the cochlear length in millimeters, and x is the distance in millimeters from the apex of the cochlea. Current accepted values for the species specific constants for the guinea pig are: A=350, a=2.1, K=0.85, and L=18.5 (15). Since we were starting with known frequencies and wanted to know where they would be localized in the cochlea we rearranged the Greenwood function to calculate a characteristic location given a specific frequency. The rearranged

function is: X=((L)Log(CF + AK)-(L)LogA)/a). Solving for x for the frequencies we tested yielded the data in TABLE 1.

We compared these lengths to the distances to the center of each cochlear turn. The distance from the base of the cochlea to the midpoint of each turn in the scala tympani of guinea pigs has been previously determined by Alec Salt.[16] His measurements, though, were taken along a different line through the cochlea than Greenwood's. Because of this difference Salt took the full length of the cochlea to be 16.4 mm rather than the 18.5 mm determined by Greenwood. To compensate for this we converted the distance from the base reported by Salt to a percentage of the whole cochlear length, which we then multiplied by 18.5. This yields the distance from the base to the center of each turn along the basilar membrane. These data are shown in TALBE 2. Because the frequencies we tested did not for the most part fall precisely mid-turn we used these numbers as a guide to estimate which turns would be most involved for each frequency. These data are shown in TABLE 3.

Hearing thresholds and histological HRs were determined for nine animals. Hearing loss at frequencies characteristic of each cochlear turn was correlated with HR for each cochlear turn. Additionally a weighted overall measure of hydrops was correlated with hearing loss at all 5 tested frequencies. Results of the HR for each turn for all animals and the average HR of all animals at each turn are shown in TABLES 4 and 5. The HR revealed that both apical and basilar turns were found to demonstrate the most significant deviations from normal (TABLE 5).

The relationship between hearing loss and HR was determined by calculating a correlation coefficient between these variables. This was calculated for the relationship between hearing loss at all tested frequencies and the HR for each individual turn and a weighted overall measure of hydrops. The weighted measure was determined by normalizing each turns HR to that turns volume percentage of the cochlea. The only statistically significant correlations were found for HR with 2 kHz and 16 kHz. These showed a statistically significant relationship to hearing loss in both the cochlear turn specific measurements and in the measurement of overall hydrops. Interestingly, though, the significant correlation found in the turn specific measurements did not arise in the turns most characteristic for those frequencies.

Statistical data summarizing our findings for the correlation between the HR in each individual turn and hearing loss are shown in TABLE 6. Only statistically significant relationships are shown with a p value. Statistical data summarizing our findings for the correlation between weighted whole cochlear hydrops and hearing loss are shown in TABLE 7. Again, p values are only given for statistically significant results. FIGURES 8 and 9 show representative graphs of significant correlations between turn specific HRs and hearing loss and weighted overall HRs and hearing loss respectively.

Our histological analysis provides a more thorough estimate of actual scala media volume than has been previously reported in animal studies utilizing histological techniques. To assess the efficacy of our technique we compared the

overall HR ratio calculated using our technique to the overall HR calculated using the technique of Klis et al. We then performed a correlation coefficient between the two HRs to see if they were statistically different. We could only do this for an overall measure of hydrops because Klis et al.'s method does not give turn specific data. Guinea pig 31 was not included in the comparison because we had inadequate histology in the left ear to duplicate the Klis method. The HRs are shown in TALBLE 8 and the correlation coefficient in FIGURE 7. These results show no statistical difference in the determination of overall hydrops, indicating that our more thorough histological analysis offers no advantage in estimating the overall degree of hydrops. It does, though, still have the advantage of being able to provide turn specific data on hydrops.

Discussion

We report for the first time a statistically significant correlation between the degree of hydrops and the degree of hearing loss in both low and high frequency ranges of guinea pigs with advanced surgically induced endolymphatic hydrops. Early reports of surgically induced endolymphatic hydrops as a model for Menière's syndrome report the qualitative relationship between the development of hydrops and hearing loss, but offer no statistical analysis.[17-18] In 1980 Fraysse et al. reported a relationship between hearing loss and a quantitative measure of hydrops from a retrospective temporal bone study of humans with Menière's syndrome. They reported a statistically significant correlation between overall degree of hydrops and hearing loss at all but the lowest frequencies. Further, they also reported a statistically significant relationship between the degree of hydrops in each cochlear turn and the hearing loss at the frequency characteristic for that turn for all cochlear turns with the exception of posterior middle (0.25 kHz). Since that time there have been a number of studies that correlated electrophysiologic measures of hearing with a quantification of hydrops in a variety of animal models of Menière's syndrome. Taken as a whole this work has shown only a weak correlation between the degree of hydrops and the amount of hearing loss that develops.

In 1990 Klis et al. reported a statistically significant correlation between overall hydrops and decrease in low frequency cochlear microphonics at 29 Hz in guinea pigs with surgically induced endolymphatic hydrops. They quantified hydrops

using a histologic approach using two slides per animal, with the most hydropic turn on a particular slide taken as a measure of the overall hydrops. They also looked at the relationship between degree of hydrops and the summating potential at 2 kHz and the action potential at 8 kHz, but found no correlation. We modified their technique by taking a measure of hydrops in all sections, and using the aggregate values as a measure of turn specific hydrops. This provides a far more extensive histologic analysis on which to base our estimates of hydrops.

Klis et al. speculate that the inconsistencies in finding a correlation may be due to differing electrophysiologic measures being more or less sensitive to various pathologies. While this may be true, it is also worth noting that hearing loss associated with endolymphatic hydrops follows a particular clinical course, with loss first developing in the lower frequencies, but ultimately progressing across the dynamic range. Klis et al. report on data that was pooled from animals sacrificed 2 and 4 weeks post surgery. This is very early in the development of hydrops, so it is possible that a relationship between hearing loss and hydrops may have developed at the higher frequencies if the pathology had progressed. Also the guinea pig hearing range extends to about 50 kHz, so at a highest frequency of 8 kHz, Klis et al. have not reported on the high frequency range.

In 2000 Bouman et al. reported on the relationship between a histologically quantified measure of hydrops and the summating potential at 2 kHz, 4 kHz, and 8

kHz in guinea pigs that had hydrops induced by an autoimmune protocol (4). They report no statistically significant relationship at any frequency. The measure of hydrops they used was an average of measurements taken from the basilar and suprabasilar turns in two slides. The middle of the basilar turn has a characteristic frequency of about 16 kHz and the suprabasilar turn of about 4 kHz, but they did not present this data separately. It is also important to remember that one should be careful about comparing these results to those of animals with surgically induced endolymphatic hydrops. It is not clear that the pathophysiology of hearing loss will be the same. Of particular note is that by six weeks past inoculation the animals in this study no longer appear hydropic. This is in striking contrast to surgically induced hydrops, which continues in time with progressive hydrops.

Our results show more correlation than previously reported, but still do not duplicate the results of Fraysse et al. Why there might be a difference at different frequencies remains to be explained, but it is of note that a statistically significant relationship was found in the high frequency range, which has previously not been reported on. The report by Fraysse et al. was in human temporal bones, and correlating the human to an animal model is fraught with difficulties. However, their findings of a correlation between hydrops and hearing loss magnitude are to some degree recapitulated now in the animal model. The reasons for this are likely multifactorial, and include the analysis of cases of advanced hydrops, detailed compilation of HR from the whole cochlea, as well as the measurement of hearing

changes in the high end of the guinea pig dynamic range. The explanation for why we found a correlation at 2000 Hz and 16,000 Hz only is speculative. It possibly relates to the manner in which pressure and anatomic changes impart injury or homeostatic changes to those particular portions of the cochlea. Whether the mechanism for hearing loss in hydrops is pressure related or due to direct mechanical changes imparted throughout the cochlea, though remains to be determined.

Our own study could perhaps have given more insight into these relationships if we had looked at lower frequencies, or used a better electrophysiological measure, such as compound action potentials. Nonetheless, the finding of greater correlation between hydrops and hearing loss than previously reported in animal studies has possible significance. Beyond working toward validating the common animal model this data perhaps sheds some light on appropriate treatment for human patients with Menière's syndrome. If in fact there is a reasonable correlation between hearing loss and the severity of hydrops, regardless of what the pathophysiology might be, this reinforces the need to vigilantly apply treatment modalities aimed at reducing hydrops.

References

1. Kimura RS, Schuknecht JF. Membranous hydrops in the inner ear of guinea pig after obliteration of the endolymphatic sac. *Pract Otorhinolaryngol* 1965;27:343-5.

2. Feldman AM, Brusilow SW. Effects of cholera toxin on cochlear endolymph production: Model for endolymphatic hydrops. *Proc Natl Acad Sci* 1976;73(5):1761-1764.

3. Lohuis PJFM, Klis SFL, Klop WMC, et al. Signs of endolymphatic hydrops after perilymphatic perfusion of the guinea pig cochlea with cholera toxin; a pharmacological model of acute endolymphatic hydrops. *Hearing Research* 1999;137:103-113.

4. Bouman H, Klis SFL, Meeuwsen F, et al. Experimental Autoimmune inner ear disease: an electrocochleographic and histophysiologic study. *Ann Otol Rhinol Laryngol* 2000;109:457-466.

5. Schuknecht HF, Northrop C, Igarashi M. Cochlear pathology after destruction of the endolymphatic sac in the cat. *Acta Otolaryngol* 1968;65:479-487.

6. Albers FWJ, Celdman JE, Huizing EH. Early hair cell loss in experimental

hydrops. *Ann Otol Rhinol Laryngol* 1987;96:282-285

7. Horner KC, Erre JP, Cazals Y. Asymmetry of evoked rotatory nystagmus in the guinea pig after experimental induction of Endolymphatic hydrops. *Acta Otolaryngol* 1989;468:65-69

8. Horner KC, Cazals Y. Contribution of increased Endolymphatic pressure to hearing loss in experimental hydrops. *Ann Otol Rinol Laryngol* 1991;100:496-502

9. Paparella MM, McDermott JC, De Sousa LCA. Meniere's disease and the peak audiogram. *Arch Otolaryngol* 1982;108:555-559

10. Klis SFL, Buijs J, Smoorenburg GF. Quantification of the relation between electrophysiologic and morphologic changes in experimental endolymphatic hydrops. *Ann Otol Rhinol Laryngol* 1990;99:566-570.

11. Fraysse BG, Alonso A, House WF. Menière's disease and endolymphatic hydrops. Clinical-histopathological correlation. *Ann Otol Rhinol Laryngol* 1980: 89(suppl 76):2-22.

12. McCormick JG, Nuttall AL. Auditory Research. In: Wagner JE, Manning PJ,

eds. *TheBiology of the Guinea Pig*. London: Academic Press, 1976;281-303

13. Megerian CA, Burkard RF, Ravicz ME. A Method for Determining Interaural Attenuation in Animal Models of Asymmetric Hearing Loss. *Audiol Neurootol* 1996;1:214-219

14. Greenwood DD. A cochlear frequency-position function for several species: 29 years later. *J Acoust Soc Am*. 1990;87(6):2592-2605.

15. Greenwood DD. Comparing octaves, frequency ranges, and cochlear-map curvature across species. *Hearing Research* 1996;94:157-162.

16. Cochlear Fluids Lab-Washington University http://oto.wustl.edu/cochlea/model/elec.htm . Accessed July 23, 2001.

17. van Deelen GW, Ruding PRJW, Smoorenburg GF, et al. Electrocochleographic changes in relation to cochlear histopathology in experimental endolymphatic hydrops. *Acta Otolaryngol* 1988;105:193-201.

18. Morizono T, Cohen J, Sikora MA. Measurement of action potential thresholds in experimental endolymphatic hydrops. *Ann Otol Rhinol Laryngol* 1985;94:191-194.

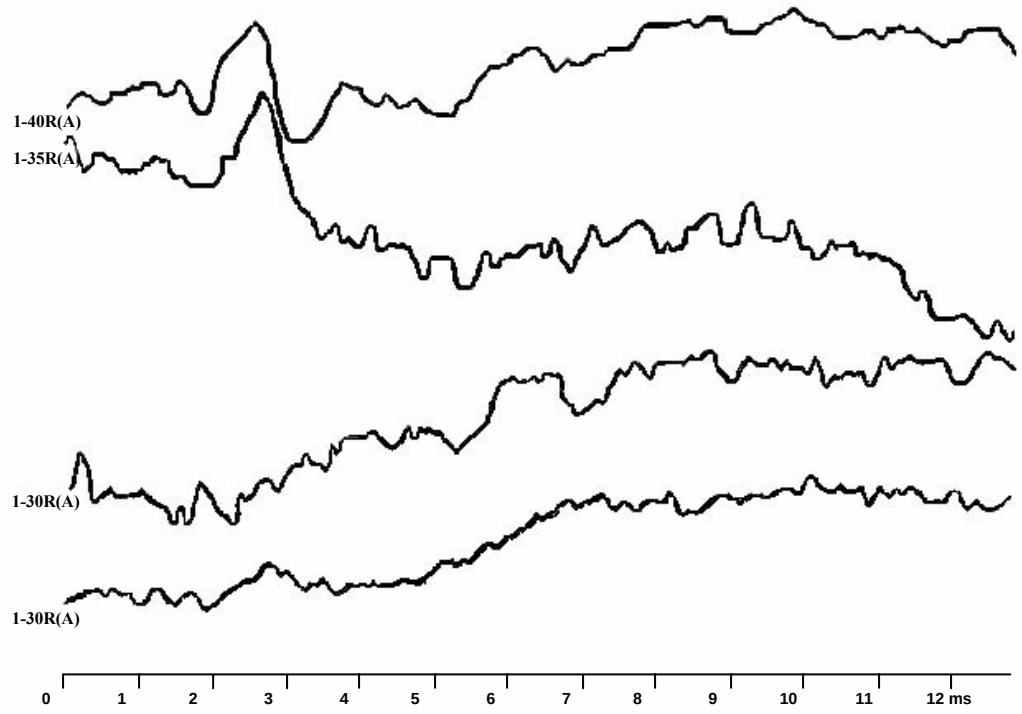

1: gpRA40A 5 Int:40 Ear:R Swp:1024 Art:3 Rate:19.3 Mode: Rare PP Amp:0.55uV:100.0K 100.0-3000.0Hz

2: gpRA30A 4 Int:30 Ear:R Swp:1024 Art:3 Rate:19.3 Mode: Rare PP Amp:0.27uV:100.0K 100.0-3000.0Hz

3: gpRA30A 5 Int:30 Ear:R Swp:1024 Art:5 Rate:19.3 Mode: Rare PP Amp:0.50uV:100.0K 100.0-3000.0Hz

4: gpRA35A 1 Int:35 Ear:R Swp:1024 Art:4 Rate:19.3 Mode: Rare PP Amp:0.35uV:100.0K 100.0-3000.0Hz

Figure 1:

Representative audiogram at 16,000 Hz (right ear) from a normal hearing animal before surgical obliteration of the endolymphatic duct and sac. Threshold was estimated at 35 dB SPL.

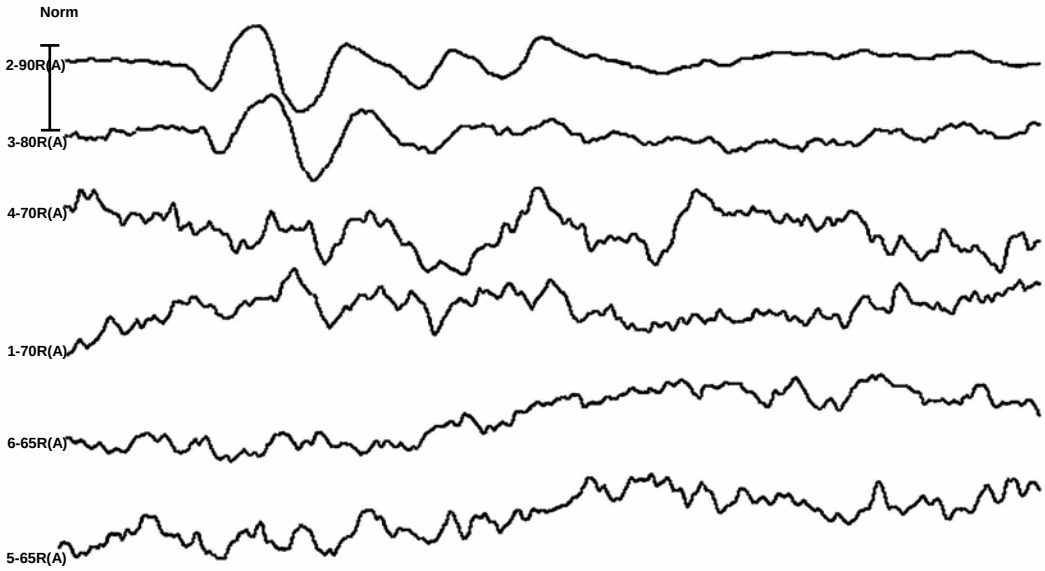

0 1 2 3 4 5 6 7 8 9 10 11 12 ms

Num	Filename	Int	Ear	Stim	Swps/Art	Rate	Mode	PP Amp	Gain (K)	HP (Hz)	LP(Hz)
1	gpRA70A.8	70SPL	R	16000Hz(1)	1024/0	19.3	Altr	0.23	100.0	100.0	3000.0
2	gpRA90A.4	90SPL	R	16000Hz(1)	491/0	19.3	Altr	1.96	100.0	100.0	3000.0
3	gpRA80A.5	80SPL	R	16000Hz(1)	411/0	19.3	Altr	0.84	100.0	100.0	3000.0
4	gpRA70A.9	70SPL	R	16000Hz(1)	1024/0	19.3	Altr	0.21	100.0	100.0	3000.0
5	gpRA65A.8	65SPL	R	16000Hz(1)	1024/0	19.3	Altr	0.22	100.0	100.0	3000.0
6	gpRA65A.9	65SPL	R	16000Hz(1)	1024/0	19.3	Altr	0.29	100.0	100.0	3000.0

Figure 2

Representative audiogram at 16,000 Hz (right ear) 22 weeks after surgical obliteration of the right endolymphatic duct and sac in the guinea pig presented in Figure 1. Threshold was estimated at 70 dB SPL, with an overall threshold shift of 35 dB SPL..

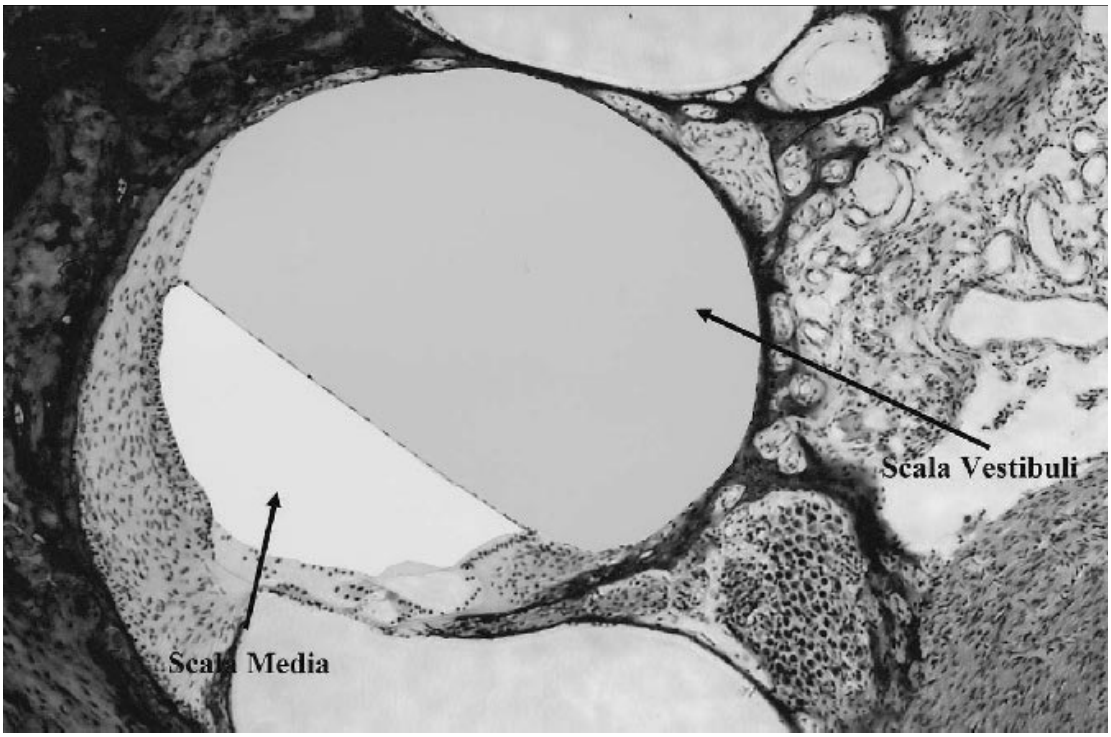
Scala Vestibuli
Scala Media

Figure 3

Morphometric analysis of a control (left) ear from guinea pig 35, showing measured scala media and scala vestibule areas (200x).

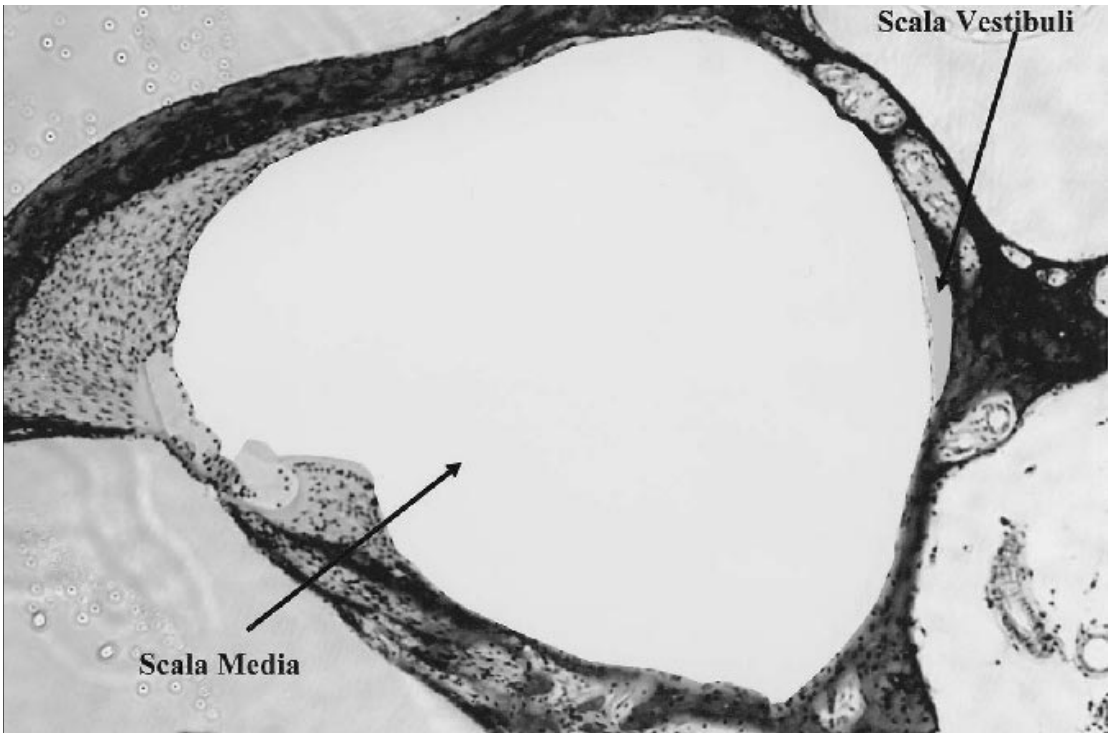
Scala Vestibuli
Scala Media

Figure 4

Morphometric analysis of the operated (right) ear from guinea pig 35, showing measured scala media and scala vestibule areas. Note dilatation of scala media indicating severe hydrops (200x).

Frequency	Distance from the apex
2000 Hz	7.2 mm
4000 Hz	9.6 mm
8000 Hz	12.1 mm
16000 Hz	14.7 mm
32,000 Hz	17.3 mm

Table 1
Tested hearing frequencies and their corresponding distance from the apex of the cochlea

Turn	Distance from the base measured in the scala tympani	Percentage from the apex	Distanced from the apex on the basilar membrane
basilar	2.1 mm	0.88	16.1 mm
supra-basilar	7.5 mm	0.54	10.0 mm
sub-apical	11.6 mm	0.29	5.3 mm
apical	15.1 mm	0.07	1.3 mm

Table 2

Conversion of distance from the base to distance from the apex, compensating for cochlear path.

Frequency	Representative turn
2,000 Hz	Turn 3 or Turn 2
4,000 Hz	Turn 2
8,000 Hz	Turn 2 or Turn 1
16,000 Hz	Turn 1 or Turn 2
32,000 Hz	Turn 1

Table 3
Estimated correlation between tested frequency and cochlear turn

animal	basilar turn	suprabasilar turn	subapical turn	apical turn
Gp 17	3.57	2.07	2.39	1.78
Gp 31	3.53	3.70	3.47	2.36
Gp 33	1.09	1.04	1.31	2.29
GP 34	1.75	1.15	1.55	2.60
Gp 35	4.5	3.31	3.34	2.96
Gp 36	7.36	4.53	4.32	2.29
Gp 37	5.76	3.91	3.69	2.72
Gp 42	1.30	0.86	0.93	1.25
Gp 51	1.61	1.93	3.52	2.91

Table 4
HR for all animals at all turns

turn	average hydropic ratio
Basilar	3.39
Suprabasilar	2.50
Subapical	2.72
Apical	3.35

Table 5
Cochlear turn versus average hydropic ratio (HR)

Turn	Frequency	R^2	p
1	2000 Hz	0.7003	0.0025<p<0.005
1	4000 Hz	0.3293	
1	8000 Hz	0.0385	
1	16,000 Hz	0.3690	
1	32,000 Hz	0.2204	
2	2000 Hz	0.6731	0.01<p<0.020
2	4000 Hz	0.2788	
2	8000 Hz	0.0172	
2	16,000 Hz	0.4286	0.025<p<0.05
2	32,000 Hz	0.1555	
3	2000 Hz	0.4450	0.025<p<0.05
3	4000 Hz	0.2535	
3	8000 Hz	0.0164	
3	16,000 Hz	0.5459	0.01<p<0.02
3	32,000 Hz	0.154	
4	2000 Hz	0.1769	
4	4000 Hz	0.0281	
4	8000 Hz	0.0296	
4	16,000 Hz	0.0459	
4	32,000 Hz	0.00003	

Table 6

Statistical data summarizing the correlation between the HR in each individual turn and hearing loss at the frequencies represented at those turns. Only statistically significant relationships are shown with a p value.

Frequency	R^2	p
2000 Hz	0.7433	0.005<p<0.01
4000 Hz	0.3265	
8000 Hz	0.0293	
16,000 Hz	0.6590	0.025<p<0.05
32,000 Hz	0.2046	

Table 7

Whole cochlea hydrops correlations with frequency.

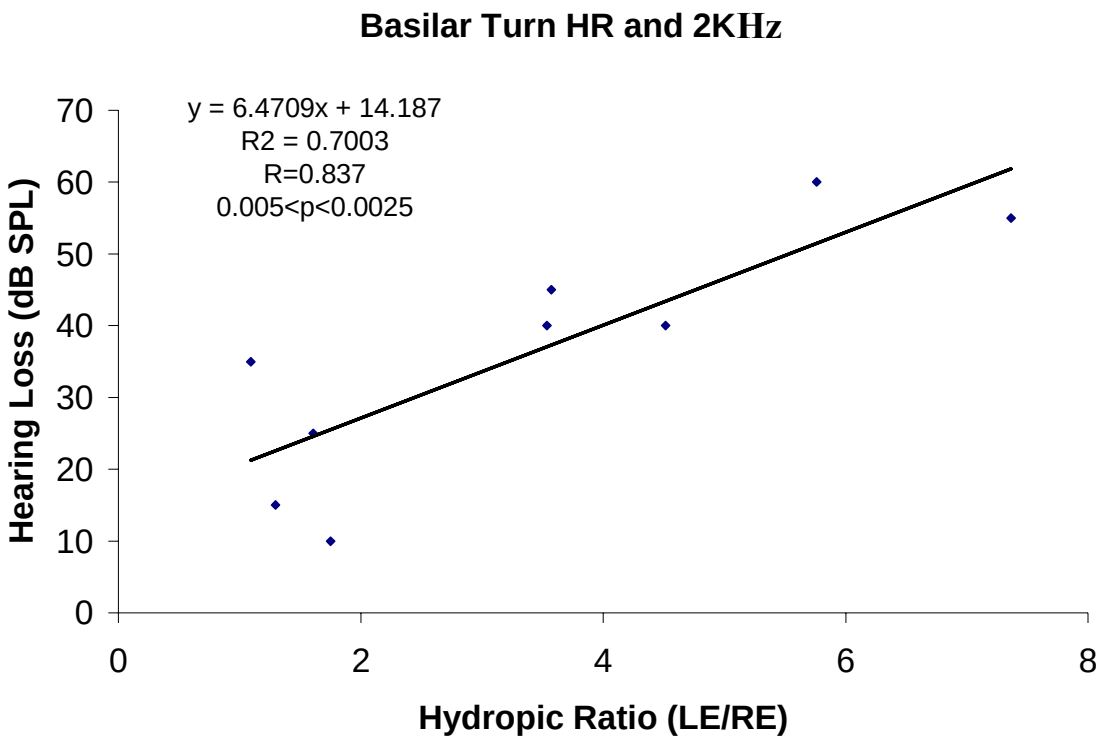
Basilar Turn HR and 2KHz
y = 6.4709x + 14.187
R2 = 0.7003
R=0.837
0.005<p<0.0025
Hearing Loss (dB SPL)
70
60
50
40
30
20
10
0
0
2
4
6
8
Hydropic Ratio (LE/RE)

Figure 5

Statistically significant correlation between the HR in the basilar turn and hearing

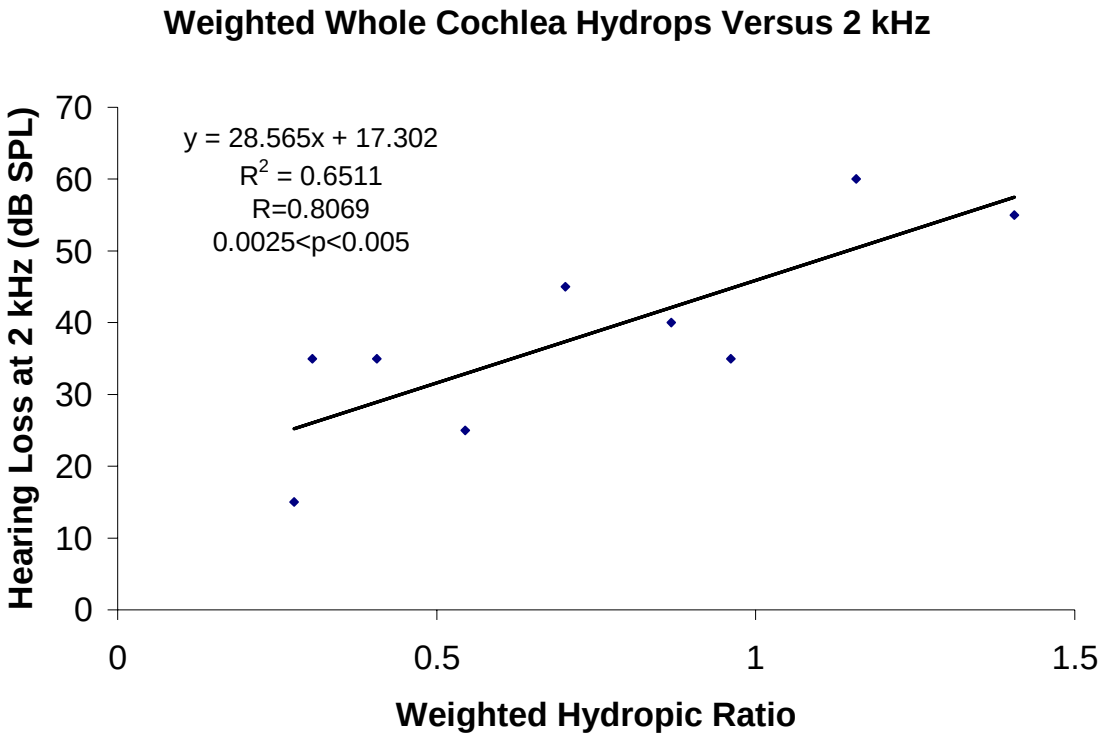
Weighted Whole Cochlea Hydrops Versus 2 kHz
y = 28.565x + 17.302
R2 = 0.6511
R=0.8069
0.0025<p<0.005
Hearing Loss at 2 kHz (dB SPL)
70
60
50
40
30
20
10
0
0
0.5
1
1.5
Weighted Hydropic Ratio

Figure 6

Statistically significant correlation between a weighted overall measure of HR and hearing loss at 2 kHz

Animal	HR (Klis)	HR (Hott)
gp17	2.81	3.52
gp33	1.22	2.36
gp34	1.63	1.63
gp35	3.84	3.40
gp36	5.62	7.06
gp37	4.63	8.44
gp42	1.11	1.00
gp51	2.18	3.70

Table 8

Comparison of overall HR calculated by counting all possible cochlear areas (Hott) and 2 representative areas per ear (Klis)

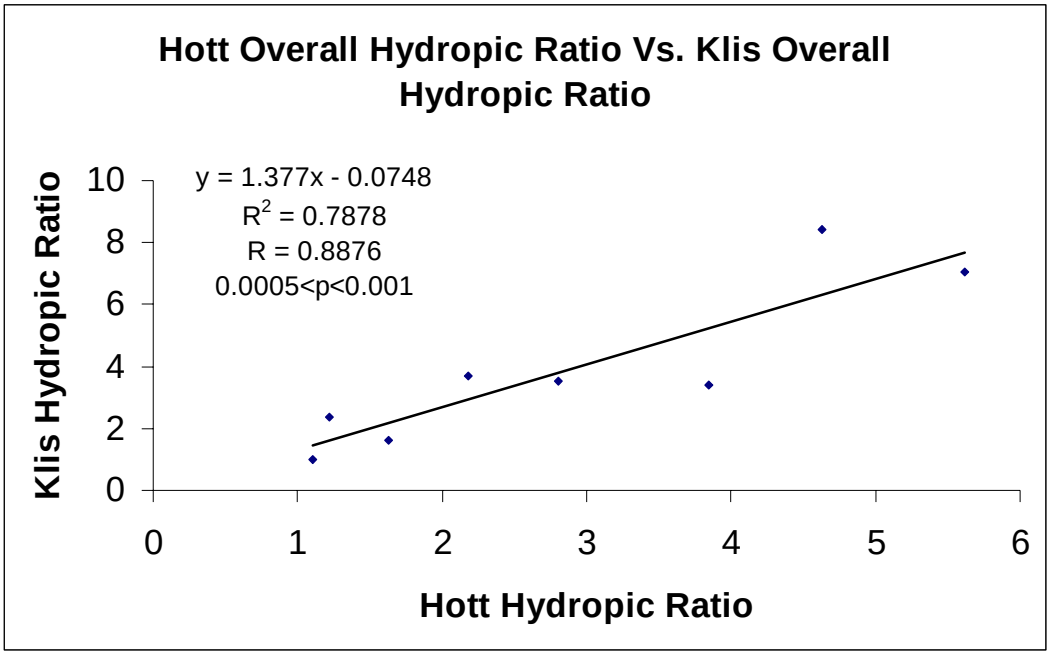
Hott Overall Hydropic Ratio Vs. Klis Overall Hydropic Ratio
y = 1.377x - 0.0748
R2 = 0.7878
R = 0.8876
0.0005<p<0.001
Klis Hydropic Ratio
Hott Hydropic Ratio
0
2
4
6
8
10
0
1
2
3
4
5
6

Figure 7

Correlation of Hott HR to Klis HR, showing no statistical difference between the two

CHAPTER 5

AMINOGUANIDINE ADMINISTRATION AND HEARING PRESERVATION IN EXPERIMENTAL ENDOLYMPHATIC HYDROPS IN THE ALBINO GUINEA PIG

Abstract

Objectives/Hypothesis. The goal of the current study was to evaluate the pharmacologic potential of aminoguanidine, a relatively specific inhibitor of the inducible isoform of nitric oxide synthase (iNOS), to protect against hearing loss in guinea pigs with surgically induced endolymphatic hydrops, the standard animal model for Menière's syndrome.

Methods. Right sided endolymphatic hydrops was surgically induced in 20 guinea pigs. Half were administered aminoguanidine in their drinking water for 22 weeks. Hearing thresholds were measured by auditory brainstem response (ABR) approximately every 2 weeks, and thresholds in treated and untreated animals were compared at 2 kHz, 4 kHz, 8 kHz, 16 kHz, and 32 kHz.

Results. Hearing was preserved in all unoperated ears and declined in all operated ears, though this was not statistically significant at 4 kHz and 8 kHz in the aminoguanidine treated group. Overall there was a statistically significant preservation of hearing in the treated verse the control group at all tested frequencies by 16 weeks.

Conclusions. Aminoguanidine appears to provide a neuroprotective effect in the hydropic cochlea that prevents hearing loss in animals with surgically induced

endolymphatic hydrops. These results are encouraging, and merit additional study to investigate the possibility of a hearing protective therapeutic intervention in humans.

Introduction

Menière's syndrome is a disorder that is characterized by idiopathic endolymphatic hydrops, with associated progressive sensorineural hearing loss and periodic tinnitus and vertigo. The reported incidence of Menière's syndrome in Europe and the United states has ranged from 7.5-157 per 100,000[1-2]. Menière's syndrome most commonly presents in patients 40-60 years of age with a slight increased incidence in women compared to men[3]. It typically presents initially with symptoms affecting a single ear, but can progress to involve the contralateral ear as well. Reports of the frequency of progression to the contralateral ear have varied widely, ranging from 2-78%[4]. It has been proposed that this unusually large range is probably related to differing diagnostic criteria and length of follow up, with the true value being closer to the higher end of the range[5].

Endolymphatic hydrops, somewhat analogous to edema of the inner ear, is a condition characterized by expansion of the scala media by excess endolymph. In principal this can be due to either an overproduction of endolymph or a lack of resorption of endolymph. However, it is not currently known whether overproduction, insufficient resorption, or a combination of these mechanisms is responsible for the findings in Menière's syndrome[7]. Further, while there is a well established association between endolymphatic hydrops and the clinical symptoms of Menière's syndrome, the mechanism by which this occurs is still a matter of speculation. The

continued lack of understanding of the pathogenesis of Menière's syndrome is in part due to a lack of understanding the basic mechanisms involved, but also, I suspect, reflects that the pathogenesis of the ubiquitous endolymphatic hydrops is likely multifactorial.

Recent studies have demonstrated a selective destruction of type II ganglion cells in the cochlea of guinea pigs with surgically induced endolymphatic hydrops, with a nearly complete sparing type I ganglion cells[8]. Exactly why this occurs is unknown, but one reasonable speculation is that because of their different anatomic associations type II ganglion cells are more susceptible to neurotoxic damage. While Type 1 ganglion cells are completely enveloped by the afferent nerve ending of the calyx, type II ganglion cells are bathed in perilymph at their basal and lateral surfaces, and thus are far more vulnerable to neurotoxic damage from the surrounding environment. It has also been reported that the inducible isoform of nitric oxide synthase (iNOS) is found in high levels in the hydropic cochlea, but not in the normal cochlea[9-10]. We postulate that excessive nitric oxide may be the neurotoxic culprit responsible for much of the damage in the hydropic cochlea. To test this theory we administered aminoguanidine, a relatively specific inhibitor if iNOS[11-13], to a cohort of guinea pigs with surgically induced endolymphatic hydrops. In this animal model of Menière's syndrome there is a characteristic sensorineural hearing loss that takes place. We hypothesize that if nitric oxide is indeed part of the pathology leading to hearing loss in Menière's syndrome, then inhibiting the formation of nitric oxide

should be protective against hearing loss, even in the presence of hydrops. To test this theory we used auditory brain stem response (ABR) to monitor hearing thresholds along a range of frequencies in aminoguanidine treated guinea pigs with surgically induced endolymphatic hydrops, the standard animal model for Menière's syndrome. To date we are not aware of any studies demonstrating pharmacological hearing protection in Menière's syndrome.

Methods and Materials

Materials. The study was carried out using 20 albino guinea pigs (Duncan Hartley strain) each initially weighing 250-300 grams. All guinea pigs obtained from the Charles River Breeding Labs (Wilmington, MA). Prior to hearing tests, guinea pigs were anesthetized by administration of pentobarbital (16.67mg/kg, IP), xylazine (3.46mg/kg. IM), and ketamine (17.28mg/kg, IM). Body temperature was maintained with an electric heating pad (Harvard Apparatus, Holliston, MA). Aminoguanidine was purchased from Sigma Aldrich (Irvine, Ca). All animals were treated in accordance with the NIH Guide for the Care and Use of Laboratory Animals, and the protocol was approved by the Animal Care Committee at the University of Massachusetts Medical School.

Induction of hydrops. Guinea pigs were anesthetized as described earlier and right-side unilateral endolymphatic hydrops was induced in the usual manner as described by Kimura and Schuknecht[14]. Briefly, the endolymphatic sac and duct were entered through a posterior cranial fossa approach, and a small surgical drill was used to enter and obliterate the endolymphatic sac and duct, the remains of which were packed with bone wax. All right ears were operated on and all left ears were kept as internal controls. Post-operatively sulfonamide antibiotics and one dose of liquid Tylenol were included in the drinking water of all animals.

Hearing Tests. All hearing thresholds were obtained using Intelligent Hearing Systems' Auditory Brainstem Response (ABR) system, version 3.6x (Intelligent Hearing Systems, Miami, Fl). Sound was introduced through a custom made sound source described in detail elsewhere[15]. Briefly, the sound source, which consisted of a Radio Shack 40-1377 'Super Tweeter' high-frequency dynamic speaker, a brass ear bar to direct sound into the ear canal, and a coupler to attach the ear bar to the speaker, was fit securely into the external auditory canal of the guinea pig. Grass subdermal needle electrodes were placed at the midline scalp and retroauricularly. Electrical activity was amplified 100,000 times and was filtered (0.1-3 kHz) with a bioamplifier. The signal was digitized by an MII signal averaging system and an IBM PC clone. Each response was the average of 1024 sweeps presented at a rate of 19.3 Hz and was stored on the PC clone. Threshold of hearing was determined to plus or minus 5 dB SPL for frequencies of 2 kHz, 4kHz, 8kHz, 16kHz, and 32kHz.

Aminoguanidine Administration. Twenty female guinea pigs were operated on to surgically induce right-sided unilateral endolymphatic hydrops. Ten of these animals were treated with aminoguanidine in their drinking water for twenty-two weeks. The remaining ten animals were left as untreated controls. The aminoguanidine in the drinking water was added at 2.0 grams per liter, and the animals were allowed free access to the water. All animals were caged individually, and hearing tests in both ears on all animals were performed approximately every 2 weeks.

Statistical Analysis. Difference in mean hearing thresholds between experimental and control groups for each measured frequency at each time point was analyzed by one way analysis of variance (ANOVA) with Tukey post hoc multiple comparisons.

Statistical significance between mean starting and ending hearing thresholds in treated and control animals in both ears was determined by paired sample t test.

Results

Aminoguanidine Tolerance. All animals appeared to tolerate aminoguanidine well, without obvious ill effect. After 22 weeks there was no significant difference in weights between the treated and untreated animals (Figure 1). This is consistent with previous reports of the use of aminoguanidine in experimental animals in which there have been no reported effects on weight, renal, or cardiovascular health.[13, 16-17]

Hearing Thresholds. Hearing thresholds for all animals were determined at 2kHz, 4kHz, 8kHz, 16kHz, and 32kHz from start to twenty-two weeks. Hearing was unaltered over time in all unoperated ears (Figures 2-3). Hearing thresholds increased in all operated ears (Figure 4-5), though this did not reach statistical significance at 4 kHz and 8 kHz in aminoguanidine treated animals. There was a statistically significant prevention of hearing loss in the operated ears of treated verse control animals at all frequencies by 16 weeks (Figures 6-10).

Discussion

Excessive production of nitric oxide related to increased levels of iNOS has been shown to be cytotoxic in many tissues and neurotoxic in the central nervous system[18]. We have hypothesized that the characteristic sensorineural hearing loss seen in Menière's syndrome may be related to a neurotoxic injury from elevated levels of nitric oxide in the inner ear. The goal of the current study was to evaluate the potential of aminoguanidine, a relatively specific iNOS inhibitor, as a pharmacologic neuroprotective agent for the preservation of hearing in albino guinea pigs with surgically induced endolymphatic hydrops, the standard animal model for Menière's syndrome.

In the current study the aminoguanidine treated animals had statistically significant protection against hearing loss. We interpret these results to indicate that neuroprotection by pharmacological inhibition of iNOS was partially protective against hearing loss in the standard animal model of Menière's syndrome.

There are some limitations of this study that will need to be addressed in future work. The amount of treated water consumed by guinea pigs was not measured, leaving it unclear how much aminoguanidine was administered. Further study in this area should attempt to quantify a dose response. Also, it will be important to look for histologic and immunohistochemical correlations to hearing protection in the cochlea of treated animals to help substantiate the mechanism by

which aminoguanidine is protective. Ultimately, if these promising results continue, this work may suggest a possible therapeutic treatment for humans. While it is premature to consider human trials with aminoguanidine for hearing preservation in Menière's syndrome, it is worth noting that the hurdle to beginning human trials is not as onerous as it might be, as aminoguanidine has already been used in FDA approved human studies[19].

References

1. Peron DL, Kitamura K, Carniol PJ, Schuknecht HF. Clinical and experimental results with focused ultrasound. *Laryngoscope* 1983; 93:1217–1221.

2. Wladislavosky-Waserman P, Facer GW, Bahram M, Kurland LT. Menière's disease: a 30-year epidemiologic and clinical study in Rochester, MN, 1951–1980. *Laryngoscope* 1984; 94:1098–1102.

4. Kitahara M. Bilateral aspects of Menière's disease: Menière's disease with bilateral fluctuant hearing loss. *Acta Otolaryngol (Stockh)* 1991; 485:74–77.

5. Balkany TJ, Sires B, Arenberg IK. Bilateral aspects of Menière's disease: an underestimated clinical entity. *Otolaryngol Clin North Am* 1980; 13:603–609.

6. Balkany TJ, Sires B, Arenberg IK. Bilateral aspects of Menière's disease: an underestimated clinical entity. *Otolaryngol Clin North Am* 1980; 13:603–609.

7. Paparella MM. The cause (multifactorial inheritance) and pathogenesis (endolymphatic malabsorption) of Menière's disease and its symptoms (mechanical and chemical). *Acta Otolaryngol (Stockh)* 1985; 99:445–451.

8. Tsuji, KL, Velazques-Villasenor, SD, Rauch, *et al*. Temporal bone studies of the human peripheral vestibular system: Meniere's disease. *Ann. Otol. Rhinol. Laryngol* 2000; 109 (Pt. 2, Suppl. 181)**:** 26–31.

9. Hess A, Bloch W, Su J, Stennert E, Addicks K, Michel O. Expression of inducible nitric oxide-synthase in the vestibular system of hydropic guinea pigs. *Neuroscience Letters* 1999 Apr 2;264(1-3):145-8.

10. Michel O, Hess A, Su J, Bloch W, Stennert E, Addicks K Expression of inducible nitric oxide synthase (iNOS/NOS II) in the hydropic cochlea of guinea pigs. *Hearing Research* 2000 May;143(1-2):23-8.

11. Bryk, R and Wolff, DJ. Mechanism of Inducible Nitric Oxide Synthase Inactivation by Aminoguanidine and L-N^6-(1-Iminoethyl) lysine *Biochemistry* 1998 37;4844–4852.

12. Brenner, T, Brocke, S, Szafer, F, Sobel, R A, Parkinson, J F, Perez, DH, and Steinman, L. Inhibition of nitric oxide synthase for the treatment of experimental autoimmune encephalomyelitis. *Journal of Immunolog* 1997;158:2940–2946.

13. Waz, W R, Van Liew, JB and Feld, LG. Nitric oxide-inhibitory effect of

aminoguanidine on renal function in rats. *Kidney Blood Pressure Research* 1997 20;211–217.

14. Kimura RS, Schuknecht JF. Membranous hydrops in the inner ear of guinea pig after obliteration of the endolymphatic sac. *Pract Otorhinolaryngol* 1965; 27:343-5.

15. Greenwood DD. A cochlear frequency-position function for several species: 29 years later. *J Acoustical Society of America* 1990; 87(6):2592-2605.

16. Selles-Navarro I, Villegas-Perez MP, Salvador-Silva M, Ruiz-Gomez JM and Vidal-Sanz M. Retinal ganglion cell death after different transient periods of pressure-induced ischemia and survival intervals. A quantitative in vivo study. *Investigative Ophthalmoogy and Visual Scienes* 1996*;* (37): 2002–2014.

17. Turner, CH, Owan, I, Jacobs, DS, McClintock, R. and Peacock, M. Effects of nitric oxide synthase inhibitors on bone formation in rats *Bone* 1996;*(* 21):487–490.

18. Dawson, VL & Dawson, TM. The Ginkgo biloba extract (EGb 761) provides a neuroprotective effect on retinal ganglion cells in a rat model of chronic glaucoma *Proc. Soc. Exp. Biol. Med.* 1996; 211, 33–40.

19. Freedman BI, Wuerth JP, Cartwright K, Bain RP, Dippe S, Hershon K, Mooradian AD, Spinowitz BS. Design and baseline characteristics for the aminoguanidine Clinical Trial in Overt Type 2 Diabetic Nephropathy *Controlled Clinical Trials*. 1999 Oct; 20(5):493-510.

Guinea Pig Weights (mean ± sd)	
Treated Initial	273 grams ± 28 grams
Treated Final	1027 grams ± 128 grams
Control Initial	285 grams ± 18 grams
Control Final	1018 grams ± 115 grams

Figure 1

Beginning and ending mean guinea pig weights in grams ± sd.

Mean Difference in Starting and Ending Hearing Thresholds in Untreated Animals in Non-Hydropic Ears

Frequency	Initial (dB SPL)	Final (dB SPL)	Difference (dB SPL)	
2 kHz	35.4 ± 3.1	37.1 ± 2.3	+1.9	***
4 kHz	36.2 ± 2.1	35.1 ± 4.2	- 0.9	***
8 kHz	18.7 ± 4.2	20.3 ± 3.3	+1.6	***
16 kHz	20.1 ± 5.2	18. 1± 4.5	-2.0	***
32 kHz	21.6 ± 4.4	25. 3 ± 5.3	+3.7	***

Figure 2

Difference between initial and final mean hearing thresholds in the unoperated, control ear of untreated animals. *** signifies lack of statistical significance, with $p>0.05$.

Mean Difference in Starting and Ending Hearing Thresholds in Treated Animals in Non-Hydropic Ears

Frequency	Initial (dB SPL)	Final (dB SPL)	Difference (dB SPL)	
2 kHz	33.4 ± 3.9	35.1 ± 4.1	+1.7	***
4 kHz	31.2 ± 9.4	36.3 ± 6.2	+5.1	***
8 kHz	20.2 ± 3.7	16.4 ± 5.0	-3.8	***
16 kHz	16.0 ± 8.3	19. 3± 5.1	+3.3	***
32 kHz	20.9 ± 4.4	23. 1 ± 7.1	+2.2	***

Figure 3

Difference between initial and final mean hearing thresholds in the unoperated, control ear of treated animals. *** signifies lack of statistical significance, with $p>0.05$.

Mean Difference in Starting and Ending Hearing Thresholds in Untreated Animals in Hydropic Ears

Frequency	Initial (dB SPL)	Final (dB SPL)	Difference (dB SPL)	
2 kHz	38.8 ± 3.8	61.3 ± 2.3	+21.5	$p<0.01$
4 kHz	35.6 ± 3.2	57.5 ± 4.2	+21.9	$p<0.01$
8 kHz	16.3 ± 4.4	42.5 ± 3.3	+26.2	$p<0.01$
16 kHz	18.8 ± 4.5	52.5 ± 8.2	+33.7	$p<0.01$
32 kHz	20.6 ± 5.6	45.0 ± 4.5	+24.4	$p<0.01$

Figure 4

Difference between initial and final mean hearing thresholds in the operated ear of untreated animals.

Mean Difference in Starting and Ending Hearing Thresholds in treated Animals in Hydropic Ears

Frequency	Initial (dB SPL)	Final (dB SPL)	Difference (dB SPL)	
2 kHz	37.5 ± 3.3	45.0 ± 6.3	+7.5	$p<0.05$
4 kHz	36.9 ± 3.7	42.5 ± 5.3	+5.6	***
8 kHz	19.6 ± 7.5	24.4 ± 6.1	+4.8	***
16 kHz	20.5 ± 4.9	32.5 ± 6.9	+12	$p<0.05$
32 kHz	23.8 ± 3.3	31.3 ± 2.1	+7.5	$p<0.05$

Figure 5

Difference between initial and final mean hearing thresholds in the operated ear of treated animals. *** signifies lack of statistical significance, with $p>0.05$.

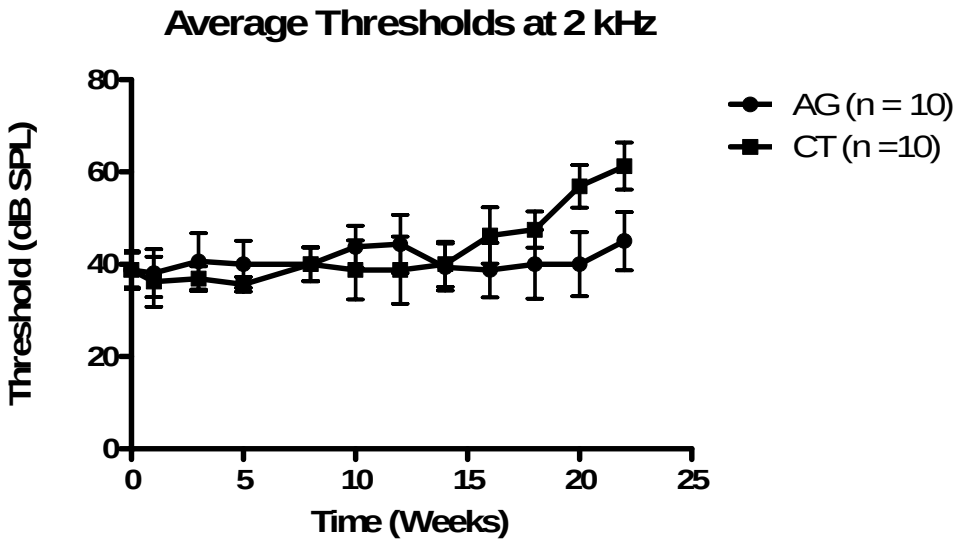
Average Thresholds at 2 kHz
Threshold (dB SPL)
80
60
40
20
0
0
5
10
15
20
25
Time (Weeks)
AG (n = 10)
CT (n =10)

Figure 6

Mean hearing thresholds at 2 kHz in aminoguanidine (AG) treated and untreated controls (CT). The difference between the means was statistically significant from 16 weeks on ($p < 0.05$).

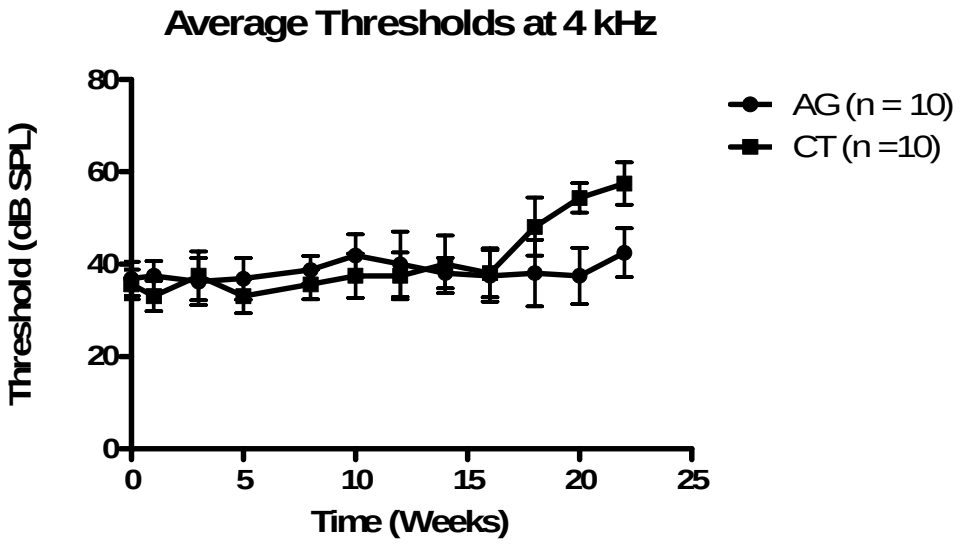
Average Thresholds at 4 kHz
Threshold (dB SPL)
80
60
40
20
0
0
5
10
15
20
25
Time (Weeks)
AG (n = 10)
CT (n =10)

Figure 7

Mean hearing thresholds at 4 kHz in aminoguanidine (AG) treated and untreated controls (CT). The difference between the means was statistically significant from 16 weeks on ($p < 0.05$).

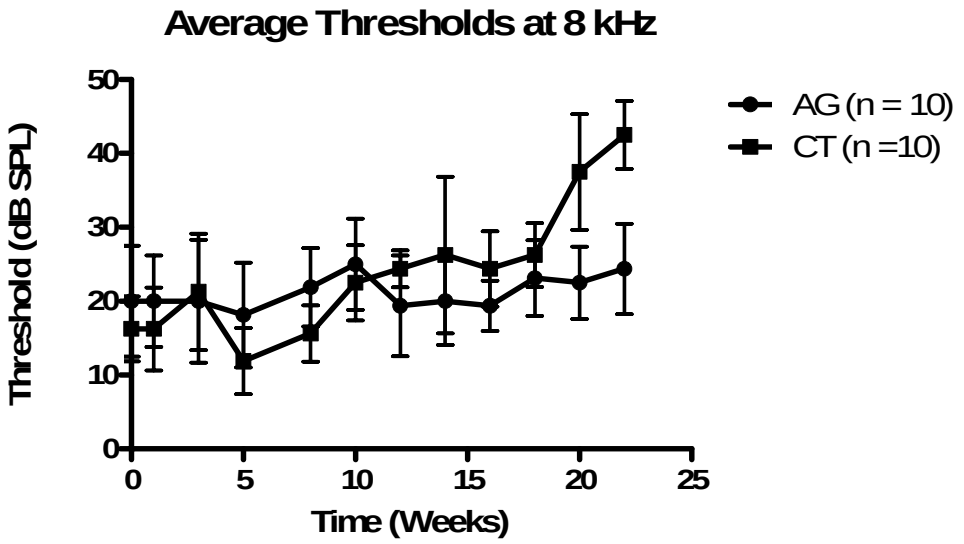
Average Thresholds at 8 kHz
Threshold (dB SPL)
50
40
30
20
10
0
0
5
10
15
20
25
Time (Weeks)
AG (n = 10)
CT (n =10)

Figure 8

Mean hearing thresholds at 8 kHz in aminoguanidine (AG) treated and untreated controls (CT). The difference between the means was statistically significant from 16 weeks on ($p < 0.05$).

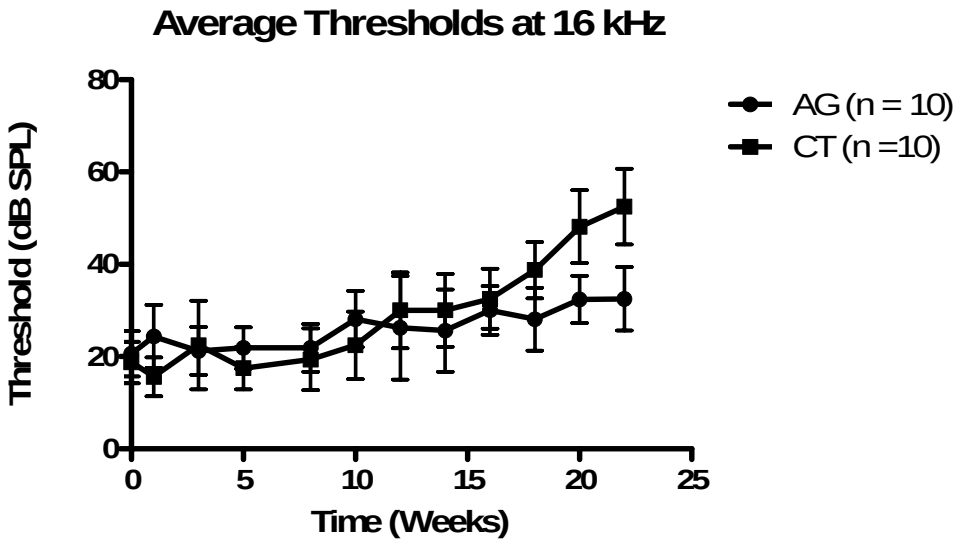
Average Thresholds at 16 kHz
Threshold (dB SPL)
80
60
40
20
0
0
5
10
15
20
25
Time (Weeks)
AG (n = 10)
CT (n =10)

Figure 9

Mean hearing thresholds at 16 kHz in aminoguanidine (AG) treated and untreated controls (CT). The difference between the means was statistically significant from 16 weeks on ($p < 0.05$).

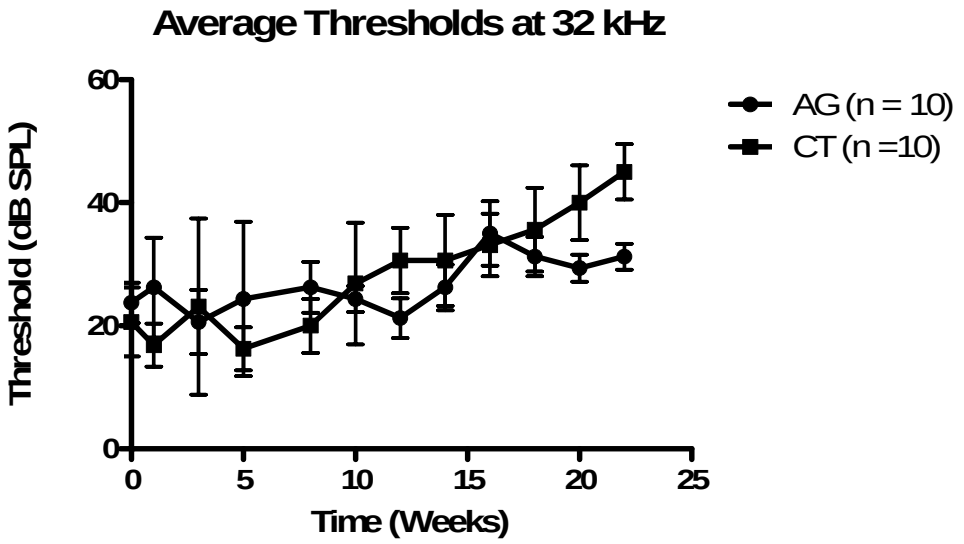
Average Thresholds at 32 kHz
Threshold (dB SPL)
60
40
20
0
0
5
10
15
20
25
Time (Weeks)
AG (n = 10)
CT (n =10)

Figure 10

Mean hearing thresholds at 32 kHz in aminoguanidine (AG) treated and untreated controls (CT). The difference between the means was statistically significant from 16 weeks on ($p < 0.05$).

Discussion

The goals of the cartilage tissue engineering research presented here were three-fold: first, to establish the chondrogenic potential of adult human nasal septal chondrocytes; second, to demonstrate the formation of small calcium alginate constructs in complex geometries with high dimensional tolerances utilizing computer-aided design and an injection molding process; and finally, to establish that calcium alginate can be reliably modified by the efficient covalent addition of peptides, and that by adding a TGF-β binding peptide we could alter the release characteristics of pre-loaded TGF-β1 from a molded alginate gel.

The data presented in this thesis are encouraging with regards to all the stated goals. As such, the work of this thesis helps to highlight the exciting potential of cartilage tissue engineering. We have shown that adult human nasal septal chondrocytes have substantial chondrogenic potential when grown within an alginate scaffold. We have shown that alginate is a versatile polymer for cartilage tissue engineering purposes, amenable to both precise shaping and modification by covalent addition of peptides, which, in principle, could serve any number of biologically important functions.

Even in light of these encouraging results, though, perhaps this work should also serve as a somewhat sober reminder that the field of tissue engineering is still in

its infancy. While the work presented here is encouraging, it is by no means definitive. Truly definitive work in cartilage tissue engineering should not only demonstrate a clinically useful method for engineering a replacement cartilage indistinguishable from healthy native cartilage, but should also show that the engineered cartilage performs in humans like healthy native cartilage for many years.

Our results are indeed encouraging, but they stem from looking at one cell source with one scaffold in one set of growth conditions. Seen in the context of the veritable panoply of well studied scaffolds, numerous cell sources, and abundant culture conditions, it is not possible to know how our results would compare to the innumerable rich opportunities that remain uninvestigated. This is part of both the excitement and the frustration of working in an emerging field.

A critical appraisal of the tissue engineering literature reveals the existence of many novel and promising biologically-based approaches for the induction of articular cartilage repair, the vast majority of which are still at an experimental phase of development. There are, however, no prospective, double-blinded clinical trials showing the efficacy of cartilage tissue engineering. The tissue engineering approaches to articular cartilage repair thus far pursued have been principally of an empirical nature and still very much at an experimental stage of development. From a clinical standpoint, where only definitive solutions count, results achieved to date are far from satisfactory with respect to repair tissue quality and durability. Success in the

future depends upon our now following a rational, rigorous approach to the problem, based on biological principles at the molecular, cellular and physiological levels.

Although it has been suggested many times that the problems of tissue engineering should be thought of as a recapitulation of embryological differentiation, this is probably not a particularly good idea.[1-3] Both the cellular microenvironments and tissue macroenvironments encountered in adult organisms are fundamentally different from those encountered in embryological environments. Apart from the signaling molecules, which are most probably the same, every other component is different, including the existence of an active immune system in fully-developed organisms. Thus, while the control available with in vitro systems is appealing, the attempt to engineer complete constructs, consisting of a matrix, cells, and bioactive signaling molecules in vitro, with the thought that terminal differentiation will occur after in situ implantation, may be overly optimistic, especially when we consider the mammalian body's own limited tissue engineering capacity, as exemplified by scar formation.

Future tissue engineering studies will need to tackle an often overlooked issue; namely, tissue integration. A tissue engineered construct must be accepted by, and become integrated with, tissue neighboring its destined site without triggering the immunological responses that would result in its resorption. Following resorption, it would inevitably be replaced by a scar-like or fiber-rich tissue bearing little

resemblance to the articular cartilage we all aspire to make. If the engineered constructs are reabsorbed and exchanged following their implantation, then the great pains we have gone to in order to created the conditions conducive to cartilage development and growth will be in vain. Additionally, as we move forward in the next generation of cartilage tissue engineering experiments we will need to pay more attention to recreation of the zonal organization in native collagen. To date engineered cartilage has been homogeneous, but if an engineered construct is to fill a full thickness defect, or even replace an entire articular surface it should be engineered to replicate the zonal architecture in native cartilage. This will require continued enhancement of our understanding of the differing molecular biology and gene expression of chondrocytes in different cartilage zones.

Part of the great challenge in moving forward in tissue engineering is the incredible complexity that arises when considering that a successful application will need to consider appropriate use of cells, polymers, and growth factors. Each of these individually is legitimately an enormous puzzle. When one starts to consider combining these issues, the magnitude of the problem increases exponentially. Certainly, the same matrix may not be appropriate for use with all tissues, and of course, different cell types may behave differently in different matrices. Best results may be achieved with three or more matrices in a single construct, but the more we start combining elements the more difficult a rigorous analysis becomes.

The potential and promise of tissue engineering to change the face of medicine is enormous. After all, in its ideal form it promises nothing less than the replacement of damaged or unhealthy tissue with a replacement, indistinguishable from healthy native tissue. Do you have osteoarthritis? Stop taking antiinflammatories, we will make you new, healthy, gleaming articular cartilage, like you had in your youth. Do you have hepatic cirrhosis? No need to wait for a transplant, we can make you a new liver. Do you have diabetes? Close the dialysis centers, we can make you new kidneys. Let's face it, to the degree that science can be sexy, this is awfully sexy stuff.

Given its revolutionary potential, it should come as no surprise that tissue engineering makes good press. When I was working on my thesis research, I appeared on the evening news (in the background) for ABC, CBS, NBC, the BBC, and the Discovery Channel. For the year 2000 change of the millennium edition, Time Magazine predicted "tissue engineer" as the number one occupation for the twenty first century. There was a period of time when the work of our lab was so often in the news when people in pain and need would contact the lab on a nearly daily basis, asking if we could help. They would volunteer to have new tissues implanted, without really understanding what we were doing. From the evening news, to the popular press, to the general public, tissue engineering has captured our imagination.

For those who work in this field, though, we must always remember that the devil is in the details, and we must remain cautious, and skeptical. The project that truly caught the attention of the world was the work of Vacanti et al in which an engineered cartilage human ear was grown on the back of an athymic mouse.[4] The press coverage was enormous, and forever changed the public perception of tissue engineering in medicine. And it probably does not even bear saying, but the public, whether they supported or decried the work, did not really understand what was done. This project like much of the work of tissue engineering was proof of principal. It demonstrated in broad strokes what the future might hold. As the field has continued to grow the real, slow, incremental work of advancing this new science has begun. And the truth is that from a basic science standpoint we are at the very beginning of understanding how a new tissue might be engineered. What is the best matrix to use? What is the best cell source to use? How should growth factors be delivered? Should we use gene therapy or encapsulate the needed growth factors in a polymer scaffold? Many researchers around the world, certainly more than ever before in history, are working toward answering these questions, but still it would be terribly premature to claim sure answers. No one has yet cured diabetes, osteoarthritis, or any other ailment by applying engineered tissues, so for some the blush of tissue engineering has begun to fade. In my opinion, this perception is really for the best. Too much publicity is not necessarily a good thing.

Tissue engineering is a field still in its infancy, and perhaps it is having some growing pains. Much of the work to date has painted with a broad brush. It has been empirical in nature, and largely about proof of principal. As the field is now maturing the time has come to get down to the detailed work of molecular biology, physiology, engineering, and gene therapy. It is time to begin the slow process of answering the detailed questions that will allow for the incremental progress of science, and I believe that is what we are now seeing in tissue engineering. Certainly the promise of tissue engineering will always fire the imagination of those who work in this field, but on a daily basis the question should not be "when can we make a tissue that serves all the functions of native tissue?", but rather "what gene is being expressed?", "how can I make this matrix stiffer?", "what is the Kd of this ligand". It is through the rigorous application of science to an endless number of small detailed questions that we will ultimately pool the data to answer the big picture questions that have captivated so many.

Tissue engineering has also begun to come up against the harsh realities of clinical medicine. This science is part of medical science, which is to say that the ultimate goal must be to produce useful products to improve human health. In some cases this calls into question the value of the project as a whole. While there is something aesthetically and intellectually appealing about creating, de novo, a new articular surface for a knee devastated by osteoarthritis, to make this a realistic project we also need to show that it is the best treatment we can offer. Meaning, if we can

make an artificial knee that provides relief from pain and adequate mobility, do we really need to be making new cartilage? As a reality check, we should recognize that making replacement tissues will almost certainly be substantially more expensive than making synthetic replacements. Making tissues requires the use of cells and bioactive molecules, which by necessity requires manufacturing in a sterile environment. Medical devices, on the other hand, containing no biological elements, are manufactured in a clean environment and the final product is subsequently sterilized. This difference in processing alone can increase costs by an order of magnitude.[5] Add to this the complexity and cost of using living cells and large quantities of growth factors, and it is clear that any tissue engineered product will need to be clearly superior to any synthetic product to have any hope of becoming part of mainstream medical practice.

At this time, the existence of so many new and encouraging biological approaches to cartilage repair still justifies the future investment of time and money in this research area, particularly given the extremely high socio-economic importance of therapeutic strategies in the prevention and treatment of common joint diseases. Reaching the stage where we are ready for clinical trials, even for very small applications, will have to come in the not too distant future in order to continue the scientific appraisal of current therapies and future novel approaches.

One of my own projects, the tissue engineered tympanic membrane patch, was funded for initial animal testing by the world's largest ENT company, Gyrus ENT. The results were good, excellent in fact, but in the end the project stalled, as so many others of its kind recently have, as the reality of the difficulty and cost of production became clearer. Still, I remain enthusiastic about tissue engineering. For the benefit of the field, though, I believe it is high time that we take tissue engineering off the evening news and leave it in the lab where it belongs. It is only there that the slow incremental work of science can happen. And slowly, as the small contributions from many labs around the world enter the scientific arena, we will begin to uncover answers. Will we every truly be able to make new cartilage, a new liver, or any other tissue one can imagine? Maybe, but truthfully, I think it is time we stopped asking that question, if only for a short time. That question belongs to the era when tissue engineering was a grand idea, the era when simple experiments fired the imagination with amazing possibilities. I believe that time has passed. Tissue engineering is still a new field, but now it is maturing, it is growing up. The work is worth doing. It is valid science, and its researchers are doing their small part to increase knowledge. And as with all such endeavors it is unclear where our work will ultimately lead until we arrive. After all, the role of serendipity in good science, from the work of Alexander Flemming to the work of Craig Mello, cannot be overlooked. Pursing tissue engineering with detail minded, rigorous science will produce interesting and valuable results. We will learn about principles of molecular biology, and the detailed nature of many tissues. And perhaps, one day, we really will replace our old tissues

like we replace our old car parts. The field of tissue engineering is just getting started, just finding its feet. And I for one look forward to seeing how this story unfolds.

References

1. Caplan AI, Elyaderani M, Mochizuki Y, Wakitani S, Goldberg VM. Principles of cartilage repair and regeneration. *Clin Orthop* 1997;00:254–69.

2. Reddi A. Role of morphogenetic proteins in skeletal tissue engineering and regeneration. Nat Biotechnol 1998;16:247–52.

3. Reddi A. Cartilage-derived morphogenetic proteins and cartilage morphogenesis. Microsc Res Tech 1998;43:131–6.

4. Cao, Yilin M.D., Ph.D.; Vacanti, Joseph P. M.D.; Paige, Keith T. M.D.; Upton, Joseph M.D.; Vacanti, Charles A. M.D. Transplantation of Chondrocytes Utilizing a Polymer-Cell Construct to Produce Tissue-Engineered Cartilage in the Shape of a Human Ear. Plastic & Reconstructive Surgery. 100(2):297-302, August 1997.

5. Personal communication with Russ Johnson, research and development project manager for Gyrus ENT.